



THE HONG KONG  
POLYTECHNIC UNIVERSITY

香港理工大學

Pao Yue-kong Library

包玉剛圖書館

---

## Copyright Undertaking

This thesis is protected by copyright, with all rights reserved.

**By reading and using the thesis, the reader understands and agrees to the following terms:**

1. The reader will abide by the rules and legal ordinances governing copyright regarding the use of the thesis.
2. The reader will use the thesis for the purpose of research or private study only and not for distribution or further reproduction or any other purpose.
3. The reader agrees to indemnify and hold the University harmless from and against any loss, damage, cost, liability or expenses arising from copyright infringement or unauthorized usage.

### IMPORTANT

If you have reasons to believe that any materials in this thesis are deemed not suitable to be distributed in this form, or a copyright owner having difficulty with the material being included in our database, please contact [lbsys@polyu.edu.hk](mailto:lbsys@polyu.edu.hk) providing details. The Library will look into your claim and consider taking remedial action upon receipt of the written requests.

# 3D PATTERN FOR KNITTED OBJECTS

CHEUNG CHUN TING

M.Phil

The Hong Kong Polytechnic University

2017

The Hong Kong Polytechnic University  
Institute of Textiles and Clothing

## 3D Pattern for Knitted Objects

Cheung Chun Ting

A thesis submitted in partial fulfilment of the requirements for the degree of Master  
of Philosophy

June 2016

**CERTIFICATE OF ORIGINALITY**

I hereby declare that this thesis is my own work and that, to the best of my knowledge and belief, it reproduces no material previously published or written, nor material that has been accepted for the award of any other degree or diploma, except where due acknowledgement has been made in the text.

\_\_\_\_\_ (Signed)

Cheung Chun Ting (Name of student)

## ABSTRACT

This study attempted to develop a theoretical basis for knitting three-dimensional (3D) shapes. This generic and scientific study aimed at converting 3D data cloud into a 3D knitted shape. An approach of 3D data cloud conversion of a freeform surface based on its geometry, instead of finite elements in many present researches, was introduced. In order to preserve the target 3D shape in knitting, a series of experiments was carried out to reconstruct the 3D form from its data cloud. The relationship between 3D scanned data and two-dimensional (2D) knitting structure was examined. This study involved two parts, 3D data cloud conversion and 3D shape knitting. In order to develop a complete 3D shape knitting theory on freeform shapes, surfaces which would be examined in this study were categorised into three types by means of the Theory of Gaussian Curvature. As a freeform shape can be zoned into different atlases according to their curvatures, surfaces with zero, positive and negative Gaussian curvature were contemplated and taken to experiments separately in the study. All of them underwent a process of capturing 3D data cloud by 3D scanning, flattening the 3D form into a 2D plane as in cartography and reconstructing the 3D form by aligning knitting loops onto the plane.

The scope of the study focused on weft knitting with double-bed flatbed knitting machines, so as to develop and establish a complete basis of theory proposed with fundamental knitting techniques and components. Ground on the knitting constrains in flatbed weft knitting, a knitting mechanism in 2D, knitted fabrics grow only in length upon a width depending on the number of needles to be selected, but not in depth in 3D. Discussions on how a 2D knitting mechanism was capable of creating a 3D shape by specific loop alignment methods were raised.

## ACKNOWLEDGEMENT

My whole-hearted thanks go to the Lord Jesus Christ.

With gratitude and humility, I acknowledge the numerous people who have contributed to the investigation of this study that constitutes my thesis. I especially owe intellectual debt to Dr. Roger Ng, my enlightenment preceptor and MPhil chief supervisor, who gave me insightful advice and valuable lessons on the study.

Special thanks to my MPhil co-supervisor Dr. T. Y. Lo for his beneficial guidance and inspirations.

I must also express my deepest thanks to Dr. Zhou Jinyun, my MPhil co-supervisor for his technical support at all times.

Above all, I wish to express my sincere gratitude to my parents, family and friends who sustained me in studying, as well as in listening my frustrations throughout the writing of thesis

## TABLE OF CONTENTS

<b>CERTIFICATE OF ORIGINALITY .....</b>	<b>iii</b>
<b>ABSTRACT.....</b>	<b>iv</b>
<b>ACKNOWLEDGEMENT.....</b>	<b>v</b>
<b>CHAPTER 1.....</b>	<b>1</b>
<b>INTRODUCTION .....</b>	<b>1</b>
<b>1.1 Background of Study.....</b>	<b>3</b>
1.1.1 Gaussian Curvature .....	3
1.1.2 3D Data Cloud .....	4
1.1.3 3D Shape Knitting.....	6
<b>1.2 Objectives .....</b>	<b>8</b>
<b>1.3 Statement of Problems .....</b>	<b>9</b>
<b>1.4 Theses Framework .....</b>	<b>10</b>
<b>CHAPTER 2.....</b>	<b>13</b>
<b>LITERATURE REVIEW .....</b>	<b>13</b>
<b>2.1 3D Data Cloud .....</b>	<b>13</b>
2.1.1 3D Data Acquisition.....	15
2.1.2 3D Data Processing .....	16
2.1.3 Geometric Feature Recognition .....	18
2.1.4 Surface Feature Extraction.....	19
2.1.5 Distortion in Flattening .....	20
2.1.6 Surface Mapping .....	21
2.1.7 Surface Mesh Flattening .....	22
2.1.8 Summary .....	23

<b>2.2</b>	<b>3D Knitting.....</b>	<b>24</b>
2.2.1	Knitting Fundamental .....	25
2.2.2	Knitting Science .....	27
2.2.3	Shaping Methods.....	31
2.2.4	Knitted 3D Shapes .....	35
2.2.5	Shaping Calculation .....	36
2.2.6	Summary .....	39
<b>CHAPTER 3.....</b>		<b>40</b>
<b>METHODOLOGY .....</b>		<b>40</b>
<b>3.1</b>	<b>3D Data Cloud Conversion.....</b>	<b>42</b>
3.1.1	3D Data Acquisition and Processing .....	42
3.1.2	Feature Recognition and Extraction.....	43
3.1.3	Polygonal Mesh Mapping and Flattening .....	44
<b>3.2</b>	<b>3D Shape Knitting .....</b>	<b>45</b>
3.2.1	Loop Alignment .....	46
3.2.2	Knitting Validation .....	47
<b>3.3</b>	<b>Result Evaluation .....</b>	<b>47</b>
<b>3.4</b>	<b>Conclusion.....</b>	<b>48</b>
<b>CHAPTER 4.....</b>		<b>50</b>
<b>ZERO GAUSSIAN CURVATURE.....</b>		<b>50</b>
<b>4.1</b>	<b>3D Data Cloud Conversion.....</b>	<b>51</b>
4.1.1	3D Data Acquisition and Processing .....	51
4.1.2	Feature Recognition and Extraction.....	56
4.1.3	Polygonal Mesh Mapping and Flattening .....	56
<b>4.2</b>	<b>3D Shape Knitting .....</b>	<b>59</b>
4.2.1	Loop Alignment .....	59



4.2.2	Knitting Validation .....	62
<b>4.3</b>	<b>Evaluation .....</b>	<b>64</b>
<b>4.4</b>	<b>Conclusion.....</b>	<b>69</b>
<b>CHAPTER 5.....</b>	<b>.....</b>	<b>71</b>
<b>POSITIVE GAUSSIAN CURVATURE .....</b>	<b>.....</b>	<b>71</b>
<b>5.1</b>	<b>3D Data Cloud Conversion I .....</b>	<b>72</b>
5.1.1	3D Data Acquisition and Processing .....	73
5.1.2	Feature Recognition and Extraction.....	74
5.1.3	Polygonal Mesh Mapping and Flattening .....	75
<b>5.2</b>	<b>3D Shape Knitting I.....</b>	<b>78</b>
5.2.1	Loop Alignment .....	78
5.2.2	Knitting Validation .....	82
<b>5.3</b>	<b>Evaluation I.....</b>	<b>86</b>
<b>5.4</b>	<b>3D Data Cloud Conversion II.....</b>	<b>91</b>
5.4.1	Surface Flattening .....	92
<b>5.5</b>	<b>3D Shape Knitting II.....</b>	<b>93</b>
5.5.1	Loop Alignment .....	93
5.5.2	Knitting Validation .....	95
<b>5.6</b>	<b>Evaluation II .....</b>	<b>98</b>
<b>5.7</b>	<b>Conclusion.....</b>	<b>104</b>
<b>CHAPTER 6.....</b>	<b>.....</b>	<b>106</b>
<b>NEGATIVE GAUSSIAN CURVATURE .....</b>	<b>.....</b>	<b>106</b>
<b>6.1</b>	<b>3D Data Cloud Conversion.....</b>	<b>107</b>
6.1.1	3D Data Acquisition and Processing .....	107
6.1.2	Feature Recognition and Extraction.....	107
6.1.3	Polygonal Mesh Mapping and Flattening .....	108

<b>6.2</b>	<b>3D Shape Knitting .....</b>	<b>110</b>
6.2.1	Loop Alignment .....	110
6.2.2	Knitting Validation .....	113
<b>6.3</b>	<b>Evaluation .....</b>	<b>115</b>
<b>6.4</b>	<b>Conclusion.....</b>	<b>118</b>
<b>CHAPTER 7</b>	<b>.....</b>	<b>120</b>
<b>CONCLUSION</b>	<b>.....</b>	<b>120</b>
<b>REFERENCE</b>	<b>.....</b>	<b>124</b>

## LIST OF FIGURES

Figure 1.1	Examples of each type of Gaussian curvature : (a) zero Gaussian curvature (a cylinder) (Andymsp, 2010), (b) positive Gaussian curvature (a sphere) (Quickfur, 2012) and (c) negative Gaussian curvature (a hyperboloid) (Köller, 2011).....	4
Figure 2.1	3D data cloud of a torus: (left) front view and (right) side view (Kieff, 2012) .....	16
Figure 2.2	Demonstration of a successive loop formation (Raz, 1991) .....	26
Figure 2.3	An illustration of (a) a single wale and (b) a single course highlighted in a plain knitted fabric .....	26
Figure 2.4	Illustration of (a) interlock gating and (b) rib gating of double-bed knitting machine.....	27
Figure 2.5	Illustration of loop configuration for calculation.....	29
Figure 2.6	Illustration of (a) loop overlapping in inside narrowing and (b) hole formation in inside widening. ....	34
Figure 3.1	Framework of the study methodology .....	41
Figure 3.2	Side view of Artec Eva handheld 3D scanner .....	43
Figure 3.3	Triangle subdivision process proposed and illustrated by McCartney and his team (2004).....	45
Figure 4.1	A digital image of the shape with a surface with zero Gaussian curvature indicated in yellow.....	50
Figure 4.2	Front view of Artec Eva handheld 3D scanner with indications .....	53
Figure 4.3	Demonstration of the 3D data cloud of the target with a lopsided polar coordinate using an Artec Eva handheld scanner .....	54
Figure 4.4	An image of proceeding scanning.....	54

Figure 4.5	An image of the scan with noise and unrelated data.....	55
Figure 4.6	An image of the data cloud after preliminary processing .....	55
Figure 4.7	An image of the flattened 2D plane of the surface with zero Gaussian curvature used .....	58
Figure 4.8	An illustration of the plane marked with measurement references....	62
Figure 4.9	Knitting programme of target object of zero Gaussian curvature.....	63
Figure 4.10	An image of the finished 3D knitted shape of zero Gaussian curvature on the target object.....	64
Figure 4.11	The pictures of positioning a knitting shape of zero Gaussian curvature onto the target: (a) target shape with black and red reference marking tapes; (b) the seam of the knitting shape lying on the black reference marking tape; (c) the edge of the knitted shape top below the rib trim lying on the upper red reference marking tape and (d) the edge of the knitted shape bottom lying on the lower red reference marking tape.....	67
Figure 4.12	The scanned images of (a) target image and (b) the knitted shape of surface with zero Gaussian curvature .....	68
Figure 4.13	The procedures of measuring cpc with counting 70 successive loops... ..	68
Figure 5.1	Image of the egg-like shape with a surface with positive Gaussian curvature .....	72
Figure 5.2	A finished 3D data cloud of the target object .....	74
Figure 5.3	A diagram of Sobel mask of half of the target shape of positive Gaussian curvature.....	75
Figure 5.4	An illustration of constant size of triangulation and possible errors .	76
Figure 5.5	An illustration of subdivided triangulation and less possible errors..	77

Figure 5.6	One of the two identical 2D planes with two opposite halves of positive Gaussian curvature for method 3DSL-1 and 2DSL-1 .....	77
Figure 5.7	Illustration of parallel of latitudes on a sphere.....	80
Figure 5.8	Illustration of parallel of latitude on target object as for method 3DSL-1 .....	81
Figure 5.9	A half plane marked with 2D curved lines and vertical reference line for method 3DSL-1 .....	81
Figure 5.10	A half plane marked with 2D straight lines and vertical reference line for method 2DSL-1 .....	81
Figure 5.13	Knitting Programme of (a) method 3DSL-1 and (b) method 2DSL-1... ..	85
Figure 5.14	(a) The front view and (b) the side view of the 3D knitted shape by method 3DSL-1.....	85
Figure 5.15	(a) The front view and (b) the side view of the 3D knitted shape by method 2DSL-1.....	86
Figure 5.16	The front view of scanned images of (a) target image, (b) 3D knitted shape by method 3DSL-1 and (c) 3D knitted shape by method 2DSL-1 .....	89
Figure 5.17	The top view of scanned images of (a) target image, (b) 3D knitted shape by method 3DSL-1 and (c) 3D knitted shape by method 2DSL-1 .....	89
Figure 5.18	An illustration of one of the newly flattened 2D planes for method 3DSL-2 and 2DSL-2.....	93
Figure 5.19	An illustration of 2D curved lines from 3D straight lines in loop alignment method 3DSL-2.....	95
Figure 5.20	An illustration of 2D straight lines directly marked onto the plane in loop alignment method 2DSL-2.....	95

Figure 5.21	Knitting programme of method 3DSL-2 of the two planes .....	96
Figure 5.22	Knitting Programme of method 2DSL-2 of the two planes.....	97
Figure 5.23	(a) The front view and (b) the side view of the 3D knitted shape by method 3DSL-2.....	97
Figure 5.24	(a) The front view and (b) the side view of the 3D knitted shape by method 2DSL-2.....	98
Figure 5.25	The front view of scanned images of (a) target image, (b) 3D knitted shape by method 3DSL-2 and (c) 3D knitted shape by method 2DSL-2 .....	101
Figure 5.26	The top view of scanned images of (a) target image, (b) 3D knitted shape by method 3DSL-2 and (c) 3D knitted shape by method 2DSL-2 .....	102
Figure 5.27	An illustration of the shape induced by method 3DSL-2 .....	102
Figure 6.1	A digital image of the shape with a surface with negative Gaussian curvature indicated in red.....	106
Figure 6.2	A diagram of Sobel mask of half of the target shape of negative Gaussian curvature.....	108
Figure 6.3	An illustration of mesh mapping with smaller triangles on the convex area of the surface with negative Gaussian curvature.....	109
Figure 6.4	The flattened plane of the surface with negative Gaussian curvature with olive-shape empty space indicated in grey .....	110
Figure 6.5	A 90° rotated plane of the target .....	112
Figure 6.6	The rotated plane marked with measurement lines for loop alignment .....	112
Figure 6.7	Knitting programme of the target object of negative Gaussian curvature .....	114

Figure 6.8	The knitted shape of surface with negative Gaussian curvature on the target .....	114
Figure 6.9	Applying double tape to the target edge to hold the fabric edge .....	116
Figure 6.10	The scanned images of (a) target image, (b) 3D knitted shape of surface with negative Gaussian curvature.....	117

## LIST OF TABLES

Table 4.1	Table of appearance observations of three samples of zero Gaussian curvature .....	69
Table 4.2	Table of loop density of three samples of zero Gaussian curvature .....	69
Table 5.1	Table of appearance observations of three samples of positive Gaussian curvature by method 3DSL-1.....	90
Table 5.2	Table of appearance observations of three samples of positive Gaussian curvature by method 2DSL-1.....	90
Table 5.3	Table of loop density of the three samples by Method 3DSL-1 .....	91
Table 5.4	Table of loop density of the three samples by Method 2DSL-1 .....	91
Table 5.5	Table of appearance observation of three samples of positive Gaussian curvature by method 3DSL-2.....	102
Table 5.6	Table of appearance observation of three samples of positive Gaussian curvature by method 2DSL-2.....	103
Table 5.7	Table of loop density of the three samples by Method 3DSL-2 .....	103
Table 5.8	Table of loop density of the three samples by Method 2DSL-2 .....	104
Table 6.1	Table of appearance observation of three samples of negative Gaussian curvature .....	117
Table 6.2	Table of loop density of three samples of negative Gaussian curvature.... .....	118



## CHAPTER 1

### INTRODUCTION

Transformation of three-dimensional (3D) scanned anthropometric data into developable 2D pattern had been investigated and discussed in depth already. Most of the existing studies, however, considered anthropometric features, non-elastic woven materials and cut-and-sewn process only. In this study, an approach of converting 3D data cloud of a freeform surface based on its geometry, instead of finite elements in many present researches, into a 3D knitted shape was introduced. This study was a generic and scientific study of 3D knitted shape control on the relationship between 3D scanned data and two-dimensional (2D) knitting structure. It involved two parts, 3D data cloud conversion and 3D shape knitting. In order to develop a complete 3D shape knitting theory on freeform shapes, surfaces which would be examined in this study were categorised into three types by means of the Theory of Gaussian Curvature.

This study attempted to lay the theoretical basis for knitting 3D shapes from 3D data cloud captured by 3D scanning into a developable 2D plane as in cartography to retrieving the 3D form by aligning knitting loops onto the plane. Ground on the knitting constrains in flatbed weft knitting, a knitting mechanism in 2D, knitted fabrics grow only in length upon a width depending on the number of needles to be selected, but not in depth in 3D. Discussions on how a 2D knitting mechanism was capable of creating a 3D shape by specific loop alignment methods were raised. As a freeform shape can be zoned into different atlases according to

their curvatures, surfaces with zero Gaussian curvature, positive Gaussian curvature and negative Gaussian curvature were contemplated and taken to experiments separately in the study. To start with, by using a 3D scanner, a target object of each type of curvatures was scanned, and its 3D data cloud derived was flattened into a 2D plane based on its geometric properties. Measurements and corresponding dimensional information were taken before developing a knitting sequence that was based on loop alignment onto the plane. With the knitting sequence, 3D shape knitting was proceeded.

The scope of the study focused on single jersey of weft knitting with double-bed flatbed knitting machines, so as to develop and establish a complete basis of theory proposed with fundamental knitting techniques and components. Seamless knitting technique was not considered here, but it had high potential to be an advanced tool for 3D shape knitting in the future. However, to develop a theory for weft knitting, it should start with basic knitting techniques first. After finding out the possibilities and limitations in 3D shapes with basic knitting techniques in this study, further research on other knitting methods could be developed based on the established theory. Therefore, double-bed flatbed knitting machines as the fundamental computerised knitting equipment were mainly focused. In this study, scanning and knitting were carried out by means of the Artec Eva handheld 3D scanner and Shima Seiki SES-122S computerised automatic flatbed knitting machine respectively.

## 1.1 Background of Study

Surfaces with each type of three Gaussian curvature types were experimented and analysed in this study. Each section of one type was divided into two areas, 3D data cloud to 2D plane transformation and 3D shape knitting. This study aimed at developing a theoretical study on controlling and producing a knitted fabric with a required 3D form of the target captured by the 3D scanner.

### 1.1.1 Gaussian Curvature

The value of the Gaussian curvature  $K$  at a surface point depends only on its geometrical shape but not the space it embeds according to Lo (2015). Lo also mentioned  $K$  is the product of the principal curvatures  $\kappa_1$  and  $\kappa_2$ .

$$K = \kappa_1 \kappa_2$$

By the definition in the book of Gallier (2011), a surface  $X$  can be categorized into four different shapes according to the Gaussian curvature value on  $X$ .

Elliptic:  $K > 0$ ;

Hyperbolic:  $K < 0$ ;

Parabolic:  $K = \kappa_1 \kappa_2 = 0$ , when  $\kappa_1 \neq 0$  or  $\kappa_2 \neq 0$ ;

Planar:  $K = \kappa_1 \kappa_2 = 0$ , when  $\kappa_1 = \kappa_2 = 0$ .

Therefore, surface of a planar or a parabolic shape has zero Gaussian curvature; that of an elliptic shape has positive Gaussian curvature; and a hyperbolic shape negative Gaussian curvature. Surfaces of each type of constant curvature include cylinders and cones for zero Gaussian curvature, spheres for positive curvature and hyperboloids for negative curvature. Figure 1.1 illustrated each type respectively.

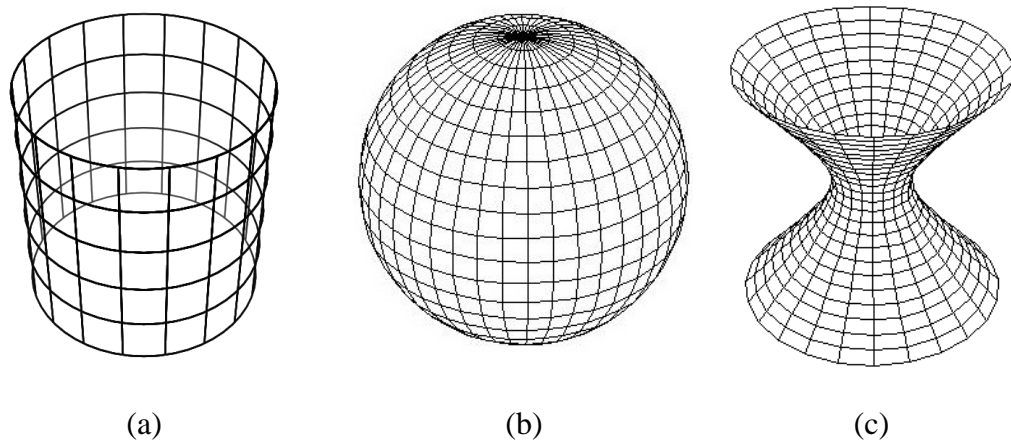


Figure 1.1 Examples of each type of Gaussian curvature : (a) zero Gaussian curvature (a cylinder) (Andymsp, 2010), (b) positive Gaussian curvature (a sphere) (Quickfur, 2012) and (c) negative Gaussian curvature (a hyperboloid) (Köller, 2011)

### 1.1.2 3D Data Cloud

To capture the geometric features and dimensions of an object, to date, 3D scanning, a non-contact measurement system, is a significant tool. It provides accurate digitised 3D data from the scanned target, as its information obtaining system is consistent. With the assistance of the up-to-date automatic frames alignment computer aided design (CAD) software, scanned images are ready to be visualised in a digital 3D manner. There are different types of 3D scanners such as a

large set of stationary scanning machinery, desktop scanner and portable handheld scanner. They are designed for different size or features of objects to be scanned as their coordinate system for figure registration may vary depending on the geometry of the object.

The discrete 3D data cloud obtained is, however, neither readily available for measurement collection nor containing readable indications or landmarks. The 3D data cloud of an undevelopable surface is needed to be processed and flattened to be a developable plane. From the statement of the Gauss egregium theorem, it is known that distortion is inevitable in the process of mapping a 3D form onto a 2D plane (Benítez et al. 2004). This is also a tumbling stone for accurate mapping in cartography throughout ages. So the simultaneous distortion in distance, area or angle from transforming 3D data cloud into a 2D plane before converting back to a 3D shape in knitting is unavoidable.

Many researches were done on flattening 3D surfaces of a closed-form object base on their well-recognised geometry. For freeform objects, researches had a tendency to solve surface unfolding by using finite elements but not by geometry. This study allowed for this research gap that an approach handling freeform surface flattening based on its geometry was to be found. Cartographic projections such as central projection and area-preserving projections were taken into considerations for planar geometry mapping.

### 1.1.3 3D Shape Knitting

Since the Industrial Revolution, knitting had gained an outburst of increased productivity as the invention and development of knitting machines was started in that period of time (Brackenbury, 1992). The technology of knitting became a popular scope in textile industry. And even if 3D shape knitting machines and technology had not been available yet, the potential of this versatile idea had been realised long before. 3D knitting has become more prevalent since when the development of significant flatbed knitting technology and computer aided design (CAD) system started in mid-1990s (Underwood, 2009). The two world-leading automatic flatbed knitting machine companies who have put effort into 3D shape knitting investigation are Shima Seiki of Japan and Stoll of Germany. Their technical development of 3D seamless knitting is recognised that they are Shima Seiki's WholeGarment® and Stoll's Knit-and-Wear®. However, 3D seamless knitting technology will not be engaged in this study. The idea of seamless knitting is joining the knitted components together in the knitting process in order to eliminate linking afterwards. The 3D form of the end product is actually constructed by the shapes of the knitted components instead of by linking. This statement supports the significance of the aim of the study that is, through 3D data cloud conversion and flattening, the appropriate shapes of knitted components for the corresponding 3D form are determined. Besides, in the CAD system of seamless knitting, it is required to draw the programme of the panels one by one separately that these panels can be referred to the 2D planes suggested in this study. And this study will tell how these 2D planes would be achieved to knit an accurate 3D shape. Therefore, in order to

develop a fundamental theory of 3D knitted shapes reconstruction, double-bed knitting as the weft knitting basic knitting model was considered and double-bed flatbed knitting machines were used as the start for establishing the theory of the study.

The concept of 3D shape knitting refers to constructing a knitted fabric which intimately possesses a solid form when relaxed. Shaping is the basic techniques of knitting elements such as widening and narrowing in a horizontal direction of the flat knitting process. The employment of shaping techniques gives a contour or a form to a knitted fabric. The capability of 3D shape knitting has captured the interest of the field of textile design and technology. It offers enormous opportunities to form knitted constructions. Although certain amount of in depth investigations of 3D shaping control in flatbed knitting had been carried out in the industry, they are not well recorded in the academic field or disclosed to the public due to industrial confidentiality, the top secret of technology investment. Taking Shima Seiki's latest exhibition held in the US in February and May in 2016 as an example, they only exhibited about the new features and improved functions of the new computerised flatbed knitting machine, SRY123LP, the new WholeGarment<sup>®</sup> machine, SWG091N2, and the new SDS-ONE APEX 3D design system, but not any theories or principles in details (Knitting Industry, 2016a & 2016b). Even both Shima Seiki and Stoll have applied many patents for their own techniques, many of them are concerning stabilising knitting with advanced machine setting, 3D design and simulation (Google). For 3D shape knitting, they only mentioned shaping by narrowing and widening, which are the basic shaping techniques, but not how the knitted shape could be controlled. Despite the technical and theoretic details are

closed, it is possible to learn the concept of some kinds of 3D knitting.

WholeGarment<sup>®</sup> of Shima Seiki uses four needle beds and Knit-and-wear<sup>®</sup> of Stoll applies half gauge knitting on a two-needle-bed machine. Both machines associated with corresponding hardware facilitating linking and needle transfer allow 3D seamless knitting. Other efforts on 3D shape include changing loop length and utilisation of knitting structure combinations. But there is not clear explanation of determining the target shape. To make an academic contribution towards 3D knitting technology, this study attempts to fill the research gap with the direction of using a two-needle-bed machine in full gauge to knit the 3D shape in plain knit.

## **1.2 Objectives**

The prime objective of this study was to convert 3D data cloud into a knitted 3D shape. The shaped knitted fabric possessed and reflected the geometric features of the scanned object. This would be further knowledge advancement to recent knitting technology. Furthermore, in the process of this study, relationships between 3D data cloud and flattening, and between loop mapping and 3D knitted shapes were investigated.

Main goal:

- To convert 3D data cloud into a 3D knitted shape

Sub-goal:

- To extract information and measurement from scanned data



- To investigate and develop loop alignment methods to reconstruct the 3D shape
- To examine and to verify the flatbed knitting machine capability to 3D shaping knitting techniques

### **1.3 Statement of Problems**

This study proposed an idea of attaining 3D knitted shapes from scanned 3D data cloud, while some obstacles were raised in the research gap. Despite there are many different projections in cartography for surface flattening, the applications of these are on a sphere, namely the Earth. Besides, a freeform object has one or more types of surfaces in terms of Gaussian curvature. These surfaces can be partitioned into different curvature zones based on their types. Experiments and investigations on each curvature type were carried out separately to tackle the stated problems.

Moreover, the question of how the plane to be executed in knitting was raised. The ultimate concern was to manipulate courses of knitting loops to create a relaxed form with a 3D manner. The construction of weft knitting is a 2D mechanism. A knitting fabric could only be in desired width and length only in terms of structural means, but in depth, neglecting the textural means which was only locally 3D instead of globally 3D. Also it was needed to consider what measurements were critical to the 3D shape knitting and how the relevant information from the 3D data cloud could be extracted. In order to tackle these problems, an investigation framework was proposed.

## 1.4 Theses Framework

This theses framework set out the practical procedures of the research study, in which there were three experimental sections, examining the three types of Gaussian curvature, zero, positive and negative. Each section was for one type and covered both the conversion of 3D data cloud obtained by 3D scanner into a developable plane and the subsequent 3D shape knitting. The experiments were compared and analysed qualitatively and quantitatively, followed with a discussion. This study was organised into 7 chapters and they were: Chapter 1 Introduction; Chapter 2 Literature Review; Chapter 3 Methodology; Chapter 4 Zero Gaussian Curvature, Chapter 5 Positive Gaussian Curvature, Chapter 6 Negative Gaussian Curvature and Chapter 7 Conclusion.

Generally speaking, the first two chapters provided a research direction and existing literary information related to the relationship between 3D data cloud and 3D shape knitting accordingly. Chapter 3 stated a procedure summary of investigating the possibility of the study validation. Chapters 4, 5 and 6 listed out the generic survey and the experimental practice of capturing the three types of Gaussian curvature surfaces and later reconstructing their 3D in knitting. And the last chapter concluded the study and the theory established.

Chapter 1 brought an introduction to the study topic. This first phase was to understand the background knowledge of research direction and provide a general picture of the study.

Importantly the second part (Chapter 2) reviewed the past and present literature regarding to the two areas in this study: conversion of scanned 3D data into a plane; and 3D shape knitting, and it gave further context for the study. For the first area, information from 3D data collection to data cloud processing of 3D developable surface draping; and from geometric features extraction to 3D surface mapping and flattening were examined. For the second area, knitting technology and background were provided to draw the concepts together and studied the basic knitting principles and terminology, including knitting knowledge of knitting calculation and automatic flatbed knitting machine. Also this chapter accentuated the research gaps with regards to 3D data cloud and 3D shape knitting in the literature.

Underpinning the study was a concrete methodology (Chapter 3) which outlined the process of 3D data cloud processing from collection to surface development, and features extraction to surface flattening. Also it included the procedures of experimental investigation of loop mapping, knitting shaping calculation and the 3D shaped knitted fabric. The methodology to be used in this academic study considered the 3D scanning technology, cartography as well as knitting science and technology.

From the frame set for 3D data cloud transformation and 3D shape knitting in Chapter 3, the research experiments and discussions based on the relevant literature reviewed were put into practice from Chapter 4 to Chapter 6. In these three experimental chapters, surfaces with zero, positive and negative Gaussian curvatures were examined respectively, undergoing both the investigation in 3D data cloud

conversion and 3D shape knitting. A target shape of each curvature was used. The surface dimensions of the targets were collected using a portable handheld 3D scanner and shown as data clouds. The 3D discrete data points were processed for later geometric features and measurements registration. The generated developable 3D surface was mapped with triangular mesh and flattened into a 2D plate. The prepared planes were subjected to 3D shape knitting. Dimensional measurement selection method was critical to the 3D knitted shape accuracy. Dimensional information of the plane was attained for loop alignment. Different methods to manipulate loops onto the plane were discussed and a knitting sequence to be developed based on the loop alignment method selected resulted in a knitted fabric with a shape possessing the dimensions of the target object. The 3D shaped fabric was knitted by Shima Seiki SES-122S automatic flatbed knitting machine, assisted with Shima Seiki CAD system, Knit. The finished samples then underwent some necessary finishing treatments which allowed the shape to reconstruct the target 3D. They were then compared and evaluated, qualitatively and quantitatively. Suitable loop alignment methods preserving the target dimensions for particular shapes were concluded.

Chapter 7 was the conclusion of the entire study. The experimental experiences on different types of Gaussian curvature were condensed and summarised. It reinforced the reliability of the theory and established a concrete base for 3D pattern for knitted objects. With the potentiality and versatility of the practice from 3D data cloud to 3D shape knitting, this study would contribute to the advancement in 3D knitting textile technology.

## CHAPTER 2

### LITERATURE REVIEW

This chapter specifies documentation of relevant background knowledge and information to outline and understand the concept of the study. Considering 3D data cloud processing and 3D shape knitting, academic papers, journals, textbooks and correspondent materials subject to these two main directions will be reviewed.

First part is the extent of 3D data cloud and is categorised into following aspects: 3D data acquisition; 3D data processing; Geometric feature recognition; Surface feature extraction; Distortion in flattening; Cartographic surface mapping; Triangular mesh flattening; And a general summary of literature review on 3D data cloud.

The next part is review on 3D shape knitting which involves knitting basis. To be clear, the following extents cover: general knitting principles, knitting terminology, knitting machinery technology, shaping knitting techniques, 3D shape knitting technology and shaping calculation. This part ends with a summary of knitting technologies involved.

#### **2.1 3D Data Cloud**

Various industries, to date, have made use of 3D shape technology in their manufacturing process such as ship hull production, train and aircraft manufactories,

architecture and apparel and shoes industries. There has been an interest and commonness in obtaining shapes in dimensions in recent years. 3D shape data possess dimensional information in 3D and illustrate more complex human intelligence (Liu et al., 2008).

In this part, previous literature related to 3D data will be reviewed, from acquiring 3D data by scanning to processing data from undevelopable points to understandable information; from identification of geometric feature points computationally to selecting meaningful data; from science of dimensional measurement to planar flattening of 3D developable surface for subsequent study on 3D shape knitting of the derived plane. Meanwhile, for clearer understanding on the matter of mapping process from a defined shape to planar projections, cartography has been briefly studied as academic reference to secure in the knowledge of and relations between dimensional transformation and features preservation. Distortions as an inevitable consequence in dimensional transformation are investigated so as to minimise and control the error.

As the ultimate goal of the study is to develop an approach to convert 3D data cloud into knitted 3D shapes, this pure academic research is planned to derive geometric data of any given free form and simultaneously proceed 3D knitted fabrics which possess the same geometric features of the given free form by aligning knitting loops following the theoretic basis attained that is subject to cover the 3D shape.

### 2.1.1 3D Data Acquisition

For the up-to-date technology of capturing a 3D form and geometric features of an object, 3D scanners have an innovative impact and play an important role in digitising and visualising 3D projections. This is the advancement in measurement instruments. It involves modern optical technologies or laser scanning that it is possible to measure dimensions of a form accurately and consistently by capturing a large number of frames of the target from all directions surrounding it (Wang et al., 2007). Comparing to traditional methods such as taking measurements from measuring tape manually, though it can draw an estimated measurement in a short time, 3D scanning technology is more reliable and consistent in terms of accuracy. However, Wang (2007) also suggested that to ensure precision 3D data and quality of images, parameters like system calibration, white balance, stationary of object are to be controlled.

There are several types of 3D scanners that are selected according to the target features or size, including a set of stationary scanning machinery, namely whole body scanner, free-standing scanner and portable handheld scanner. Takes Anthorscan, Artec, BodyShape, Creaform, Cyberware, TC2, Triform and Vitus as some examples of 3D scanner producers and retailers around the world. As the scanning target can be any form of object in this study, the scanner to be used is needed to be capable of scanning any or majority geometric features, size or colours. A portable handheld scanner will be capable to scan object of any size, including those that are bigger than human being.

A 3D optical measurement scanning system involves a light source, while a laser measurement system has a laser emitter instead, sensors and a controller. By operating the scanner throughout the target, geometric features are captured from it and presented as a 3D data cloud. With the advanced auto-framing programme, a 3D digital object is simulated and visualised along with constructed data points. Figure 2.1 shows a demonstration of point cloud of a torus. Before information like measurements and proper flattened plane is generated, these 3D data points are subject to be processed. These data preparation procedures include parameterisation, noise reduction, features identification and extraction and data symbolisation. Previous research will be reviewed in coming sections.

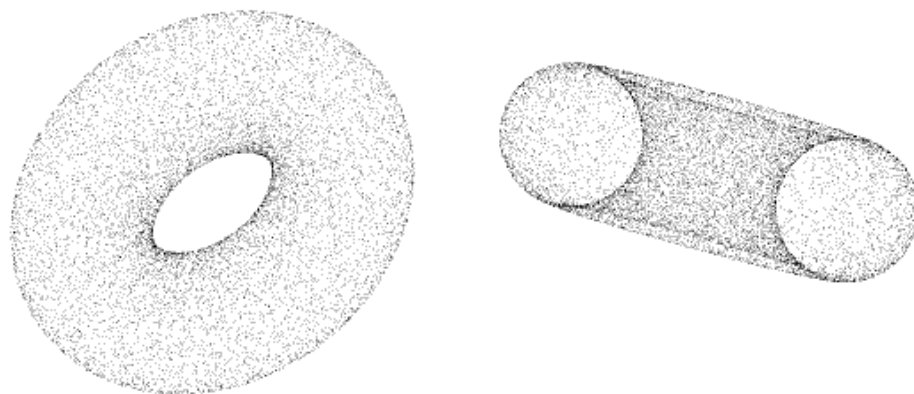


Figure 2.1 3D data cloud of a torus: (left) front view and (right) side view (Kieff, 2012)

### 2.1.2 3D Data Processing

With increasing interest in 3D shape capture technology, there are many researchers taking different approaches of processing scanned data points to become computer-recognisable, and extracting required geometric features and



understandable information from the data cloud, not only visualising the digitised form from scans.

The 3D data cloud attained from scanning is a massive set of discrete data points representing the geometric features of the scanned object. These unreadable points need to be parameterised while those extreme and non-related data points affecting the surface geometry are to be reduced.

Floater (1997) conducted a survey of mesh parameterisation and investigated a linear system graph-theory based parameterisation specially for smooth surface fitting on tessellated surfaces based on convex combination. To enhance Floater's algorithm, Hormann et al. (1999) computed the positions for interior and boundary nodes by a non-linear local optimisation algorithm following local shape preservation criteria. Desbrun et al. (2002) introduced a parameterisation algorithm capable of minimising intrinsic measurement distortion of original mesh while Levy et al. (2002) developed an algorithm of minimising angle deformation. However, both parameterisation algorithms did not consider linear stretch of the surface. To tackle the problem of mesh stretching in parameterisation process, a fast and simple low stretch mesh parameterisation was established by Yoshizawa (2004). And it was improved by introducing a diffusion process which redistributes the local stretches.

Noise presence in 3D data affects the quality and accuracy of information extraction, so some work is needed regarding to noise reduction in data processing. In Leong's journal article in 2007, some measures were introduced to define the useless or missing data points and to eliminate and fill up them respectively.

Bending value method locates cusps of a curve, but if this is not a closed loop, there will be no bending values. Curve fitting and interpolation generates a smoother curve based on low order B-spline functions. Laplace mask shares the same filtering effect as filtering with Euclidian spatial points.

### **2.1.3 Geometric Feature Recognition**

Data points in the 3D data cloud are discretely presenting on the surface of scanned object. Several related work is described to recognise geometric features of the scan as follows,

Osada et al. (2002) suggested the global geometric property D2 shape function as a 3D model with Euclidean distances histograms between any two points on the surface of a shape. But it is not capable of capturing detailed shape properties. Tae (2002) proposed three basic functions to select landmarks of the 3D data which are layer searching function for maximum and minimum girth, width and depth, position searching function for extreme point position and curvature monitoring function for a point of maximum curvature change. Wang (2007) and Leong (2007) presented different algorithms such as Laplace and Sobel masks for detecting features and determining curve properties to identify body landmarks automatically without pre-marking. Leong also defined feature points and feature lines by their respective geometries and the intersection curve of one plane passing through the scanned surface and specific features. However, they focused on only human body instead of all kind of shapes.

Kang et al. (2002) suggested finding the optimal number of sections partitioning horizontally from a scanned figure following the Euclidian distance for identifying features, but Kang only considered human body clustering. Bezdek (1981) and Huang (2011) proposed mathematical approaches, using graphs and matrix, of clustering algorithm by k-means and fuzzy c-means (KFC) and identification of topological difference between data cross sections respectively to define optimal number of clusters.

#### **2.1.4 Surface Feature Extraction**

To extract measurements such as the circumference or the length of the surface features identified in previous step, cross sections or longitudinal sections of the developed surface with defined features are sliced into layers along particular axis or projected into graphs. From 3D data cloud, it is possible to attain information in one, two or three dimensions. However, it is noted that surface feature extraction involves dimension reduction of feature data, from high dimensional data points to a lower dimension (Liu et al., 2008).

Dekker et al. (1999) introduced an automatic measurement system that can indicate landmarks from 3D data by segmentation, but it is limited to anthropometric feature recognition. Vranic et al. (2002) suggested extracting features of an enclosing sphere based on a rendered perspective projection. By extending the concept of a scalar function, namely Reeb-graph, Xiao et al. (2003) developed a topological framework which handled data efficiently. Another work of Xiao et al. (2004) improved the topological framework by employing geodesic. Leong et al.

(2007) proposed an algorithm for automatic body feature extraction by computations in 2D depth space of 3D data cloud. Wang (2007) developed a four-step automated dimension measurement system for digital 3D data, including body segmentation, landmark extraction, clustering and matching. Both algorithms from Leong and Wang, however, focus only on human body features. Liu et al. (2008) proposed a mathematical method of 3D shape retrieval by means of Spherical Healpix projection that could capture and extract main features of a surface.

### **2.1.5 Distortion in Flattening**

It is a fact that geometric distortion exists simultaneously in dimensional transformation and is inevitable. So the surface of a 3D object cannot be expressed completely in a plane without any distortion in terms of lengths, angles and areas according to the Gauss egregium theorem (Carmo 1976), unless the whole surface is in zero Gaussian curvature. So if the surface is isometric, there will not be any distortion in flattening. Criteria are set to decide which of these three parameters to be preserved prior to the others depending on different applications. For example, angle preservation for a map of the Earth for navigation is of higher importance as for practical calculations (Benítez et al., 2004).

Ng (2006a, 2006b, 2006c) derived several mathematical methods for identifying and determining the amount of distortion in distance and area of textile materials from surface to a plane using Stereographic Draping method and bicubic Bezier patch. For textiles, both rigid and flexible materials, covering a surface,

preservation of angles between any three given points are less important than that of areas and distances of them.

Azariadis et al. (2002) developed an energy function that linked geometric distortion to strain energy. Ohsaki et al. (2003) used finite elements to identify tensile distortion energy for architectural purpose.

### **2.1.6 Surface Mapping**

Surface mapping has drawn interest from cartographer and mathematicians for ages and mapping was considered a mathematic discipline in early times (Atchison et al., 2011). According to Lanius (2003), by mathematical definitions, a map refers to “a set of points, lines, and areas all defined both by position with reference to a coordinate system and by their non-spatial attributes”. Therefore, accurate mapping, or projection of a surface, is an important process in surface flattening. Mapping can be carried out by projecting in different manners such as a plane, a cylinder or a cone.

The following projections are some classical projections to be discussed. Gnomonic projection is a kind of central projections. It takes the centre of the sphere as the centre of the projection. However, taking a sphere as an example, this projection can project the surface less than a hemisphere that the great circle of the projecting equator cannot be projected onto the plane infinitely. And it is not conformal, which means it does not preserve angles between curves, and not area-preserving (Polking 2000).

Both Polking (2000) and Benítez (2004) used calculus to prove that the Stereographic projection which is also a kind of central projection is conformal but it does not preserve area. Both the Mercator projection and the Lambert equal-area projection, or called Archimedes projection, preserve surface area and are kinds of cylindrical projection. But only the Mercator projection among two does not have angle distortion.

Apart from cartographic projections, some researches on polygonal finite elements for mapping surface on a plane have been conducted. Tae et al. (1999) utilised quadrilateral meshes to reflect shear fabric behaviour in projection. Tae et al. (2002) applied triangular elements to preserve lengths in projection. Liu et al. (2008) used quadrilaterals of varying shape in equal area to project a sphere onto the Euclidean plane by a Spherical Healpix Extent Function.

### **2.1.7 Surface Mesh Flattening**

Efficient surface flattening is a very important stage in transforming 3D data cloud to a plane. Different approaches discussed below are effort made to minimise surface flattening problems which lead to stretch or extra folds of surface covering materials or distorted or cracked images on planes.

Parida et al. (1993) introduced cuts and overlaps in the plane developed from complex surfaces by cracking and overlapping triangles on the surface to compensate for orientation constrain. But the algorithm suggested might have

calculation errors. Tae et al. (1999) developed a strain reduction method to adjust diagonal distance and edge lengths of quadrilateral meshes. Based on cutting lines, Wang et al. (2002) developed an algorithm using a stretch energy distribution map while Sheffer (2002) and Wang et al. (2004) identified the shortest cutting path. Shaffer et al. (2002) proposed an Angle Based Flattening (ABF) method to minimise angular deformation and further improved ABF to reduce length distortion. However, they have not described methods for preserving surface area. Wang et al. (2004) introduced a woven mesh model, including tendon node mapping (TNM) and diagonal mode mapping (DNM), to minimise length and area distortion between nodes based on geodesic curve algorithm from Kumar et al. (2003) and strain energy minimisation. And this approach defines planar cuts in a natural manner. McCartney and his team (2004) proposed a surface flattening method with the triangulation process by which more triangles in different sizes were used on surfaces with high variable curvature. By applying a combination of surface parting and overlapping, elliptical and hyperbolic shapes are flattened with minimised distortion. This is useful for this study that both positive and negative Gaussian curvature surfaces were examined.

### **2.1.8 Summary**

Current researches and work done about 3D data cloud from data attainment to data processing, and from a not developable surface to a defined planed have been reviewed. To conclude the process, 3D data of a target object is, firstly, attained by using a 3D scanner. Second, data cloud attained is parameterised and processed by identifying the object's geometric features. And the feature information such as

measurements and locations is extracted for the planar development. Then the surface with polygonal mesh developed is flattened under the priority over area preservation to distance preservation. The plane is, finally, ready for subsequent procedures of 3D shape knitting.

## **2.2 3D Knitting**

The ultimate result from 3D data cloud is the 3D shape knitted fabric which is able to cover the target surface captured. The flattened plane mentioned in previous section is critical to 3D shape knitting as flat bed weft knitting is a mechanism which knitting movement carries out in only two dimensions. In other words, knitting cam bringing yarn carriers moves towards left and right only. The relationship between this knitting mechanical constraint and the application of cuts during surface flattening determines the geometry of the outcome, namely 3D knitted shape. Not all the information achieved from the developed plane are applicable to 3D shape knitting since surface measurements and plane measurements obtained are of differences.

In this section, flatbed, or V-bed, weft knitting fundamental information and techniques are reviewed to reinforce background knowledge. Knitting science such as loop length, take down tension of machine to knitted fabric, knitting tension and tightness factor will be discussed to maintain 3D knitting consistency. Different weft knitting theoretic shaping methods and practical shaping researches are reviewed. And shaping calculation for validating 3D shape knitting in practice is



studied. However, related and published studies concerning similar idea of 3D data cloud to 3D shape knitted are very few.

### **2.2.1 Knitting Fundamental**

To understand the significance of this study, it is important to know the mechanism and basic principle of knitting. The literature about flat knitting from Raz in 1991 stated that a certain amount of knitting needles, with a hook and a latch each, are allocated side by side in a knitting machine. As yarn is fed across the machine, adjacent loops are formed in a horizontal row from needle to needle. This statement has clearly pointed out that the mechanism of flatbed weft knitting is a two dimensional movement.

Figure 2.2 shows a demonstration of one unit of successive loop formation. Assembling to definitions of a knitted wale and a knitted course from Raz (1991) and Brackenbury (1992), a wale refers to a vertical row of loops generated by one knitting needle during a continuous knitting sequence while a course refers to a horizontal row of loops produced by a needle after one and the other (Figure 2.3). The cam system of flatbed weft knitting machine allows formation of one course of loop in one knitting cycle, not like circular knitting (Ray 2012). Special features of a double-bed flatbed automatic knitting machine include racked rib structure and loop transfer. Racking in flatbed machines allowing interlock gating and rib gating (Figure 2.4) facilitates these features. Cam carriage bringing yarn carrier, or yarn feeder, feeding with yarn moves on both needle beds.

The term “gauge” in English system refers to the number of needles per inch (npi). The higher the gauge number the knitting machine is, the finer the needles and yarns should be applied, and thus a finer knitted fabric can be produced. The number of loops in a particular area of the knitted fabric describes the fabric density which involves course density and wale density of the fabric. The fabric produced is then drawn downwards from the gap between two needle beds by a comb or take down rollers subsequently.

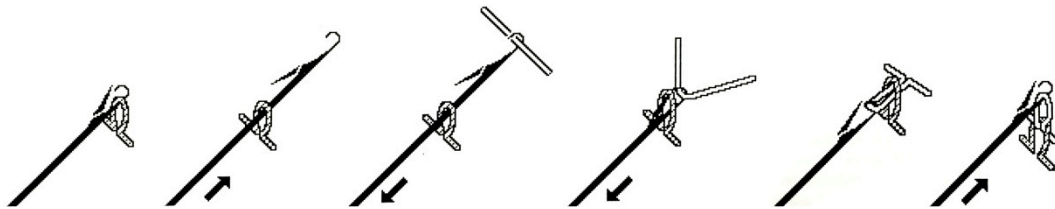


Figure 2.2 Demonstration of a successive loop formation (Raz, 1991)

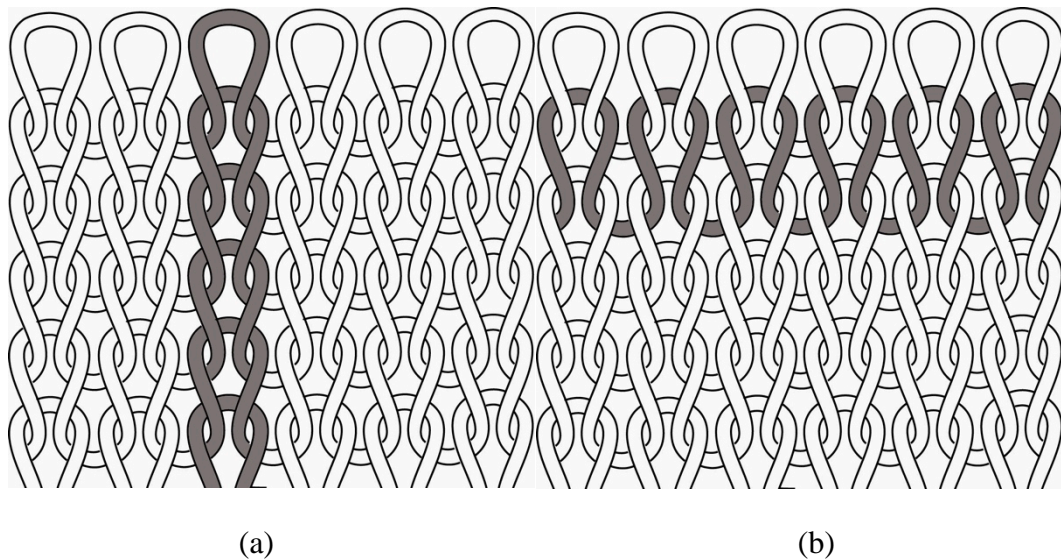


Figure 2.3 An illustration of (a) a single wale and (b) a single course highlighted in a plain knitted fabric

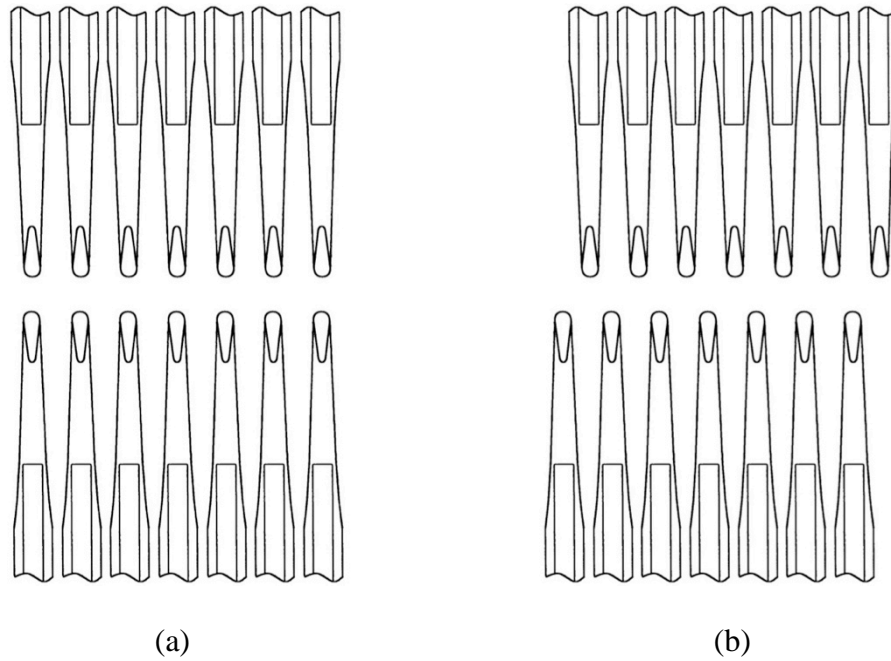


Figure 2.4 Illustration of (a) interlock gating and (b) rib gating of double-bed knitting machine

## 2.2.2 Knitting Science

This section discusses knitting technologies in a scientific way that concerns knitting parameters which alter the consistency of a knitting process. A sample swatch as a control is always prepared before actual knitting process that it consists of useful information to be followed. This quantified information determining the quality of fabric directly focuses mainly on fabric density which refers to loop length and knitting tension. Take down tension and tightness factor are also knitting constants to be controlled for the knitting consistency.

### 2.2.2.1 Loop Length

Knitting science studies the mechanism of loop formation. The dimensional properties of a knitted fabric are governed by two most important input parameters, namely loop length and loop shape in relaxed state. The shape of a loop is built after relaxation of a knitted fabric. It is also related to yarn properties, finishing treatment to the fabric and knitting structure. There is sometimes requiring more than one complete loop to configure a knitted structure and to define a repeating unit, a term is given for this knitted structure, which is structural knitted cell (SKC). The relationship between fabric dimension and loop length influences the behaviour of a knitted structure. However, combinations of stitches are not the focus of this study in which only simple plain knit is considered to be the basic knitting unit. So loop shape can be neglect and the length of a loop becomes the main parameter to knitted fabric fundamental to be concerned. Loop length is set during loop formation and depends on the knitting machine setting.

Loop length is classified into two types, theoretical loop length and actual loop length (Ray, 2012). Theoretical loop length is the length calculation obtained from machine gauge and stitch cam setting. The distance gap in centimetres between two sinkers can be measured by Equation (1).

$$w = 2.54 \times [ 1 / (\text{gauge number})] \quad (1)$$

And ‘*h*’ represents the depth of needle position in between the sinkers pulling down the yarn. Theoretical loop length ( $l_t$ ) is then being expressed in Equation (2). Figure 2.5 explains the loop configuration.

$$l_t = 2 \times (w^2 + h^2)^{0.5} \quad (2)$$

Actual loop length ( $l_a$ ) is the loop measurement taken from a knit down. But directly measuring a tiny single loop is difficult. To make it relatively efficient and accurate, a yarn unwinding method is used that a certain amount of loops on the same course, 100 wales for example, is marked and unravelled. By straightening the crimps presented in the yarn without stretching it, the length of that amount of loops, namely course length, is then easily measured. And the length of one single loop can be calculated afterwards by Equation (3).

$$l_a = (\text{Course length}) / (\text{number of loops}) \quad (3)$$

Nevertheless, there is significant difference between two types of loop lengths. This can be explained by presence of the action of robbing back which is not considered merely in theoretical loop length.

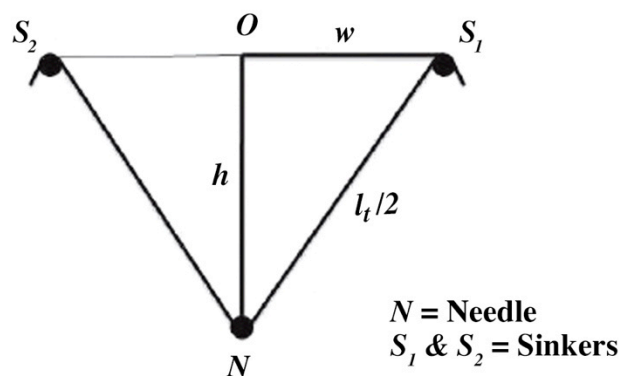


Figure 2.5 Illustration of loop configuration for calculation

### 2.2.2.2 Tightness Factor

Loop length has a direct relation to the tightness factor (TF) of a knitted fabric. TF is a relative tension ratio of area one loop occupied to area an actual loop occupied. In other words, it refers to the relationship between yarn count and loop length.

In Tex system, where TF is tightness factor, Tex is Tex count and  $l_a$  is actual loop length in millimetres.

$$TF = (\text{Tex})^{0.5} / l_a \quad (4)$$

In English system, where N is English count,

$$TF = 1 / (N^{0.5} \times l_a) \quad (5)$$

### 2.2.2.3 Fabric Density

Apart from loop length and tightness factor, another parameter is used to qualify a knitted fabric, namely stitch density. Stitch density is the total number of knitted loops, or called needle loops, in a measured area of a fabric. It is a multiplier of course number and wale number (Spencer, 2001). Course number and wale number are the linear density measurements of a knitted fabric. They are recorded as course per centimetre (cpc) or per inch (cpi) and wales per centimetre (wpc) or per inch (wpi) respectively.

#### **2.2.2.4 Fabric Take Down**

Fabric take-down allows successive formation of knitted loops in a course by applying take-down tension to the fabric produced, preventing the previous loops from riding up with the ascending needle (Raz, 1991 and Ray, 2012). Otherwise, new loops cannot be formed when needle hooks have not been cleared. To prevent it, take down comb and rollers are equipped in a computerised knitting machine. The comb is firstly subject to the first course of knitted fabric and pulls down it until reaches beyond fabric rollers, which then grab the fabric on both front side and back side and withdraw the fabric by continuous rolling. Sub-rollers are small rollers between the needle beds and fabric rollers to facilitate the take down action. The take down mechanism also manipulates collection fabric produced and maintains a constant fabric length. The force, namely take down tension, applied to the fabric downwards contributes to a constant loop length. In general, higher the take down tension applies, longer the loop length possesses, unless too high tension breaks the yarn.

Nonetheless, loop length, stitch density and take down tension affect the dimensions of knitted fabric, a 3D knitted shape, to be clear, depends on the loop-oriented alignment while these input parameters should be monitored to keep it consistent. This will be discussed in detail in Chapter 4.

### **2.2.3 Shaping Methods**

To change dimensions of a knitted fabric, shaping as a unique characteristic of weft knitting is involved. Movements of knitted loops reduce or increase the number of wales to be knitted, namely fashioning, so as to narrow or widen the knitted fabrics along the courses. Narrowing and widening allow for knitting according to required shape, though there are limitations of needle movement. Loop transfer, the special ability of double-bed flatbed knitting machines, is one of the ways capable to shaping. Pushing needle method for outside widening, binding off for casting off a series of loops securely and partial knit for changing dimensions will be discussed in this section.

Loop transfer does not involve loop formation. It is a knitting technique that transfers loops from one needle in one needle bed to the other needle in the opposite needle bed. With this mechanism and assisting with racking of needle bed, loops can be transfer in the same bed in two transfer operations. First, a loop is transferred to the nearest empty needle located in the opposite needle bed in interlock gating. Then the needle bed is racked sideways by required needle space, depending on the how many needles to be reduced or added. The loop is transferred again to a needle in the original needle bed.

For narrowing, both inside and outside narrowing involve loop overlapping and this loop arrangement leads to a fashioning mark. In inside widening, a hole is formed as a loop is transferred to the adjacent needle (Figure 2.6). This can be solved by application of a tuck, a split stitch or retaining a previous loop when only one-needle hole appears. So if to prevent holes formed by adjacent multi-needle widening, it should be controlled to one needle or single needle in separate wales



only. By loop transferring, the vertical look of a wale is deformed and the width of fabric is changed.

Outside widening is executed by introducing a needle next to the selvedge during knitting and thus an additional successive loop is formed on the edge. Due to knitting constraint, only one needle is added along a course each time. By this way of widening, there will not be any obvious marks on the fabric.

Binding off is a knitting process which moves a loop to the next loop sequentially from the edge (Choi et al., 2008). It is a combination of loop transfer and racking and it can narrow down a course by more than one needle loop, yet preventing unravel of loops. It is also a utilisation of edge finishing. Choi and his team (2014) investigated the tensile strength and elongation of different methods of binding off but had not point out any shaping difference or influence.

Traditional shaping methods for flatbed weft knitting usually contemplate shaping in two dimensions only, by controlling the horizontal measurement, namely wale shaping. For 3D shaping, partial knitting, which is capable of knitting in three dimensions as course shaping, could be used. It is a knitting technique but not special knitting structures. It is a process of knitting a selected range of needles while holding the unselected loops in place. Tuck stitch is usually applied to fill the holes developed simultaneously and which gives a mark on the appearance of the fabric. In this way, the perpendicular order of course number and wale number is altered, and thus the knitted fabric is allowed to grow in three dimensions. However, in terms of 3D knitting, partial knitting is mostly applied in 3D textural structures

concerning different stitch constructions (Blaga et al., 2011). Cai and Guo's research (2014) used partial knitting to produce novelty stitches, flares and ruffles. Ray (2012) and Ma et al. (2013) suggested different methods to achieve 3D knitted shapes such as course shaping, wale shaping, combination of stitches or yarns, changing knitting parameters or application of cut-and-sewn. But most of these methods were not suitable for this study. Besides, Ma had not proposed a concrete algorithm of partial knitting control for a particular 3D shape after all. Partial knitting was widely used in seamless knitting to produce garments though seamless knitting was excluded in this study. Shima Seiki launched its new WholeGarment® machine to produce athletic performance apparels, gloves and socks (Stitch World, 2015).

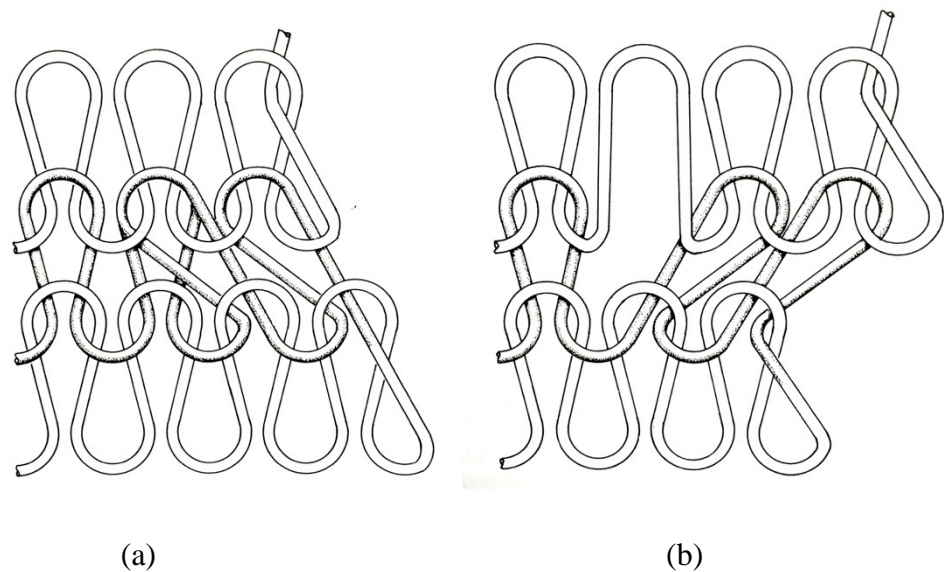


Figure 2.6 Illustration of (a) loop overlapping in inside narrowing and (b) hole formation in inside widening.

#### 2.2.4 Knitted 3D Shapes

There were several researches about course shaping, namely partial knitting, applications and few about knitting 3D shapes by using 2-needle-bed knitting machines from 3D data. Research from Ma and Lamar (2013) talked about partial knitting as a shaping method to produce 3D shapes without a seam as in cut and sewn. Huang et al. (2007) used some statistic measures to generate desirable knitted shape of a particular area from collected 3D scanning data. But the outcome of knitted shape was in two dimensions. In knitwear design, partial knitting was also used to achieve flare, bell-shaped and asymmetric hems (Yang and Mao, 2009; Xu et al., 2011; Radvan, 2013). Yang and Mao (2009) and Xu et al. (2011) investigated partial knitting applications but no application control or attainment of target shape was suggested. In Matković's (2010), bishops' gloves from the 12<sup>th</sup> century and stockings from the 19<sup>th</sup> century were displayed and the shape of them were achieved by partial knitting though their final shapes were flat and in 2D. Research by Hills (1989) mentioned the first stocking frame that it was able to carry out course shaping to create the shape of 2D stockings. Partial knitting was also used to achieve locally 3D texture on a knitted fabric. Pan et al. (2009) suggested ideas of 3D knitting but only focused on textural 3D effects. Tatsushi et al. (1998) proposed a method of generating knitted fabric shape which covered a shape and is represented by mesh. However, this method only followed the shape of the fabric draped onto the object surface that it was not knitting exactly the object shape. Song, Wu and Wei (2006) suggested a computational method with mathematical models based on the principle of 3D knitting. Partial knitting was applied to create the forms of hemisphere, tubes, cones and cuboids but their mathematical models could only be applied to these

particular shapes only. It did not cover the making up of the pattern. And there was not any relation with scanned 3D data. Belcastro (2009) also suggested a mathematical method to knit surfaces such as a sphere and a torus but it was only a pattern to produce knitted shapes with knitting techniques such as partial knitting, not a method to produce accurate size and form of the shape. McCann et al. (2016) also suggested knitting patterns to produce knitted shape in 3D forms such as clothes for dolls, knitted snakes and robots. To achieve these shapes, partial knitting was applied but not a method to produce accurate shapes. Igarashi et al. (2008) proposed a 3D knitting model that converted 3D mesh into 3D hand-knitted shapes. Nonetheless, the method of parallel winding strips as knitting pattern instructions would induce 3D shape distortion when using flatbed weft knitting. Two recent researches used 3D data to knit 3D garments by using seamless knitting (Mahbub et al., 2014 & Maghrabi et al., 2015). First, seamless knitting was not considered in this study. Second, since they were making garments, ease allowance was added to the product. Inestimable error in fitting would then be induced as the knitted fabric draped. Although course shaping was used to knit the shape of the bust part, the fitting assessment was subjective. Also, in Maghrabi et al.'s research (2015), horizontal measurements taken by TC<sup>2</sup> were used which were 3D parallel measurements. Using this kind of measurements in weft knitting would induce shape distortion. Explanations would be found in Section 5.

### **2.2.5 Shaping Calculation**

To plan the shaping operations accurately, some knitting calculations are required. Before the curves can be calculated, some basic measurements such as

fabric width and fabric length must be obtained first. With the width ( $W_{cm}$  or  $W_{inch}$ ) required and wale spacing which is wales per centimetre (wpc) or wales per inch (wpi), the number of wales can be calculated as follows,

$$\text{No. of wales} = W_{cm} \times \text{wpc} \quad \text{or} \quad \text{No. of wales} = W_{inch} \times \text{wpi} \quad (6)$$

The resulting number is the number of needles to be selected and loops to be formed to compose the fabric width. The number of course calculation follows the same concept.

$$\text{No. of courses} = L_{cm} \times \text{cpc} \quad \text{or} \quad \text{No. of courses} = L_{inch} \times \text{cpi} \quad (7)$$

Where  $L_{cm}$  = fabric length in centimetre and  $L_{inch}$  = fabric length in inch  
 cpc = courses per centimetre and cpi = courses per inch

When the loop length and wale and course spacing is fixed, the fabric width and length are depending on the number of wales and courses. Hence, more wales produce a wider fabric while more course a longer.

As wales and courses are straight lines of successive loops, this knitting constraint restricted the vertical and horizontal dimensions of a knitted fabric. To knit a curved edge, the curve is divided into several diagonal straight lines so as to calculate the number of wales and courses involved using the right angle triangle theory in each diagonal line section. Brackenbury (1992) mentioned that the max fashioning frequency in every two courses is two loops. This follows the order 1:1.3

of courses per unit length to wales per unit length. However, this theory of “normal ratio” is no longer a guideline for this study as the present computerised knitting machines allow loop transfer by 3 or 4 loops with appropriate knitting setup and technique. Also, this guideline is for preparing an estimated knitting shape. This study is in a different direction that it tries to capture the actual shape of object by scanning and knits the actual shape instead of estimates the shape under the guidelines.

Following equations explain the calculation of fashioning frequency of a knitted fabric.

$$\text{Freq.} = C / F \quad (8)$$

Where Freq. = Fashioning frequency,

C = number of courses in a fashioning section

F = number of fashioning

As the first and last course should be applied a fashioning if any, the equation should be modified to Equation (9).

$$\text{Freq.} = C / (F + 1) \quad (9)$$

### 2.2.6 Summary

The literatures provide concrete basic knowledge of knitting technology fundamentals. Loop consistency by maintaining equal loop length and regular knitting structure is the important criteria to quality control in knitting. Accurate knitting calculation and appropriate knitting machinery setup allows better knitting performance. By controlling these knitting parameters, knitting errors can be minimised to acceptable range. And the recent research focusing on 3D knitted shapes suggests some research gaps to be considered. The utilisation of combining partial knitting and wales shaping possess great potential in 3D shape knitting but yet its performance control needs to be investigated and managed. Upon the background information, the development of 3D shape knitting has a clearer direction and the trace of 3D data cloud conversion to knits to follow.

## CHAPTER 3

### METHODOLOGY

To develop a possible algorithm that was able to convert 3D data cloud of a target freeform object into a 3D knitted shape, a series of actions covering surfaces with all three types of Gaussian curvature was planned. Each type of surfaces followed the procedures concerning the two areas mentioned, 3D data cloud conversion and 3D shape knitting. Figure 3.1 described the framework of the study methodology.

The surface of an object could be divided into three types of curvatures based on the principle of Gaussian curvature. By zoning the surface according to its curvature type, the atlases of the surface obtained were studied separately. To complete an approach for free forms, surfaces with three different objects with zero, positive and negative Gaussian curvature were examined in order to cover all possibilities of a freeform object in the according sequence. Experiments of each type were carried out for three times repeatedly to ensure an accurate and precise result.

The first part of the procedures concerned 3D data cloud conversion. The 3D surface was captured and processed before it was being flattened into a 2D plane compatible with the knitting process. Knitting loops were manipulated onto the plane and a knitting sequence was then developed based on the loop alignment method used. The finished knitted fabrics were linked and were subjected to post-



treatments to resume the target 3D.

To judge the 3D knitted shape accuracy, qualitative and quantitative evaluations were carried out. For assessing the dimensions of a drapery knitted shape, it was put onto the target object for comparison. The contour and appearance of the shape were examined visually and the loop density was also measured. It was believed that if the knitted shape possessed the same dimensions of the target, there shall not be folds, bumps or stretched loops on its surface.

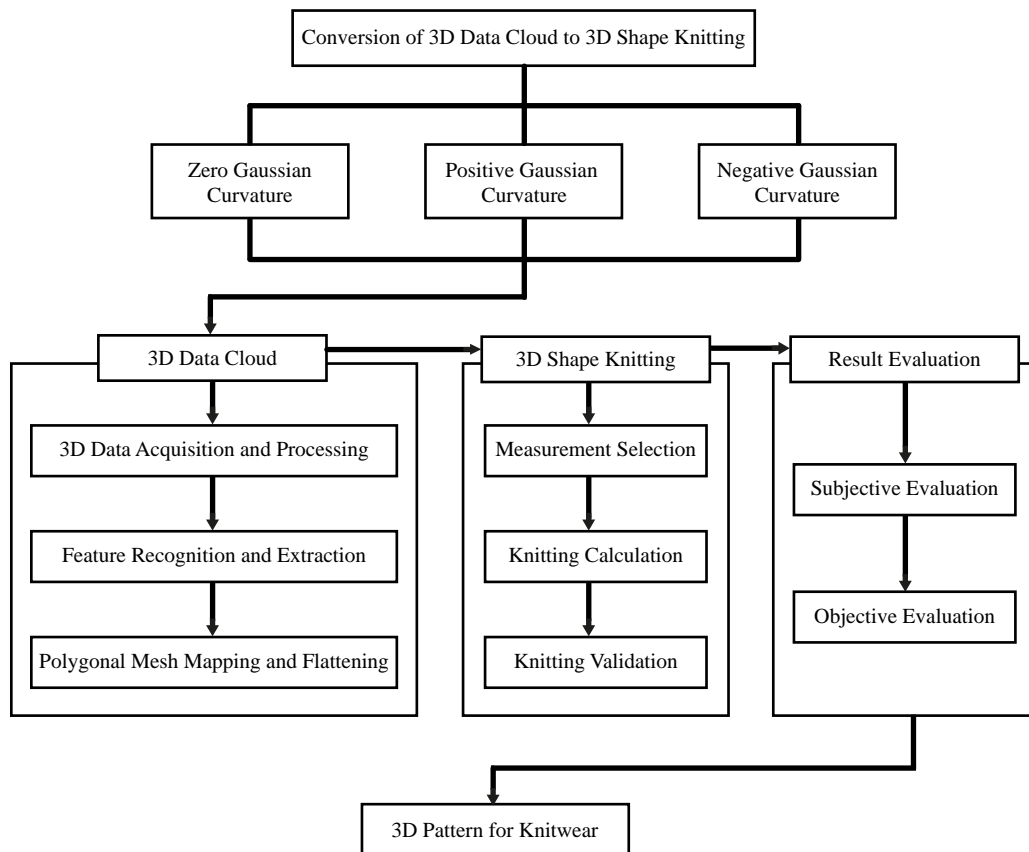


Figure 3.1 Framework of the study methodology

### **3.1 3D Data Cloud Conversion**

At first, the target object geometrical features were captured by a handheld 3D scanner. The data cloud underwent a series of data processing and its features were recognised and extracted. The 3D surface was mapped with polygonal mesh and flattened into a 2D plane.

#### **3.1.1 3D Data Acquisition and Processing**

First of all, a selected object was scanned by a portable 3D scanner, Artec Eva handheld 3D scanner (Figure 3.2.) The geometric data of the object was captured, shown as a 3D data cloud that performed the digitised appearance of the object with unreadable information and possessed discrete points in an undeveloped structure. The 3D data cloud was processed with the aid of Artec Studio 9 CAD system, by which failed frames and data points were filtered out, noise was reduced and the axis was rotated to a proper position, so that it was ready for later geometric features recognition.

A handheld scanner allowed for capturing objects in any size and shape anywhere, but the accuracy of data depends on the skill level of the operator and the immobility of the target. The higher the quality of 3D data cloud attained, the easier and faster the processing effort was required.



Figure 3.2 Side view of Artec Eva handheld 3D scanner

### 3.1.2 Feature Recognition and Extraction

Since the local Cartesian coordinates of the 3D data cloud attained might not be aligned at the same direction as that of the actual target possesses due to the manual scanning operation, correcting the orientation of axis of the whole data cloud was important to the accuracy of the later feature recognition and extraction. The discrete data points were connected based on Cubic Bezier Curve so as to drape a continuous 3D surface. Features of free forms could be very different from others. So features recognition techniques such as Sobel mask, Laplace mask, bending value method and curve fitting and interpolation from the research of Leong and his team (2007) were used to identify possible vertexes and extreme points, reduce noise reduction, define change of curvature and generate smooth curve respectively. Feature landmarks or structure lines were also drawn to define the working surface

area and carry out necessary geometric segmentation. And so cross-sectional area, circumference and any other geometric information of the target could be established and measured.

### **3.1.3 Polygonal Mesh Mapping and Flattening**

Considering the use of the 2D plane to be flattened as for subsequent loop alignment, area preservation in surface flattening as in cartography was applied. The approach of applying triangular mesh to the 3D surface is referencing to the triangulation method of McCartney and his team (2004). An equal sized polygonal mesh was mapped on the surface in initial and the triangles were divided into smaller ones to manipulate the high-energy concentration areas where there was severe curvature change. This subdivision process minimised the area-preserving error. Figure 3.3 showed the process of the triangle subdivision.

In flattening, surface of an elliptical shape splits at the sides while that of a hyperbolic shape overlaps according to McCartney et al.'s research. In this study, cuts and folds were inserted to places where were under strain and stretch in the area-preserving flattening process. Specific placement of cuts and folds were discussed in different experimental sections.

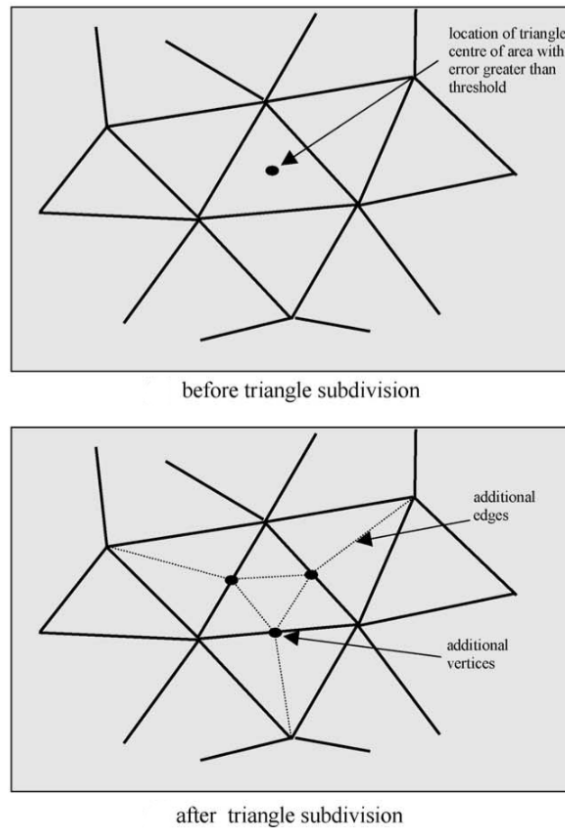


Figure 3.3 Triangle subdivision process proposed and illustrated by McCartney and his team (2004)

### 3.2 3D Shape Knitting

In this part, an idea of critical importance to this study that how loop alignment on the 2D plane reconstructs the target 3D was introduced. The knitting loops were aligned based on the measurement taking method of the flattened plane. Different loop alignment methods were proposed.

To start with, a reference knitted swatch was firstly produced. This swatch provides loop density references, including loop length, course per centimetre (cpc) and wale per centimetre (wpc), for working the knitting sequence. Knitting process

in 12 gauge was carried out after the knitting programme was designed. The finished knitted fabrics underwent necessary post-treatments including linking and fabric relaxation to resume the target dimensions. Sampling was repeated three times to ensure experimental accuracy and consistency.

### **3.2.1 Loop Alignment**

Before measurement of the flattened plane can be taken, the ways to determine what and how dimensional information to be collected were decided. There were two loop alignment methods proposed in this study. One is loop alignment following the 3D horizontal straight lines, as the same idea of parallels of latitude in cartography, while the other one is based on the 2D horizontal straight lines. The knitting loops were manipulated following the directions and the pathways of measurements. They were elaborated in details in the section of positive Gaussian curvature, Chapter 5.

To reconstruct the 3D shape, shaping knitting techniques were applied. For specific cases, partial knitting was used to facilitate knitting a continuous fabric. With the reference to the loop density of the reference swatch prepared initially, a knitting sequence was prepared based on the loop alignment method used. Knitting errors and limitations were also discussed.

### **3.2.2 Knitting Validation**

A knitting programme was designed based on the compiled knitting sequence using Shima Seiki's SDS-ONE APEX 3 CAD system. Knitting was carried out with the Shima Seiki SES-122S flat bed automatic knitting machine in 12 gauge. One end of 2/30 Nm 100% Merino Wool yarn was used for the 12 gauge knitting setup. To be consistent and accurate, the knitting machinery setting such as stitch length and take down tension should be taken under control. A trial was made before actual sampling to double check if the machine setting was correct. One hundred (100) wales of the trial were unvalued to make sure the loop length was the same as the reference swatch. And after that, the actual knitted fabrics were linked and underwent relaxation to reconstruct their natural 3D shapes from deformation. The post-treatments were carried out in standard room temperature and pressure. The wetted knitted shapes in 30°C warm water for 10 minutes were dehydrated and tumble dried with 1 kilogram (KG) dummy fabrics for enough agitation for 30 minutes. The finished shapes were steamed and laying flat for two days before evaluation for dry relaxation.

### **3.3 Result Evaluation**

The finished knitted shapes possessing the target 3D were subject to evaluation. Their appearances and loop density, cpc and wpc, were judged and compared qualitatively and quantitatively respectively. Although qualitative analysis is less consistent than quantitative analysis that its result may vary from

person to person, both kinds of evaluation methods are important to the study that each tackles different shape accuracy characteristics.

Before evaluating the 3D shape, the knitted shape was firstly measured its loop density when relaxed. These values of the shape lying freely on a surface were the evidence of correct machinery setting. The criteria of assessing a 3D knitted shape accuracy was based on its fitting, appearance and smoothness of seams when it was put onto the target object for visual comparison. A 3D knitted shape with the appearance of extra folds, bumps, stretched loops or wavy seams was defined as not in accurate dimensions. The knitted shape was also scanned and its geometry of the digital image was compared with that of the target object. For the quantitative evaluation with 95% confidence level, the loop density difference tolerance of the knitted shape comparing with the reference swatch was set to  $\pm 5\%$ . A shape with more than  $\pm 5\%$  loop density difference was considered possessing an inaccurate 3D shape. Loop density of three different interior points' regions of each knitted shape was measured to ensure result accuracy, without the inclusion of boundary points. As measuring cpc is carried out along a wale, the three regions were located in the front, either side and back for each sample. And for measuring wpc along a course, the three regions were located on the top, middle and bottom.

### **3.4 Conclusion**

This generic study aimed at converting 3D data cloud directly into 3D knitted shape. The process involved would contribute to academic advancement that the relationship between 3D data and knitting was investigated. A complete procedure



from 3D data cloud to a 2D plane development and from planar loop alignment to successive 3D knitting process was proposed. All three kinds of Gaussian curvature surfaces were examined to establish a concrete theoretic basis for freeform shapes.

As it involved two areas for each experimental section, 3D data cloud conversion and 3D shape knitting, there were many parameters that could alter the final outcome. It was important to control and minimise unwanted parameter changes throughout the process. Experimental consistency allowed higher accuracy and certainty to the algorithm and, hence, better quality of the study.

Moreover, this study enhanced the utilisation of 3D data of freeform objects that based on the Gaussian curvature. Experiments were repeated to investigate various surfaces. Different degrees of Gaussian curvature were entertained in surface flattening with distortions controlled. And all planes attained must be flattened following the knitting constraint.

Furthermore, it was of an utmost importance to determine which planar measurements were useful to 3D knitting. This was the key to establish knitting loops alignment to reconstruct a 3D form. With the proper area-preserving planar flattening method and loop alignment method, 3D pattern for knitted objects could be estimated and controlled.

## CHAPTER 4

### ZERO GAUSSIAN CURVATURE

In this first experimental section, a surface with zero Gaussian curvature was put to tests, undergoing the process of both 3D data cloud conversion and 3D shape knitting. A spinning cone was selected as the target object. Figure 4.1 showed a digital image of the cone with a surface with a constant curvature to be used indicated in yellow. According to the Gauss egregium theorem (1976), a surface with zero Gaussian curvature can be flattened without distortion in distances, areas and angles. So the 3D surface in yellow selected from the scan was directly unfolded with the area preserved. The flattened 2D plane was then aligned with loops based on the planar dimensions.



Figure 4.1 A digital image of the shape with a surface with zero Gaussian curvature indicated in yellow

## **4.1 3D Data Cloud Conversion**

This part recorded and discussed the procedure of converting the 3D data cloud of a surface with zero Gaussian curvature into a 2D plane. It involved mainly three stages, 3D data acquisition and processing, feature recognition and extraction, and polygonal mesh mapping and flattening.

### **4.1.1 3D Data Acquisition and Processing**

To capture and digitise the geometry of the selected cone, Artec Eva handheld 3D scanner was used. It was an optical measurement 3D scanner that projected visible lights and captures maximum sixteen frames in a second. Figure 4.2 indicated the position of the light emitters and cameras of Artec Eva. The frames were aligned in real time to form a precise single image of the scanned object in an ideal case. In practical, to operate a handheld scanner required some operating skills. The light emitters must be pointing perpendicularly to the target surface wherever and whenever scanning was processing. The scanning distance limitation of Artec Eva was 50 cm to 100 cm. From all angles it must be scanned to attain a full image of the target.

As the starting point and the starting angel from the centre of the gravity of the target varied every time, the xyz-axis location and direction might differ, resulting in poor alignment of the local Cartesian Coordinates System of the data cloud. Figure 4.3 showed a demonstration of the 3D data cloud of the target with a lopsided polar coordinate using an Artec Eva handheld scanner. This was different

from stationary 3D scanners by which the scanning image was standing upright as the scanned target. However, this kind of scanners could only cope with objects with limited size or registered features. By contrast, handheld scanners had more advantages in target options. Despite the fact that it had more flexibility in scanning, the 3D data cloud attained needed further realignment to tune back the correct position the same as the target.

During scanning, the object must be set still to prevent resonant noise. Upon this concern, dead objects were easier to be handled while live objects had fail images such as incompatible frames easily. To keep scanning data consistent in scanning of targets for later comparison, setting and positioning of the scanning target was required to remain the same. In this case, resonant noise was minimised as the cone used was a dead object.

Figure 4.4 showed an image during scanning. The box underneath was for holding the scanning target and giving different dimensions to the sensor for easier target tracking, though the data of the box was useless to the study and was removed later on. After scanning, a large number of frames were captured. The attained 3D data cloud was brought to preliminary data processing using Artec Studio 9.0 CAD programme. Incompatible frames were separated and realigned with the base image. Frames that failed realignment were removed. With the assistance of this CAD programme, useless data points of unrelated objects, namely general noise, for example the table or floor under the object, contained in frames were filtered. An image of the scan with noise and unrelated data was shown in Figure 4.5. Small amount of missing data in the same area appears as a hole in the image while large

amount of missing data shows unfinished image. The later one, hence, required rescanning.

Holes were filled with the aid of CAD system. However, there was still noise of unwanted data points present in the data cloud but they were not easily noticed in the CAD system. It required an effort of more precise data processing in later stage. After preliminary noise elimination and holes filling, the position of the data cloud was checked. Rotation of xyz-axis was carried out when the data cloud was not standing upright as the real object. The processed data points were saved in stl format. Figure 4.6 showed a processed 3D data cloud of the cone.

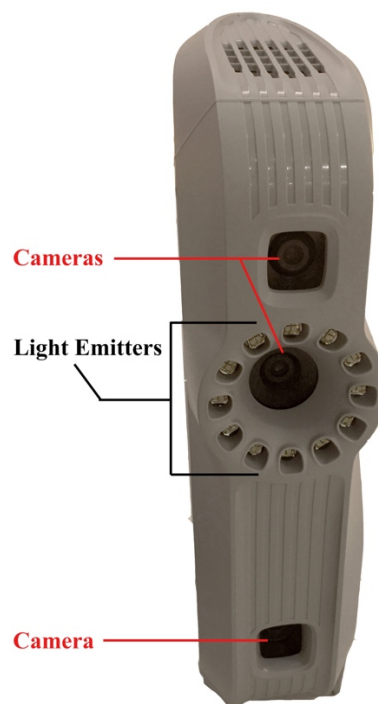


Figure 4.2 Front view of Artec Eva handheld 3D scanner with indications

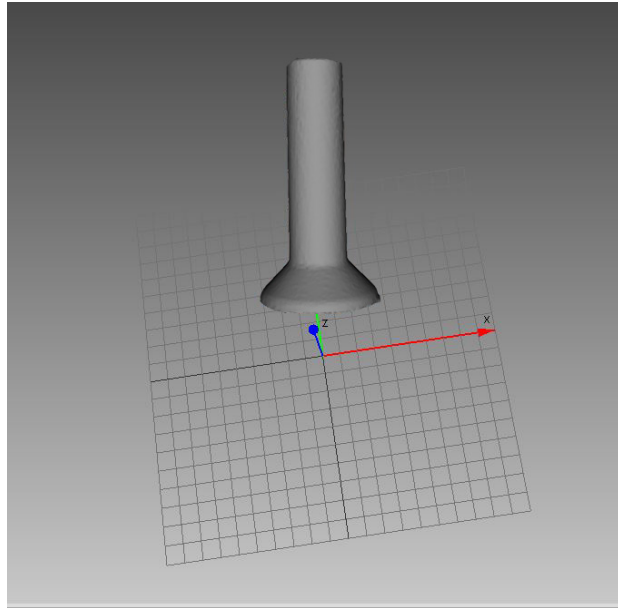


Figure 4.3 Demonstration of the 3D data cloud of the target with a lopsided polar coordinate using an Artec Eva handheld scanner



Figure 4.4 An image of proceeding scanning

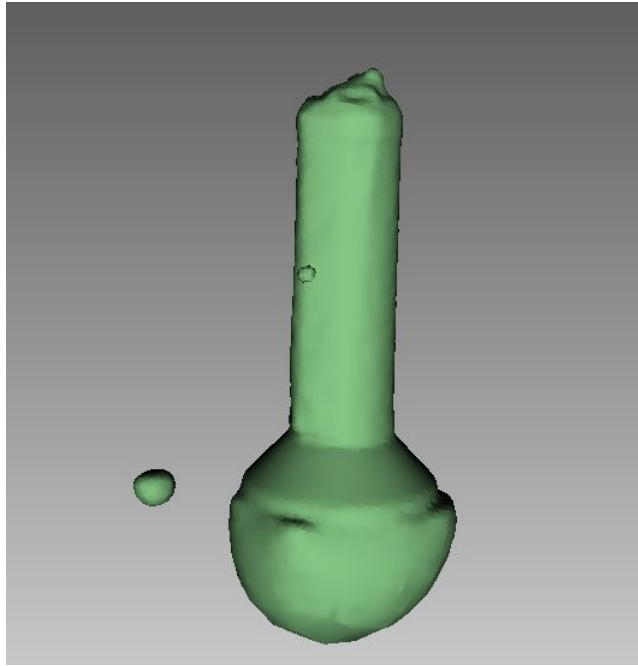


Figure 4.5 An image of the scan with noise and unrelated data

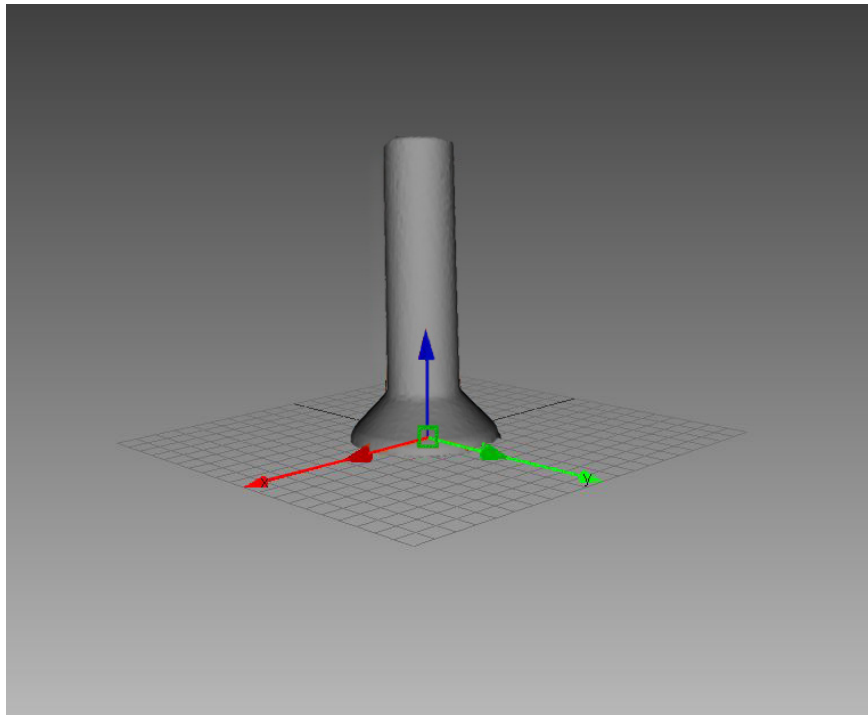


Figure 4.6 An image of the data cloud after preliminary processing

### **4.1.2 Feature Recognition and Extraction**

Before scanning, the cone was marked with marking tape to locate the top edge of the surface to be worked on. The geometry of the tape on the cone surface was recorded in scanning though it was small. Therefore, from the data cloud, it should be able to recognise the target surface, indicated in yellow in Figure 4.1. By referencing the features recognition method suggested in the research of Leong and his team (2007), the noise on the cloud surface was filtered out by using the Laplace mask. The cutting planes of the target surface top and bottom were defined by using the Sobel mask and the bending value method. The surface area between the two cutting planes was the experimental surface with zero Gaussian curvature. This area was selected and was subject to next stage for mapping and flattening.

### **4.1.3 Polygonal Mesh Mapping and Flattening**

The surface was draped with a polygonal mesh on the target surface using the method proposed by McCartney and his team (2004). Regions that had a larger curvature change were covered with more and smaller triangles to minimise error between the target surface and the mesh. From the triangle subdivision process (Figure 3.3), a triangle was divided into 4 smaller triangles with its centre point remaining the same as the centre point of the smaller triangle in the centre to minimise errors in higher curvature vales. Considering the optimisation of the mesh unit size, the smallest triangle size must be related to a knitting unit. Therefore, the size of a knitting unit was obtained from a reference fabric swatch which determines



the loop density to be used in the following experiments, more explanation of the reference swatch was in Section 4.2.1.

Given the loop density values,

Course per cm (cpc) = 8.928571, and

Wale per cm (wpc) = 6.56168

$$\begin{aligned} \text{The length of a knitting unit} &= 1 / 8.928571 \\ &= 0.1120 \text{ cm} \end{aligned}$$

$$\begin{aligned} \text{The width of a knitting unit} &= 1 / 6.56168 \\ &= 0.1524 \text{ cm} \end{aligned}$$

$$\begin{aligned} \text{The area of a knitting unit} &= 0.1120 \times 0.1524 \\ &= 0.0170688 \text{ cm}^2 \end{aligned}$$

By dividing a knitting unit by half to form a triangle,

$$\begin{aligned} \text{The area of a triangle} &= 0.0170688 / 2 \\ &= 0.0085344 \text{ cm}^2 \\ &= 85.344 \mu\text{m}^2 \end{aligned}$$

So the area of the smallest triangle of the mesh generation = 85.344  $\mu\text{m}^2$

By considering a triangle unit was divided into four smaller ones in the subdivision process,

$$\begin{aligned} \text{The area of the biggest triangle of the mesh generation} &= 85.344 \times 4 \\ &= 341.376 \mu\text{m}^2 \end{aligned}$$

Therefore, the size the triangles for mesh generation in this study was in the range of  $85.344 \mu\text{m}^2$  to  $341.376 \mu\text{m}^2$ .

In this case, the target surface with a constant zero Gaussian curvature had no curvature change at all. And due to its curvature property, it can be flattened without any dimensional distortion. The surface area was preserved. The surface was unfolded and flattened with a cut perpendicular to the bottom line. Figure 4.7 showed the flattened 2D plane. As the surface was a slightly conical shape, the flattened plane became a trapezium.

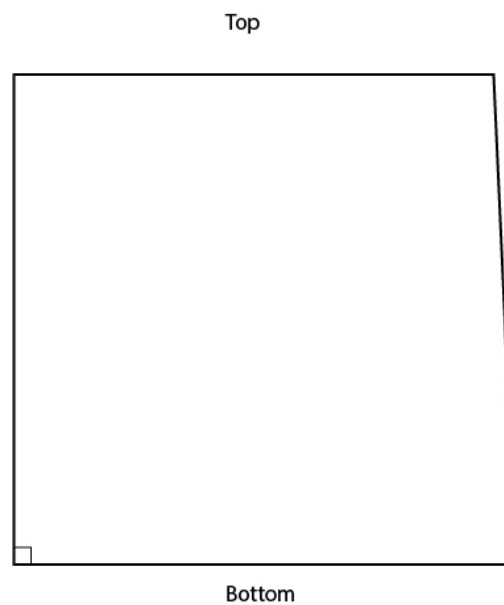


Figure 4.7 An image of the flattened 2D plane of the surface with zero Gaussian curvature used

## **4.2 3D Shape Knitting**

The procedures and details of the 3D shape to be reconstructed were discussed in this part, from the flattened 2D plane to a knitted 3D shape possessing the target geometry. Dimensional information was taken and then the flattened plane was mapped with knitting loops with the reference to loop density. A knitting sequence was prepared for knitting programme and subsequent knitting. The knitted shape was linked before subject to necessary post-treatments including washing and steaming for relaxation.

### **4.2.1 Loop Alignment**

Loop alignment was considered to be the most critical part of reconstructing the target 3D in this study. It was based on the measurement taking method which determined how the dimensions of the plane were captured and the loops were aligned following the directions and pathways of the measurements. Here were two loop alignment methods proposed, one was based on the cartographic concept of parallels of latitude while the other one was based on the direct width and length measurements to be taken from the flattened plane. So two measurement taking methods were developed based on the above ideas, in other words, the former one was based on the 3D straight lines while the later one the 2D straight lines. However, in the case of zero Gaussian curvature, according to the theory and the proof from the HYBRID-SUM model by Ng and Yu (2006a), the measurements of 3D straight lines were equal to the 2D straight lines as there were no distortions in

direct flattening. The geodesics remained the same. So the difference of the two proposed loop alignment methods was unseen in this part.

In fact, the dimensions of the flattened plane to be measured were used to determine the number of course and wale to be aligned with the reference to loop density. So the length and the width of the shape were needed to be recorded. To record the length of the shape, a vertical reference line perpendicular to the bottom line was drawn passing through the bottom and the top of the plane, marking the lowest point of the vertical reference line at 0 cm and continuing up to the top at an interval of 1 cm. For the width of the shape, horizontal lines were marked perpendicularly to the vertical reference line on the flattened plane, also at an interval of 1 cm. For any corner points in the middle and the highest point of the plane, the length of the vertical reference line and the width of the horizontal lines were also marked. As a trapezium, there was no corner points, only the highest point was additionally marked.

Since weft knitting must have a certain amount of knitted trims to start up knitting, even the least was 2 courses of knits, the height of this small amount of knits would still avoid proper positioning of the knitted shape to the conical shaped target object due to its wider base. Therefore, to avoid this situation in evaluation, the plane was placed upside down and measurements were taken from the top of the shape to the bottom. Figure 4.8 showed an illustration of the plane marked with measurement references. Knitting in this direction allowed a clean-finished edge of the knitted shape to be placed to the bottom edge of the target shape. And the start-up ribs could be hanging at the top of the target shape, where there was some empty

space that was not taken to experiment (Figure 4.1) without altering the experimental dimensions.

After all the measurements taken, the next step was calculating the knitting sequence. A knitting sequence was an instruction of how many wales to be placed upon a number of courses in a sequence to construct the knitting pattern. And to calculate the knitting sequence, loop density which were cpc and wpc should be decided beforehand. So a reference fabric swatch was need to be prepared, using the same count and content of fibre, knitting machine and set up and undergoing the same yarn relaxation treatments, so that the experimental loop density could be determined. Loop density, including loop length, cpc and wpc, of the reference swatch was also measured as a reference for following knitting checking. The cpc and wpc from the reference swatch used in this study were 8.9286 cm and 6.5617 cm respectively and the loop length was 0.6088 cm. After that, a knitting sequence of the plane of zero Gaussian curvature was worked out according to the reference loop density.

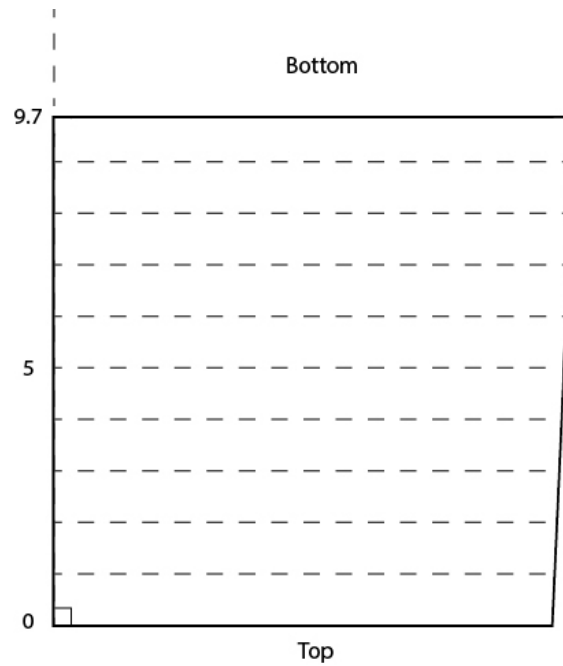


Figure 4.8 An illustration of the plane marked with measurement references

#### 4.2.2 Knitting Validation

A knitting programme was developed using the Shima Seiki's SDS-ONE APEX 3 CAD system according to the knitting sequence, shown in Figure 9.1. And knitting was proceeded by using the Shima Seiki's SES-122S automatic flatbed knitting machine. One end of 2/30 Nm 100% Merino wool was used as for 12GG knitting.

A trial sample was knitted before actual experimental sample to ensure proper knitting setting by checking the loop length to the previous reference swatch and to check if there was any knitting error. After that, the actual samples were knitted 3 times repeatedly. As the knitted samples were in a planar form, the two side edges of each were linked together to resume a conical shape. As the dry shapes stored certain amount of tension in the loops due to the friction during knitting, the

loop shapes were deformed and required relaxation to return to the natural shape. They were thus subject to post-treatments including washing, tumble drying and steaming, then were resting in flat for 2 two before evaluation. Figure 4.10 showed an image of the knitted shape put onto the target object.

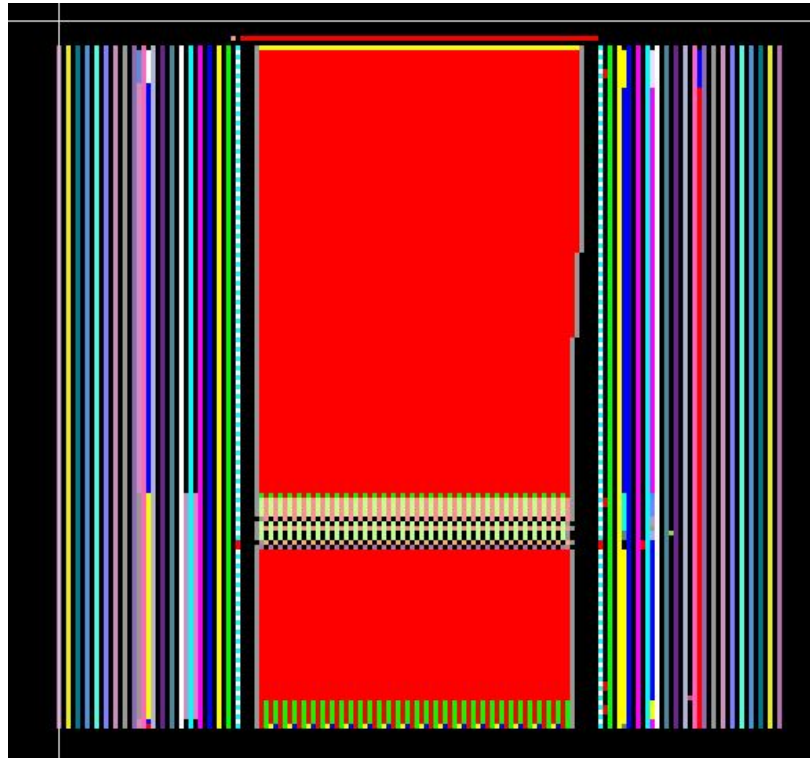


Figure 4.9 Knitting programme of target object of zero Gaussian curvature



Figure 4.10 An image of the finished 3D knitted shape of zero Gaussian curvature on the target object

### 4.3 Evaluation

As considering a knitted shape was too drapery to hold its entire shape when in a relaxed state, the knitted samples were put onto the target object to resume its initial dimensions for analysing their 3D reconstruction accuracy. To be consistent, a knitted shape was placed onto the target marked with reference lines (Figure 4.11a); its linking seam must be aligning on the black reference marking tape (Figure 4.11b); the edge of the top of the knitted shape below the rib trim and the edge of the bottom must be lying on the upper and lower red reference marking tape respectively (Figure 4.11c and Figure 4.11d) so that the shape was placed in a proper position for evaluation. A qualitative evaluating method was used by observing the visual appearance of the shape and comparing its 3D with the target object's 3D. Another method was counting the loop density of the knitted shape on the target and of it in a relaxed state as a quantitative evaluation.



To judge the appearance of a knitted shape if it possessed the target 3D, it should fit to the target object in general, without showing any extra fabrics due to too many loops, fabric pulling due to inadequate amount of loops or wavy seams due to linking yarn too tight or side seams too long. From Figure 4.10, the overall knitted shape was considered as accurate that it had no extra folds and wavy seams and it was not under tension. To be more precise, the knitted shape on the target object was further scanned. Its data was compared with the data of the target. Figure 4.12 (b) displayed a scanned image of the knitted shape. From the scanned image, it was seen that the knitted shape was possessing the required 3D. However, fabric pulling or stretched loops were not easy to be noticed by observing their appearances, especially when knitting in fine gauge as loops were too tiny, and it was even impossible to notice inadequate amount of loops from the scanning data. These qualitative evaluating methods were only suitable for assessing excess loops. The appearance observations of the samples were listed in Table 4.1.

To tackle the blind spot of the qualitative evaluations, measuring the knitted shape's loop density, which were the cpc and wpc values, as a quantitative evaluation was just ideal for it. The knitted shape was measured in two conditions, one was when laying flat as in a relaxed state and the other one was when putting onto the target shape. The tolerance was  $\pm 5\%$ . To measure the loop density, a certain amount of loops such as 50 successive loops in a complete course or wale was counted, using pins to indicate every 10 loops for easier counting. The start and end were indicated by tape with the pins removed, leaving the target loops hanging in their natural positions. Use a ruler to measure the length or use a measuring tape

for curved surfaces. After that, divided 50 courses or wales by the measured length to obtain cpc or wpc respectively. Figure 4.13 showed the cpc measuring procedures with counting 70 loops. Measuring the loop density when on the target object was to see if there was loop stretching due to missing loops; and measuring the loop density when relaxed was to double check if knitting was correct with proper cpc and wpc. Three interior regions were measured for each sample on target. Table 4.2 showed the loop density of the three samples of zero Gaussian curvature. All readings of loop density when relaxed were within tolerance which means knitting was correct. And most of the readings of cpc and wpc when on object were also within tolerance, only two wpc measurements of all were slightly beyond -5%. This was the result of measuring loops on the bottom near the linking seam in where the short linking yarn end was hidden in seam, making the bottom seam bulkier. The bulkiness given by the linking seam led to stretched loops. This situation was unseen on the top as the linking yarn end was hidden in the rib trim which was beyond the region for evaluation. Also these knitted shapes were small, the impact of seam bulkiness was stronger. In other words, the impact on bigger knitted shapes was smaller, since the error from stretched loops was well distributed. But in general, the knitted shapes had adequate amount of loops. However, this evaluating method could only find out errors in inadequate loops but not excess loops as excess loops were hanging in the extra fabric areas where were not lying on the target and thus were staying in a relaxed state. Measuring these loops only would give a result of proper loop density but would be unable to tell its error if not referring to the appearance of the shape at the same time.

After all, from the about qualitative and quantitative evaluations, the knitted shapes were successfully reconstructed the target 3D. And in order to contemplate all possible errors and distortions of the knitted shapes, both qualitative and quantitative evaluations must be carried out.

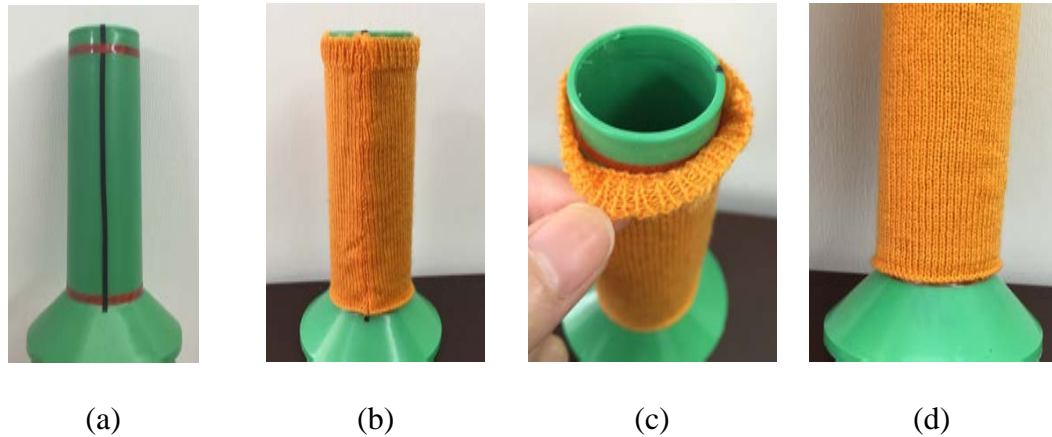


Figure 4.11 The pictures of positioning a knitting shape of zero Gaussian curvature onto the target: (a) target shape with black and red reference marking tapes; (b) the seam of the knitting shape lying on the black reference marking tape; (c) the edge of the knitted shape top below the rib trim lying on the upper red reference marking tape and (d) the edge of the knitted shape bottom lying on the lower red reference marking tape

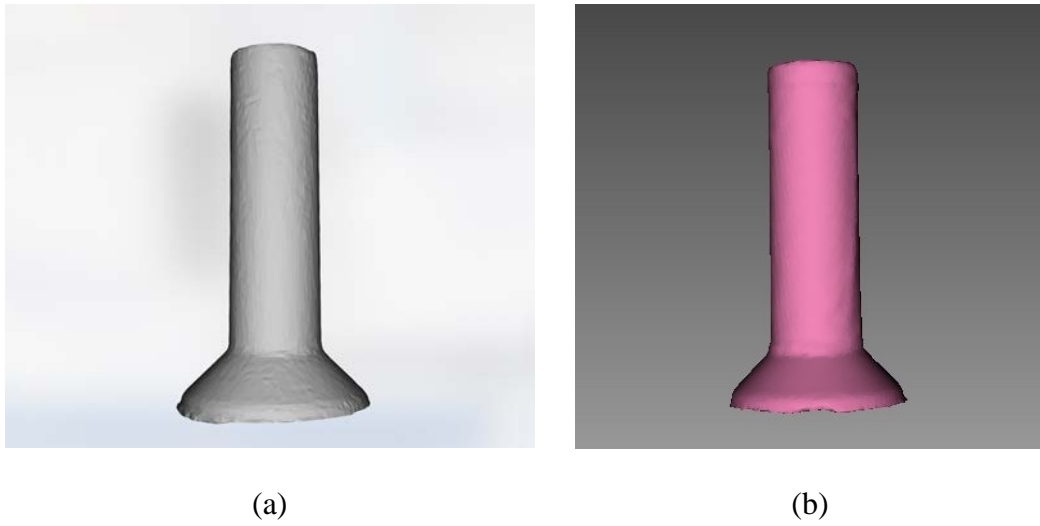


Figure 4.12 The scanned images of (a) target image and (b) the knitted shape of surface with zero Gaussian curvature



Figure 4.13 The procedures of measuring cpc with counting 70 successive loops

Item	Descriptions	Bumps / Folds	Crimps	Stretched Loops	Wavy Seam	Contour
Zero Gaussian Curvature I	Presence	No	No	No	No	Accurate
	Location					
	Remarks	N/A				
Zero Gaussian Curvature II	Presence	No	No	No	No	Accurate
	Location					
	Remarks	N/A				
Zero Gaussian Curvature III	Presence	No	No	No	No	Accurate
	Location					
	Remarks	N/A				

Table 4.1 Table of appearance observations of three samples of zero Gaussian

curvature

Item and Area	wpc	% diff	cpc	% diff	
Working loop density	6.5617		8.9286		
Zero Gaussian Curvature I	Relax	6.666666667	1.60%	9.090909091	1.82%
	On object	6.329113924	-3.54%	9.230769231	3.38%
	On object	6.349206349	-3.24%	9.345794393	4.67%
	On object	6.153846154	-6.22%	8.860759494	-0.76%
	Average on object	6.277388809	-4.33%	9.145774372	2.43%
Zero Gaussian Curvature II	Relax	6.506024096	-0.85%	9.160305344	2.60%
	On object	6.25	-4.75%	9.259259259	3.70%
	On object	6.470588235	-1.39%	9.090909091	1.82%
	On object	6.285714286	-4.21%	9.285714286	4.00%
	Average on object	6.335434174	-2.80%	9.211960879	3.17%
Zero Gaussian Curvature III	Relax	6.506024096	-0.85%	9.160305344	2.60%
	On object	6.349206349	-3.24%	9.302325581	4.19%
	On object	6.25	-4.75%	9.195402299	2.99%
	On object	6.201550388	-5.49%	9.009009009	0.90%
	Average on object	6.266918912	-4.49%	9.168912296	2.69%
Total Average on object	6.293247298	-4.09%	9.175549182	2.77%	

Table 4.2 Table of loop density of three samples of zero Gaussian curvature

#### 4.4 Conclusion

The 3D knitting pattern on a surface with zero Gaussian curvature was successfully completed from 3D data cloud to 3D knitting. The keys were preserving the surface area from the scanned 3D data cloud to the flattened 2D plane and mapping loops to the plane with the preserved area with the reference to loop

density to reconstruct the 3D. Loop alignment was technically straight forward in this chapter, though the two proposed loop alignment methods were executed as one due to the dimensional properties of zero Gaussian curvature. The two methods could be examined in the next chapter of experiments on surface with positive Gaussian curvatures. For evaluating the experimental results, it was known that the qualitative evaluations were good for finding extra folds if any but poor in notifying inadequate amount of fabrics; and vice versa for quantitative evaluations. So both were crucial to judging if the samples were able to reconstruct the target 3D.

## CHAPTER 5

### POSITIVE GAUSSIAN CURVATURE

This chapter aimed at converting the 3D data cloud of a surface with positive Gaussian curvatures into a 3D knitted shape. In the work in the previous section, a complete procedure and basic knowledge of 3D knitting pattern were established. Following this direction, an object in an egg-like shape of surfaces with positive Gaussian curvatures was selected to examine the possibilities of the two proposed loop alignment methods which were based on 3D straight lines and on 2D straight lines accordingly. It was assumed that the two loop alignment methods should induce different results on a surface with curvatures other than zero Gaussian curvature due to the distortion theory, since the Gauss egregium theorem stated that distortions were inevitable in dimensional change, though two methods were seemingly workable. Therefore, through this chapter, a theory of 3D knitting pattern on a surface with positive Gaussian curvatures and the possible loop alignment method(s) would be investigated.

Figure 5.1 showed an image of the 3D target object used in this chapter. This shape was selected as it consisted of a surface with a range of positive Gaussian curvature values, not like a sphere with only a constant curvature value. As in the last chapter, the selected shape here would undergo two parts, the 3D data conversion and 3D shape knitting, from converting the 3D data cloud into a 2D plane to aligning knitting loops onto the 2D plane to reconstruct the 3D. The finished

shape would be evaluated by both qualitative and quantitative evaluations. Same machinery, materials and loop length were used.

In the actual experiments, the first round of the experiments failed and it was unable to prove the assumption on the two loop alignment methods due to the improper planar flattening. So a second round of experiments on this shape were then carried out. To be clear, the two loop alignment methods in the first round were named method 3DSL-1 and 2DSL-1 for method based on 3D straight lines and 2D straight lines respectively while the same ideas in the second round were named method 3DSL-2 and 2DSL-2.



Figure 5.1 Image of the egg-like shape with a surface with positive Gaussian curvature

## 5.1 3D Data Cloud Conversion I

To be reminded, 3D data cloud conversion consisted of 3D data acquisition and processing, feature recognition and extraction and polygonal mesh mapping and



flattening. The surface of the shape in this part would become a 2D plane for the subsequent 3D shape knitting.

### **5.1.1 3D Data Acquisition and Processing**

The target object was scanned by using Artec Eva handheld scanner. However, a fundamental problem came across in the actual process that the target object was made of glass. In the scanning mechanism of a scanner, reflection of light or laser rays was received by the sensors for capturing images. As transparent glass allowed rays from any directions perpendicular to its surface to pass through, it was impossible to capture the geometry of objects made of this kind of material with a 3D scanner. To make the glass target capable of scanning, a light film of baby powder was spread over its surface. As baby powder fully covered the glassy surface, it provided a surface medium for light reflection during scanning while its fine particles preserved the geometric properties of the scanning surface. Marking tape was also put onto the shape for easier geometric recognition in later steps.

Artec Studio 9.0 CAD programme was used for preliminary data cloud processing. Failed frames and useless general noise were filtered and missing data shown as holes were filled. Rotation of xyz-axis was carried out to reposition the shape in a proper upright position. Figure 5.2 showed the 3D data cloud of the target object after preliminary processing.

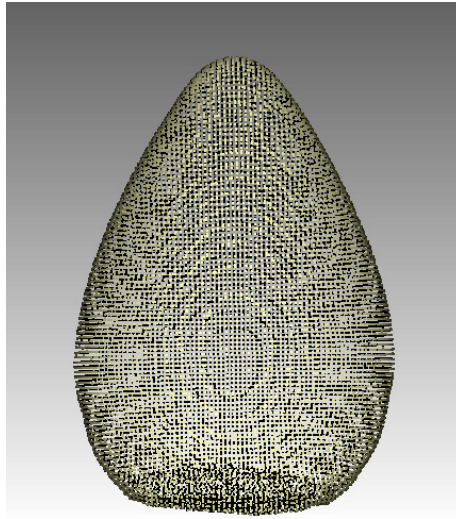


Figure 5.2 A finished 3D data cloud of the target object

### 5.1.2 Feature Recognition and Extraction

The finished data cloud was then subject to feature recognition and extraction. So its front, back, left and right were marked with marking tape for reference. By using the 1-D Sobel mask suggested in Leoung and his team's (2007) paper, the extreme convex points to the centreline on the sides of the longitudinal section of the shape were located (Figure 5.3). With the curve fitting method using a lower order B-spline, a smooth curve intersecting the bulgiest points perpendicular to the centreline was generated. For the top of the shape, the same Sobel mask was used to locate the highest extreme convex point of the shape. And the bottom curve was defined by the curve passing through the points with sudden curvature change at the bottom of the shape.

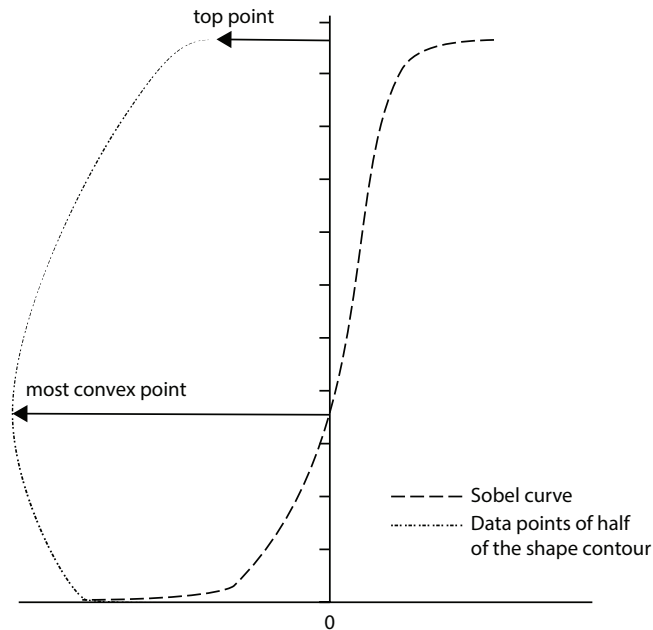


Figure 5.3 A diagram of Sobel mask of half of the target shape of positive Gaussian curvature

### 5.1.3 Polygonal Mesh Mapping and Flattening

By using the pattern flattening method proposed by McCartney and his team (2004), triangular mesh was mapped onto the surface. According to the research paper, in the area with a variation of curvature values, equal size of triangulation would induce error between the triangular mesh and the surface and the higher positive or negative curvature value gave bigger and more unacceptable error. Therefore, by applying this theory, the area with higher curvature value of the target shape should have more subdivided triangles so that the surface area could be preserved with less error. Figure 5.4 and Figure 5.5 illustrated the shape with only constant size of triangulation and the possible errors and that with subdivided triangles respectively.

Flattening was carried out with the reference to the curves obtained in the last section and the tape reference lines. In order to preserve surface area during flattening, cuts were inserted, in both horizontal directions and vertical directions. Cuts in horizontal directions allowed knitting to be carried out in a normal way, course by course, and the shape of the cut openings was achieved by partial knitting. However, cuts in vertical directions were not flavoured in knitting. Knitting shaping techniques were unable to complete the shape of cuts in this direction with its area preserved. In this case, a vertical cut would be extended to separate the plane. An assumption was drawn that the target object was of line symmetry viewing from the side and of rotational symmetry from the top, so the surface could be flattened into two symmetrical planes and the two planes were divided in the middle into two opposite halves each, shown in Figure 5.6. By considering the possibilities and productivity of knitting, two horizontal cuts were inserted to each half.

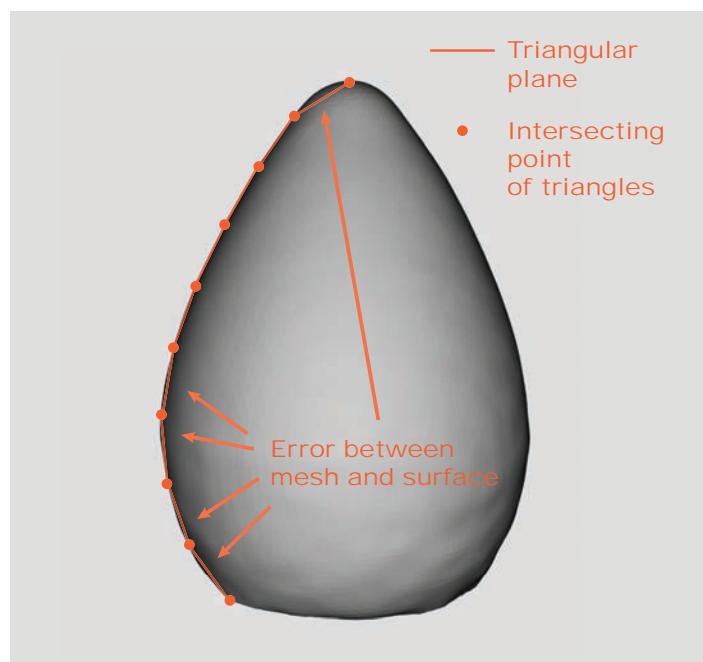


Figure 5.4 An illustration of constant size of triangulation and possible errors

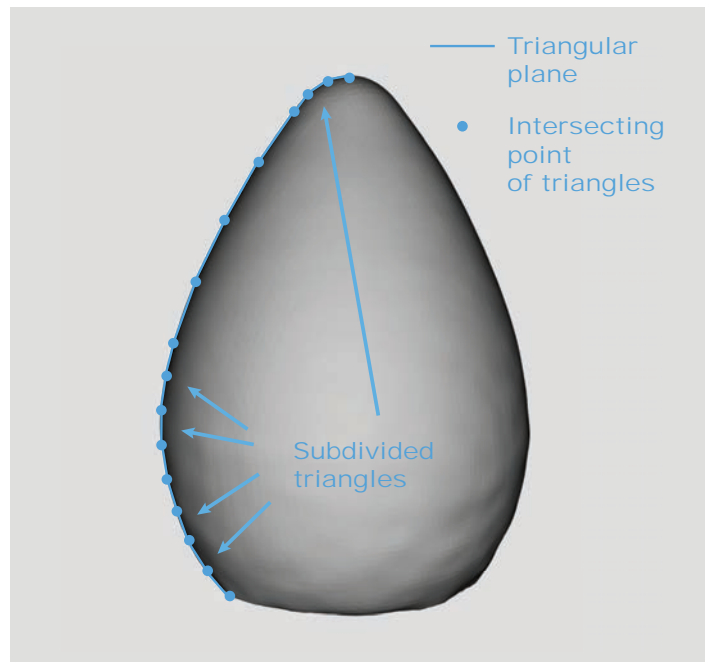


Figure 5.5 An illustration of subdivided triangulation and less possible errors

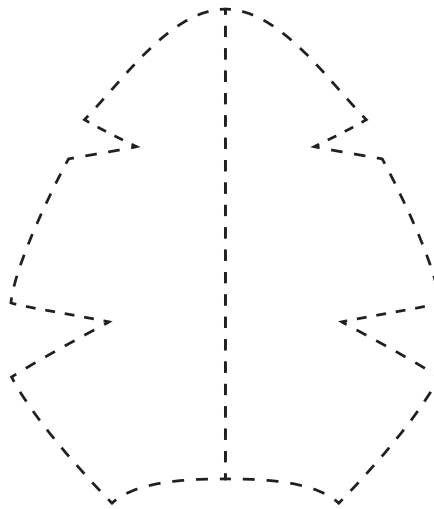


Figure 5.6 One of the two identical 2D planes with two opposite halves of positive Gaussian curvature for method 3DSL-1 and 2DSL-1

## 5.2 3D Shape Knitting I

From the previous section, two identical 2D planes of the surface of the target object were obtained. As a line symmetric plane, the following work could be done on one of the halves while the other half could then be reflected in order to save time. Therefore, in this first round of experiments, one-fourth of the entire surface in form of a 2D flattened plane was subject to the two loop alignment methods, method 3DSL-1 and method 2DSL-1. After preparing the knitting sequence, the planes were knitted down and then subject to necessary after treatments.

### 5.2.1 Loop Alignment

Two loop alignment methods, 3DSL-1 and 2DSL-1, were proposed. As mentioned, loop alignment followed the direction of the selected measurement taking method of the plane, so the width and length of the plane to be measured determined the number of wales and courses and the position of them.

Method 3DSL-1 was based on parallel of latitudes as in cartography. Figure 5.7 showed an example of it on a sphere. These parallels were shown as 3D straight lines on a 3D surface. By logical thinking, if knitting was processed from line to line following the parallel straight lines, the 3D shape could be achieved. Figure 5.8 showed an illustration of parallel of latitudes marked on the target object as for method 3DSL-1. Therefore, if these lines were marked on the 2D plane and knitting courses were aligned following this direction, method 3DSL-1 might be a possible way to reconstruct the target 3D. Loop alignment method 2DSL-1 was based on the

direct measurements of the flattened 2D plane. Surface dimensional information was neglected in this method. 2D horizontal lines were marked onto the plane for taking measurements and loops were aligned following the direction and placement of these lines to reconstruct the 3D. This idea was keeping loops alignment on the preserved surface area in a 2D mechanism.

To prepare for measurement taking for method 3DSL-1, a vertical reference line was marked in the middle of the 2D plane which was also the straight edge of the half plane, passing through the highest point of the top and that of the bottom arc of the plane. At each centimetre interval, the height of the vertical reference line was marked from the highest point of the bottom arc up to the top. The parallels of latitude marked at an interval of 1 cm on the 3D target surface were traced off on the 2D half plane. The 3D straight lines became 2D curved lines shown on the plane. For every extreme corner and the top point, its 3D straight lines was also marked and traced off. The half plane marked with reference line for method 3DSL-1 measurement taking was shown in Figure 5.9. The length of the vertical reference line was record as for calculating the number of courses in the knitting sequence. The lengths of the 2D curved lines as the width of the surface were also measured for the number of wales.

The procedures of measurement taking for method 2DSL-1 were similar to those for method 3DSL-1. A vertical reference line was marked on the straight edge of the half plane, passing through the top and the highest point of the bottom arc. But 0 cm was set at the lowest point of the plane and continued up to the top at 1 cm interval. Horizontal straight lines were also marked perpendicularly to the vertical

reference line from the lowest point of the plane up to the top at interval of 1 cm. Extreme corner points and the top point were also marked with the horizontal lines along with their height on the vertical reference line. Figure 5.10 showed a clear illustration of it. And by measuring the height of the reference line and the width of the horizontal lines, number of courses and wales for method 2DSL-1 could be calculated.

Technically before started to calculate the knitting sequence, a reference fabric swatch was needed to be prepared for acquiring the experimental loop density. In this study, as the experimental cpc and wpc were already obtained in last chapter, a new reference fabric swatch could be skipped. To be reminded, the cpc and wpc used were 8.9286 cm and 6.5617 cm respectively. A knitting sequence for each loop alignment method was then prepared.

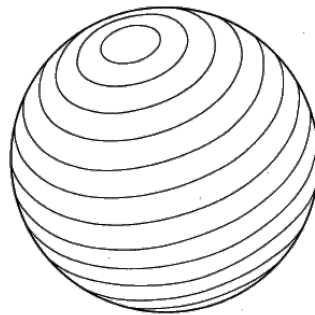


Figure 5.7 Illustration of parallel of latitudes on a sphere.



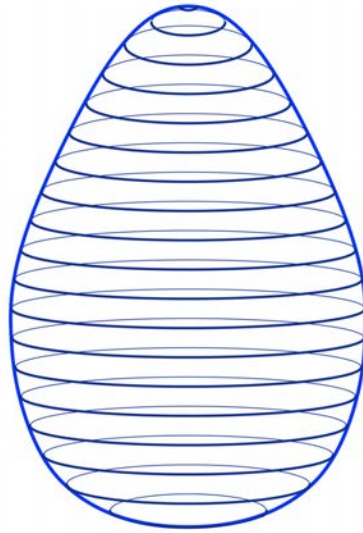


Figure 5.8 Illustration of parallel of latitude on target object as for method 3DSL-1

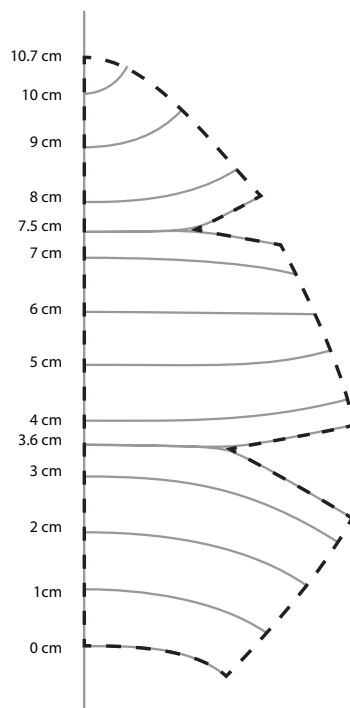


Figure 5.9 A half plane marked with 2D curved lines and vertical reference line for method 3DSL-1

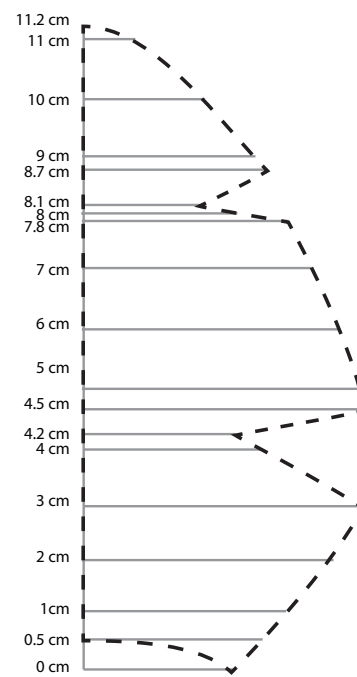


Figure 5.10 A half plane marked with 2D straight lines and vertical reference line for method 2DSL-1

### 5.2.2 Knitting Validation

Knitting programmes for loop alignment method 3DSL-1 and 2DSL-1 were prepared by using the Shima Seiki Knit CAD system following their corresponding knitting sequence. As the knitting sequence was calculated on only half of the plane, the knitting programme of the opposite half was mirrored to form a complete plane. So for each method, there were two identical knitted fabrics. Same yarn of 2/30 Nm 100% Merino wool in 1 end was used. Although it was unnecessary to prepare a new reference fabric swatch in this section, a trial swatch before actual experiments was needed. The loop density of knitted swatch must be double checked to assure the knitting set-up was correct and was following the knitting sequence. After that, each method with two identical knitted fabrics would be knitted down three times to form three repeated 3D shapes.

For knitting method 3DSL-1, as loops alignment followed the parallels of latitude, knitting loops aligned along the open edges of horizontal cuts on the flattened plane. Successive courses continued from the lower open edge to the upper open edge. The shape of vertical cuts were achieved by ordinary shaping techniques which were widening and narrowing. And although the bottom of the plane was an arc, the knitting start-up was not influenced as loops were aligned onto this curve and followed its bending direction. Figure 5.11 showed an illustration of loop alignment on half plane for method 3DSL-1.

In method 2DSL-1, knitting courses cut and fell on the open edge of horizontal cuts. Partial knitting was applied to achieve the shape of these cuts as

well as the curved top and base. Figure 5.12 showed an illustration of loop alignment on half plane for method 2DSL-1. It allowed the knitted shape to be continued without appearing cut openings or holes, but it would leave partial knitting marks on its surface. The knitting programme of method 3DSL-1 and method 2DSL-1 were shown in Figure 5.13. In practical, actual knitting of method 2DSL-1 was not as easy as of method 3DSL-1. As partial knitting was an action of knitting some of the needles while holding the rest, the furthest loop being held was under the most pulling tension giving by fabric roll, sub-rollers or the comb when the other needles were continuing loop formation. And when the furthest loop could not stand for the tension any more, it would break, leading to broken fabric and laddering. So the larger the cut opening it was on the plane, the higher tension the furthest loop was under. To ease the situation of yarn breaking caused by partial knitting, the take-down tension of the fabric roll, sub-rollers and comb must be tuned down. Although a small take-down tension might help for releasing the tension in the furthest loop during partial knitting, it might also lead to not enough pulling force for those needles which were knitting and cause unsuccessful loop formation, thus broken fabric. Therefore, a proper take-down tension of fabric roll and sub-rollers must be controlled in the part of partial knitting. And due to the issue of take-down tension and fabric edge breaking, method 2DSL-1 had been trialled for several times to get the proper machine setting.

Each two knitted fabrics from each method were linked together, forming three 3D knitted shapes of each method. They were then washed and steamed for loop relaxation to retain their proper loop position. Figure 5.14 and Figure 5.15

showed the finished images of the 3D knitted shapes by method 3DSL-1 and 2DSL-1 respectively. They were evaluated in the following section.

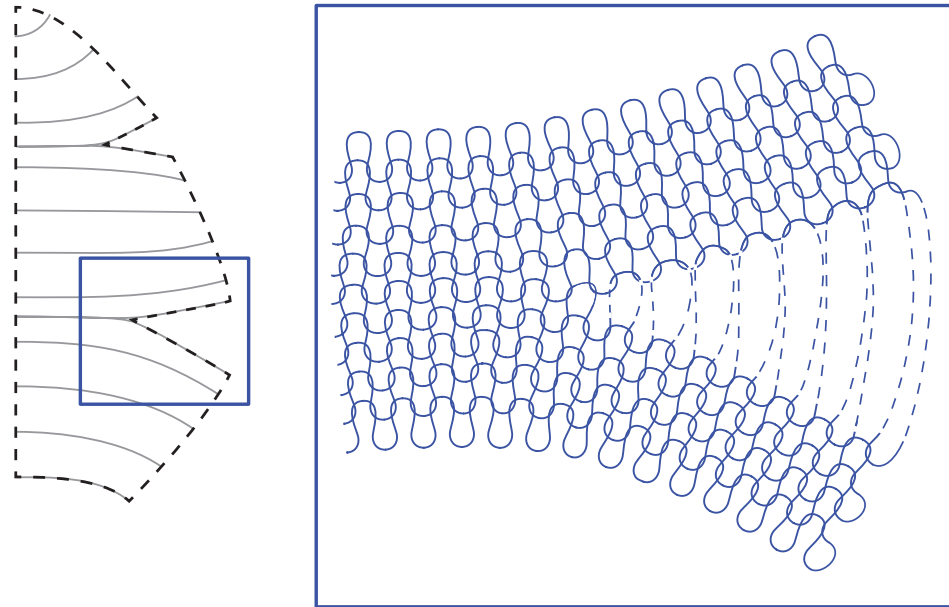


Figure 5.11 An illustration of loop alignment on half plane for method 3DSL-1

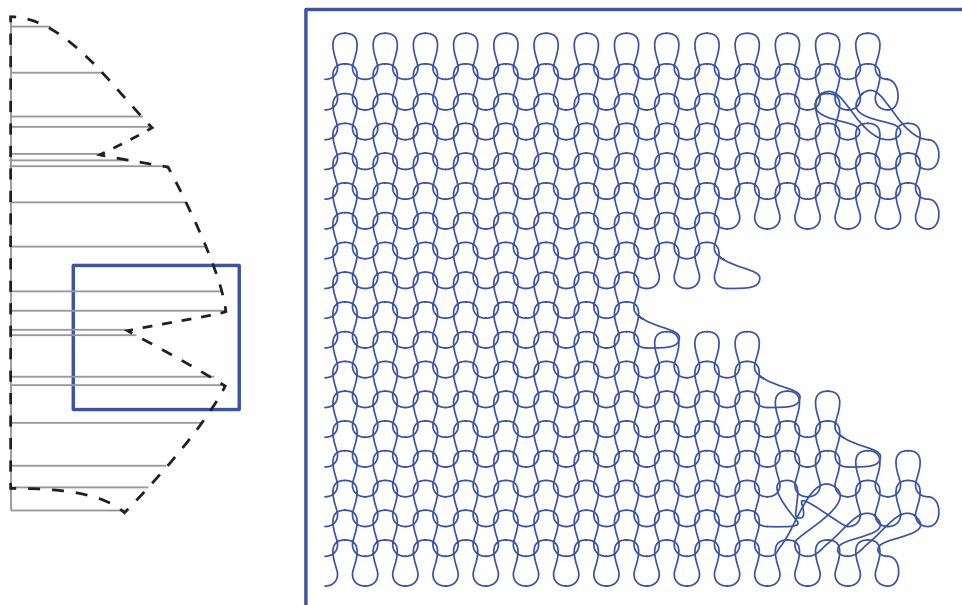


Figure 5.12 An illustration of loop alignment on half plane for method 2DSL-1

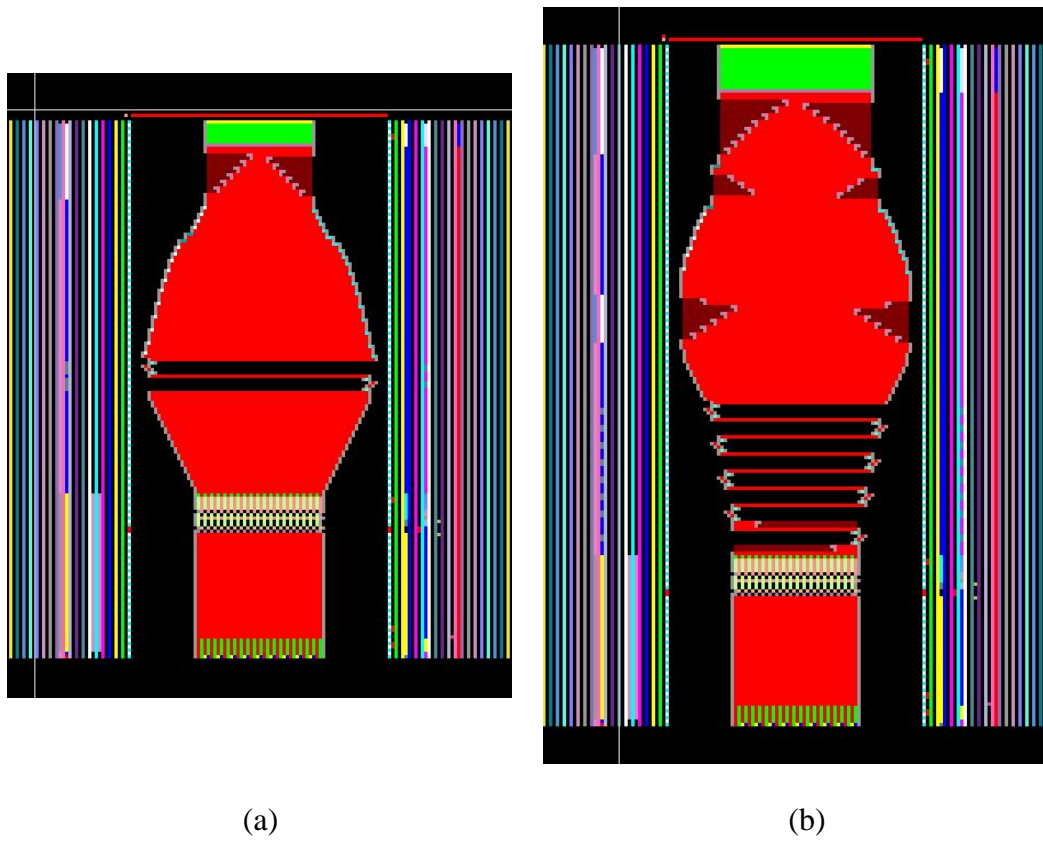


Figure 5.13 Knitting Programme of (a) method 3DSL-1 and (b) method 2DSL-1

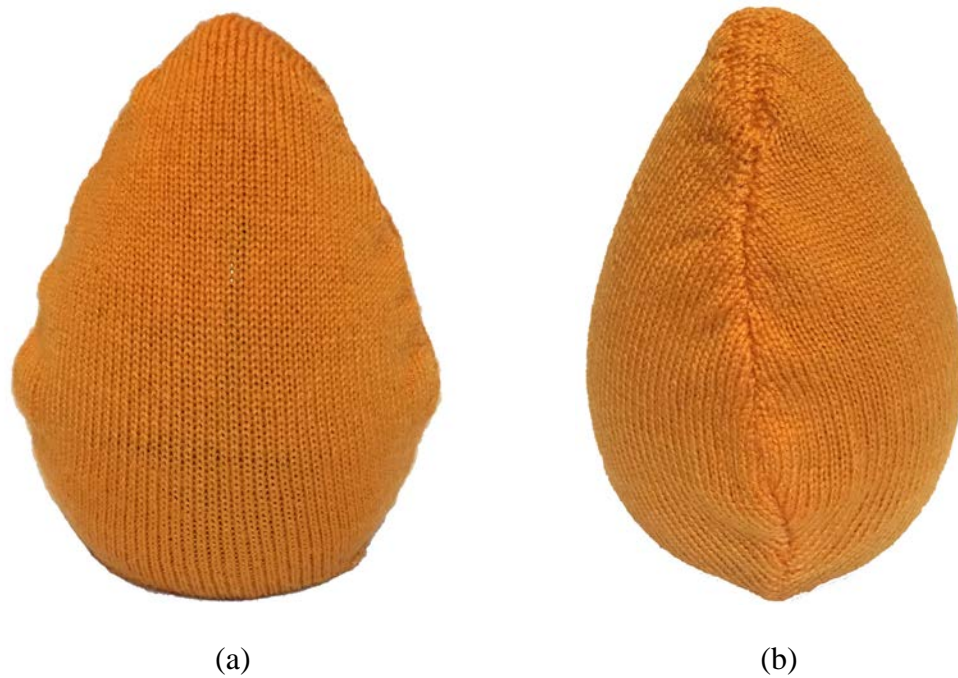


Figure 5.14 (a) The front view and (b) the side view of the 3D knitted shape by method 3DSL-1

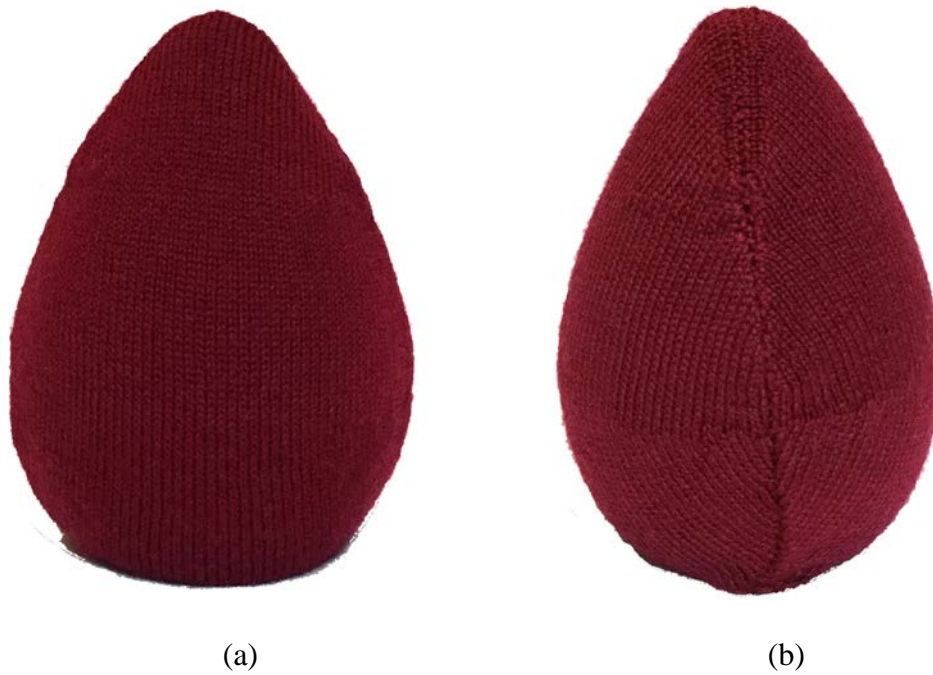


Figure 5.15 (a) The front view and (b) the side view of the 3D knitted shape by method 2DSL-1

### 5.3 Evaluation I

Both qualitative and quantitative evaluations were carried out. The 3D knitted shapes were put onto the egg-like target for visual comparison and loop density measurement.

As in last chapter, the appearances of the shapes were observed and they were also scanned for contour comparison. From Figure 5.14, method 3DSL-1 was obvious that the sides were wavy and bumps appeared on the sides of the bulgiest part. There were crimps on the linking seam. The loops in the bulgiest part looked bigger than those in upper parts, implying the loops were stretch. Method 2DSL-1 was better with smooth edges and linking seams, no extra fabrics were seen.

However, method 2DSL-1 had also the appearance of bigger loops in the bulgiest part and smaller in upper parts. Then the two shapes were scanned, shown in Figure 5.16 and Figure 5.17. The contour of method 3DSL-1 was different from the target and the edges were seriously wavy viewing from the top. Meanwhile, the top view of method 2DSL-1 showed two protrusions on the sides though its shape from front view was acceptable. These two pointed sides were caused by the linking seams as there were 4 wales of linking allowance underneath on each side. The size of loops was unable to be noticed through the scans. From the qualitative evaluation, the knitted shape by method 3DSL-1 failed to reconstruct the target 3D as its shape was distorted. The knitted shape by method 2DSL-1 was seemingly acceptable but it was yet too soon to confirm its possibility before the quantitative evaluation. Table 5.1 and Table 5.2 listed the appearance observations of samples by method 3DSL-1 and method 2DSL-1 respectively.

The knitted shapes were then subject to quantitative evaluation. Loop density of the six samples on the target object and in relaxed state was measured with a tolerance of  $\pm 5\%$ . Three interior areas were measured while on the object. The results were shown in Table 5.3 and Table 5.4 for method 3DSL-1 and method 2DSL-1 respectively. All readings of the six samples in the relaxed state were within tolerance, meaning they were knitted with correct loop density and machine settings. However, other readings were not very acceptable. And the results of method 2DSL-1 were unexpectedly poor that no specific differences were seen between method 3DSL-1 and method 2DSL-1 from the quantitative evaluation. Their total wpc values were -10.73% and -7.85% for method 3DSL-1 and method 2DSL-1 respectively, beyond the tolerance. Many of their wpc values were more

than -5% that meant loops were stretched and the 3D shapes did not have adequate amount of loops in width in many areas, while only some of the cpc values were beyond the tolerance. So from the loop density results, both methods failed to reconstruct the target 3D and this was unexpected.

It was assumed that the two loop alignment methods had different results in 3D shape knitting that at least one might work though both methods were seemingly workable. Failure for both was unpredictable. Although method 2DSL-1 showed it had not much excess fabrics from the qualitative evaluation, it was actually stretching and wrapping around the target to give a fit appearance. Method 3DSL-1 failed in the beginning that it was off from the target shape. As both methods failed, there should be an error in both methods. And went back to the surface flattening section, there was an assumption that only  $\frac{1}{4}$  of the surface was proceeded to the 3D shape knitting section. The surface information of the other  $\frac{3}{4}$  of the whole surface was missing and that could be the possible error. Although the target was seemingly symmetrical, the error existed said it might not be. Therefore, a second round of experiments starting from the surface flattening was carried out.



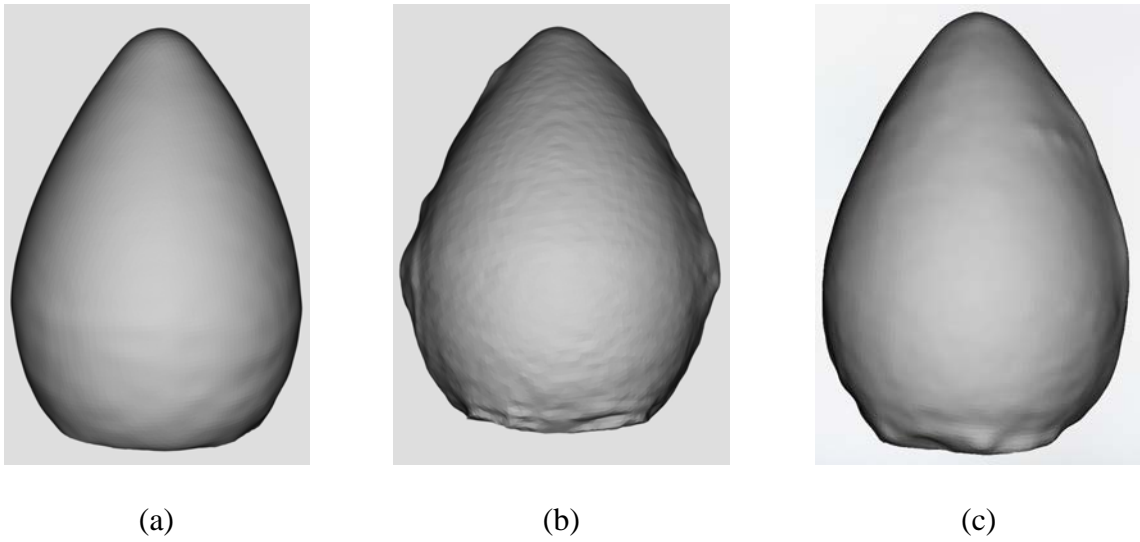


Figure 5.16 The front view of scanned images of (a) target image, (b) 3D knitted shape by method 3DSL-1 and (c) 3D knitted shape by method 2DSL-1

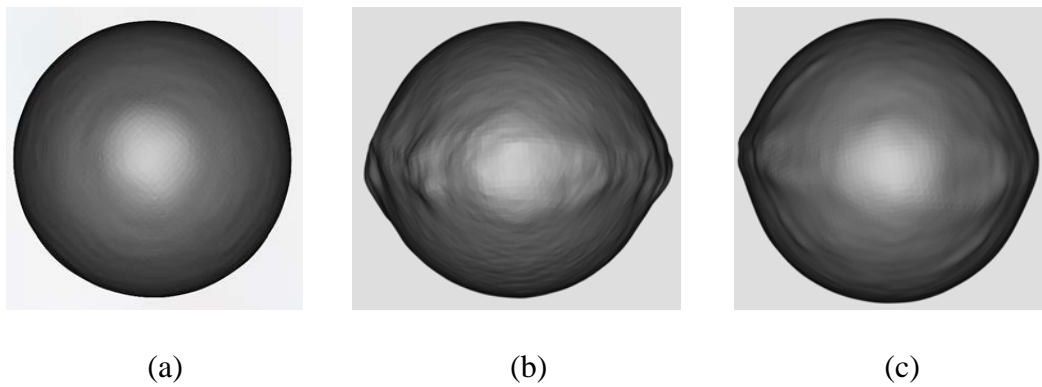


Figure 5.17 The top view of scanned images of (a) target image, (b) 3D knitted shape by method 3DSL-1 and (c) 3D knitted shape by method 2DSL-1

Item	Descriptions	Bumps / Folds	Crimps	Stretched Loops	Wavy Seam	Contour
Positive Gaussian Curvature 3DSL-1 I	Presence	Yes	Yes	Yes	Yes	Front view: distorted Top view: wavy & pointed sides
	Location	Bulgiest part sides	Linking seams	Bulgiest part	Two sides	
	Remarks	N/A				
Positive Gaussian Curvature 3DSL-1 II	Presence	Yes	Yes	Yes	Yes	Front view: distorted Top view: wavy & pointed sides
	Location	Bulgiest part sides	Linking seams	Bulgiest part	Two sides	
	Remarks	N/A				
Positive Gaussian Curvature 3DSL-1 III	Presence	Yes	Yes	Yes	Yes	Front view: distorted Top view: wavy & pointed sides
	Location	Bulgiest part sides	Linking seams	Bulgiest part	Two sides	
	Remarks	N/A				

Table 5.1 Table of appearance observations of three samples of positive Gaussian curvature by method 3DSL-1

Item	Descriptions	Bumps / Folds	Crimps	Stretched Loops	Wavy Seam	Contour
Positive Gaussian Curvature 2DSL-1 I	Presence	No	No	Yes	No	Front view: distorted Top view: pointed sides
	Location			Bulgiest Part		
	Remarks	Presence of partial knitting marks				
Positive Gaussian Curvature 2DSL-1 II	Presence	No	No	Yes	No	Front view: distorted Top view: pointed sides
	Location			Bulgiest Part		
	Remarks	Presence of partial knitting marks				
Positive Gaussian Curvature 2DSL-1 III	Presence	No	No	Yes	No	Front view: distorted Top view: pointed sides
	Location			Bulgiest Part		
	Remarks	Presence of partial knitting marks				

Table 5.2 Table of appearance observations of three samples of positive

Gaussian curvature by method 2DSL-1

Item and Area		wpc	% diff	cpc	% diff
Working loop density		6.5617		8.9286	
Positive Gaussian Curvature 3DSL-1 I	Relax	6.66666667	1.60%	9.090909091	1.82%
	On object	5.882352941	-10.35%	9.090909091	1.82%
	On object	4.761904762	-27.43%	9.090909091	1.82%
	On object	5.517241379	-15.92%	9.375	5.00%
	Average on object	5.38718046	-17.90%	9.185606061	2.88%
Positive Gaussian Curvature 3DSL-1 II	Relax	6.779661017	3.32%	9.090909091	1.82%
	On object	5.925925926	-9.69%	8.163265306	-8.57%
	On object	5.882352941	-10.35%	9.090909091	1.82%
	On object	6.666666667	1.60%	8.333333333	-6.67%
	Average on object	6.158315178	-6.15%	8.529169243	-4.47%
Positive Gaussian Curvature 3DSL-1 III	Relax	6.557377049	-0.07%	8.888888889	-0.44%
	On object	5.357142857	-18.36%	8.163265306	-8.57%
	On object	6.666666667	1.60%	8.571428571	-4.00%
	On object	6.060606061	-7.64%	8.421052632	-5.68%
	Average on object	6.028138528	-8.13%	8.385248836	-6.09%
Total Average on object		5.857878055	-10.73%	8.700008047	-2.56%

Table 5.3 Table of loop density of the three samples by Method 3DSL-1

Item and Area		wpc	% diff	cpc	% diff
Working loop density		6.5617		8.9286	
Positive Gaussian Curvature 2DSL-1 I	Relax	6.666666667	1.60%	9.0909	1.82%
	On object	5.882352941	-10.35%	8.695652174	-2.61%
	On object	5.714285714	-12.91%	8.602150538	-3.66%
	On object	6.086956522	-7.24%	9.259259259	3.70%
	Average on object	5.894552174	-10.17%	8.85235399	-0.85%
Positive Gaussian Curvature 2DSL-1 II	Relax	6.779661017	3.32%	9.090909091	1.82%
	On object	5.797101449	-11.65%	8.823529412	-1.18%
	On object	5.882352941	-10.35%	8.695652174	-2.61%
	On object	6.842105263	4.27%	8.510638298	-4.68%
	Average on object	6.173853218	-5.91%	8.676606628	-2.82%
Positive Gaussian Curvature 2DSL-1 III	Relax	6.722689076	2.45%	9.259259259	3.70%
	On object	5.309734513	-19.08%	9.302325581	4.19%
	On object	6.451612903	-1.68%	8.928571429	0.00%
	On object	6.451612903	-1.68%	9.2	3.04%
	Average on object	6.070986773	-7.48%	9.143632337	2.41%
Total Average on object		6.046464055	-7.85%	8.890864318	-0.42%

Table 5.4 Table of loop density of the three samples by Method 2DSL-1

## 5.4 3D Data Cloud Conversion II

A second round of experiments using the same target object of surface with positive Gaussian curvature was proceeded. To avoid the error of partial surface

dimensions used only in last section, the whole surface area was examined here. The same data cloud was used with the same work of data processing and feature recognition, only the part of surface flattening was redone.

#### **5.4.1 Surface Flattening**

The entire surface of the target shape was to be flattened. With the same idea of inserting cuts to preserve surface area, three horizontal cuts were inserted instead of two to increase area preservation accuracy. Vertical cuts were added as flattening needed and were extended to separate the planes for easier knitting. Two flattened 2D planes were achieved, with similar appearance yet non-identical. The two sides of each plane were not exactly mirrored. With the correct dimensions of the whole surface, the two planes were subject to 3D knitting. Figure 5.18 showed one of the newly flattened 2D planes.

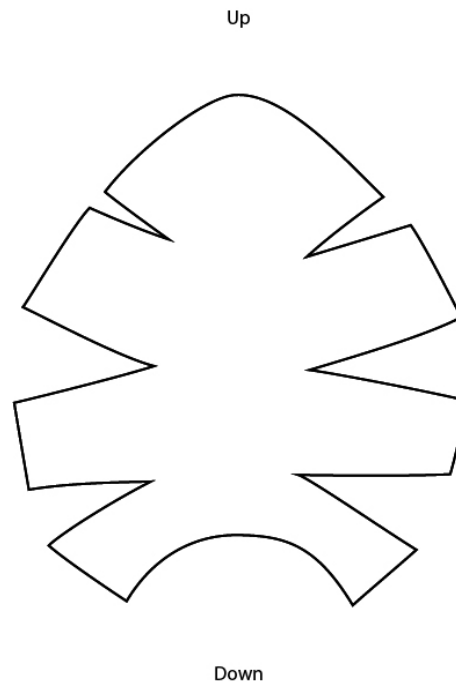


Figure 5.18 An illustration of one of the newly flattened 2D planes for method 3DSL-2 and 2DSL-2

## 5.5 3D Shape Knitting II

The two proposed loop alignment methods were experimented again. Assumption on their different results remained. As the plane changed, the two methods were named method 3DSL-2 for the one based on the parallels of latitude and method 2DSL-2 for horizontal lines to be marked on the plane. The experiments were carried out with the same procedures.

### 5.5.1 Loop Alignment

Two loop alignment methods with the same proposed ideas were carried out, method 3DSL-2 and method 2DSL-2. Their measurement taking methods remained

the same, only the 2D planes were changed. Cpc and wpc for knitting sequence calculation also remained the same as 8.9286 cm and 6.5617 cm respectively.

For method 3DSL-2, a vertical reference line was placed in the middle of the plane, intersecting the highest point of the top and that of the bottom arc. The bottom arc intersecting point was set as 0 cm. Parallels of latitude as 3D straight lines at an interval of 1 cm were traced from the 3D surface off to the 2D plane becoming 2D curved lines. Knitting loops were aligned following the directions of these lines. The height of the vertical reference line was recorded and the length of the 2D curved lines were also measured as the width of the surface. These were done on both planes. The measurements were calculated with the reference to the experimental loop density values and developed a knitting sequence. Figure 5.19 showed an illustration of loop alignment method 3DSL-2.

After marking a vertical reference line as in method 3DSL-2, the starting point 0 cm in method 2DSL-2 was set to the lowest point of the whole plane and continued up to the top at 1 cm interval. Horizontal lines as 2D straight lines were marked perpendicularly to the vertical reference line from the lowest point of the plane and up to the top also at 1 cm interval. For every extreme corners of the plane, a horizontal line was marked and its height on the vertical reference line was recorded. As two sides of the plane were not identical, measurements of both were separated. The height of the vertical reference line and the width of the horizontal lines were measured and subject to knitting sequence calculation. The other one of the flattened planes underwent the same procedures. Figure 5.20 showed an illustration of the loop alignment method 2DSL-2.

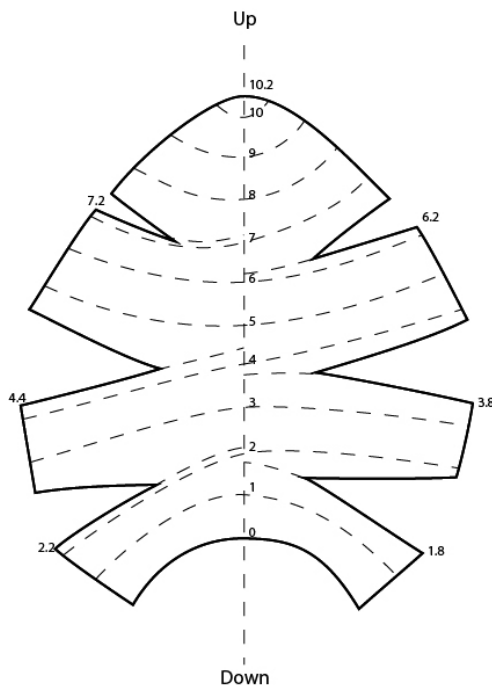


Figure 5.19 An illustration of 2D curved lines from 3D straight lines in loop alignment method 3DSL-2

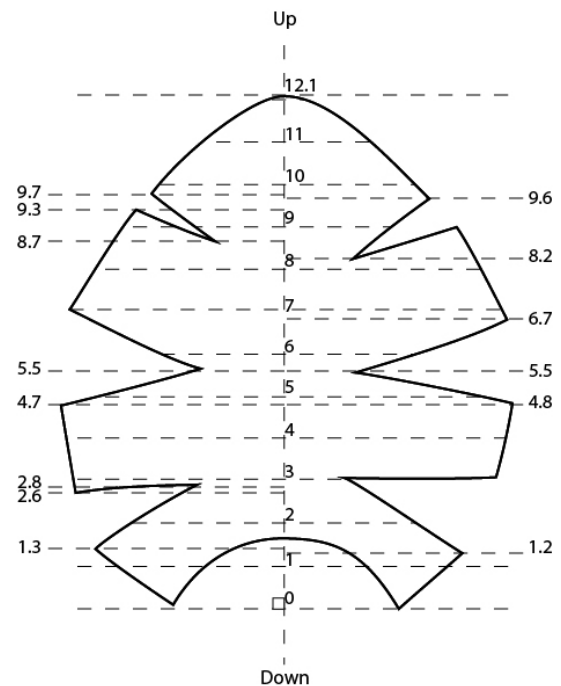


Figure 5.20 An illustration of 2D straight lines directly marked onto the plane in loop alignment method 2DSL-2

### 5.5.2 Knitting Validation

The knitting sequences were transformed into knitting programmes of method 3DSL-2 and method 2DSL-2 shown in Figure 5.21 and Figure 5.22 respectively. Trials using the same yarn and machine were carried out to make sure the machine setting, knitting programme and loop densities were correct. Knitted fabrics by method 3DSL-2 and 2DSL-2 were produced afterwards. As loop aligned following the 2D straight lines in method 2DSL-2, partial knitting was applied to achieve the shape of the cuts to a continuous knitted edge. Two similar but different knitted fabrics of each method were linked to together to form its 3D shape. Each

method was repeated three times and there were 6 samples in total. They were then subject to after treatments for relaxation. Figure 5.23 and Figure 5.24 showed the finished 3D knitted shape of method 3DSL-2 and method 2DSL-2.

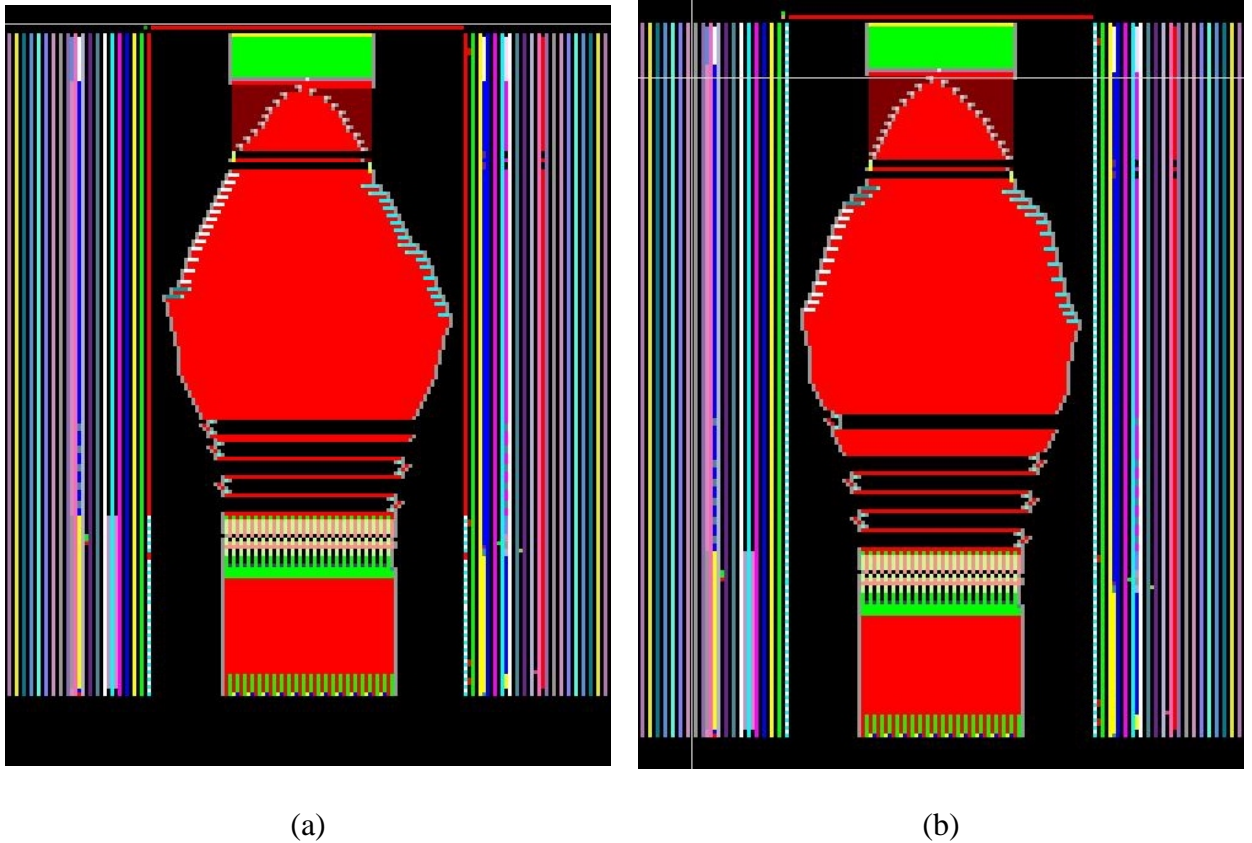


Figure 5.21 Knitting programme of method 3DSL-2 of the two planes



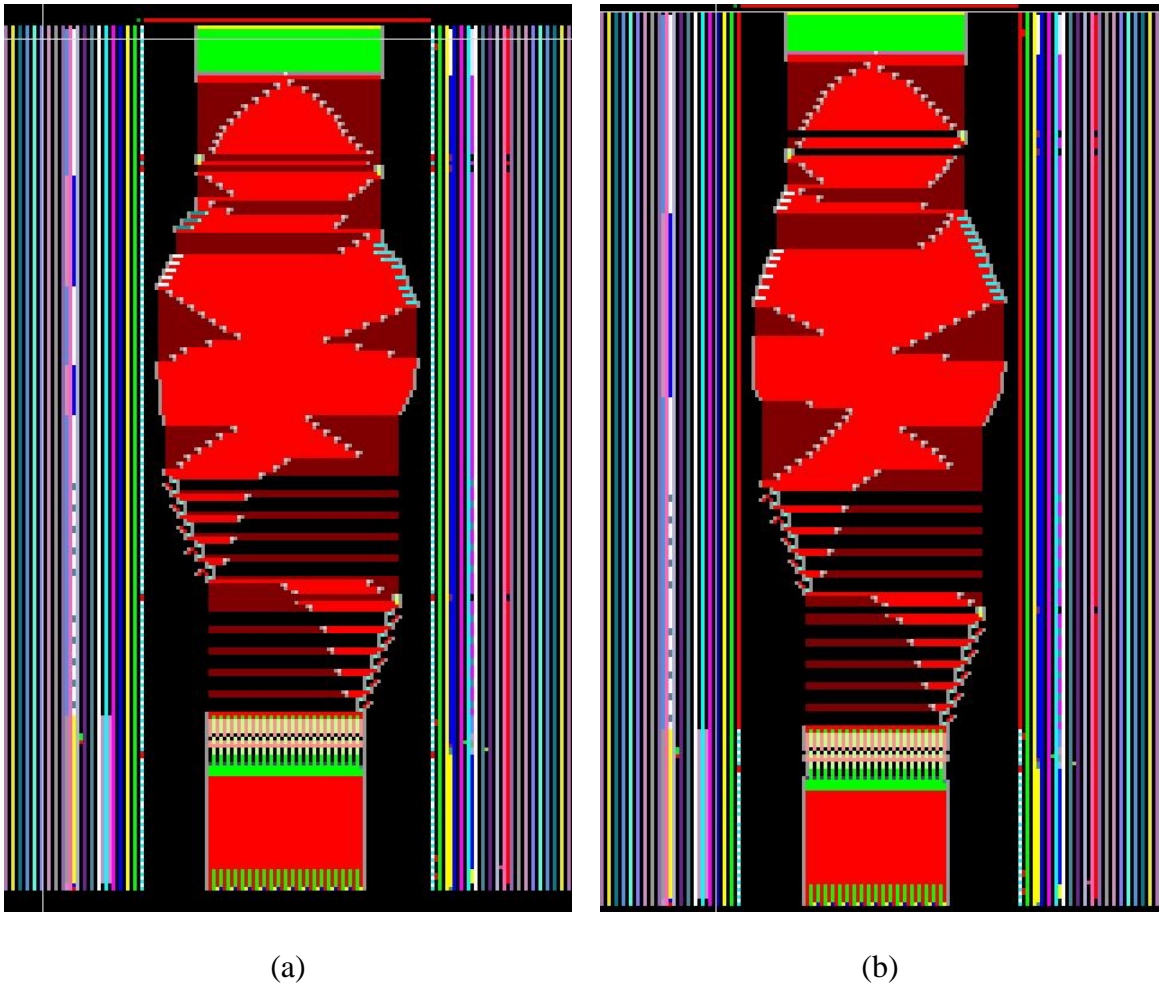


Figure 5.22 Knitting Programme of method 2DSL-2 of the two planes

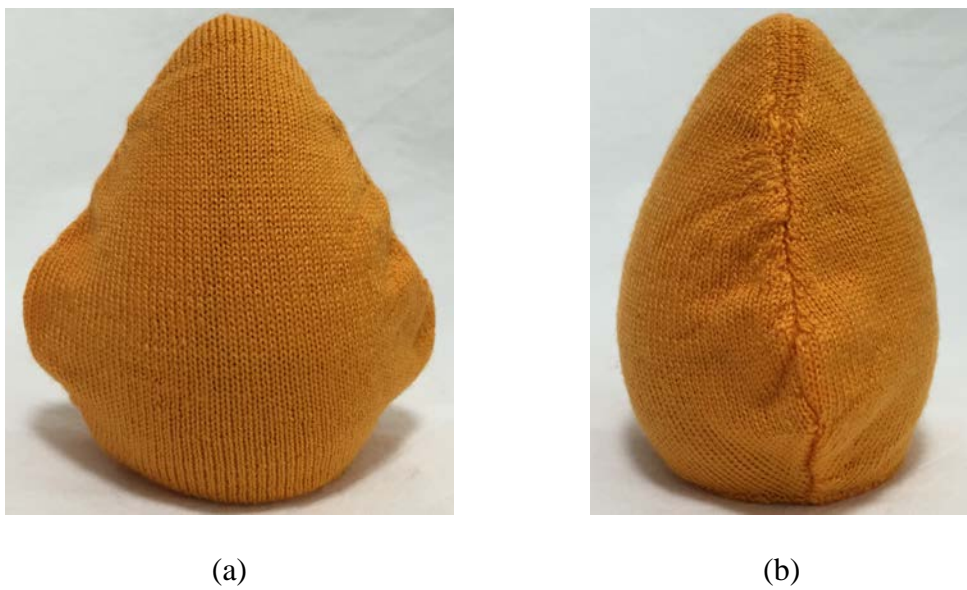


Figure 5.23 (a) The front view and (b) the side view of the 3D knitted shape by method 3DSL-2

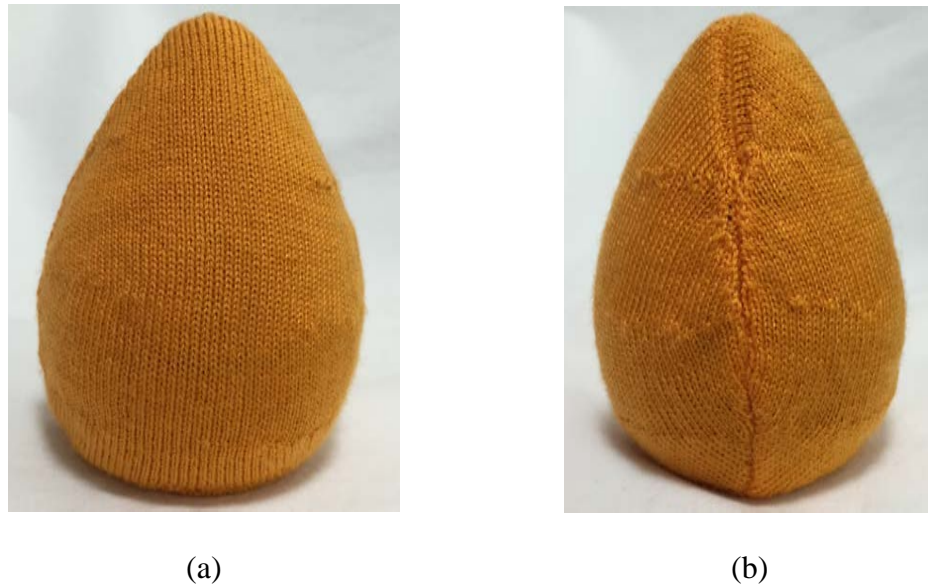


Figure 5.24 (a) The front view and (b) the side view of the 3D knitted shape by method 2DSL-2

## 5.6 Evaluation II

Six sample, three for each method, were produced for assessment of their 3D shape accuracy. All went through the qualitative and quantitative evaluations. Their appearance, shape and loop density values were compared.

Three repeated knitted shapes by method 3DSL-2 on the target object were observed. Their contours were different from the target 3D from the front view as those by method 3DSL-1. There were bumps at two sides and wavy edges due to excess fabrics. The loops in the bulgiest part were less dense than those in area around 1 cm below the tip. The elongated loops implied the bulgiest part did not have sufficient fabrics even though the sides had extra fabrics. The geometrical dimensions of the target were not preserved in these knitted shapes. The linking

seams were wavy with crimps from the side view. This was the result of side seam too long. For those by method 2DSL-2 in the front view, the edges were smoother and the shape was seemingly correct without extra folds. The loop size was even. From the side view, the link seam was clean and relatively straight, but there were some partial knitting marks. The samples by both methods were also scanned for comparison, shown in Figure 5.25 and Figure 5.26. From the front view of the scanned images, the shape by method 3DSL-2 was distorted while that by method 2DSL-2 possessed the same shape. The top view of method 3DSL-2 became a lemon shape with two protrusions on the sides while that of method 2DSL-2 was in a round shape as the target. The linking seams on method 2DSL-2 were not as obvious as those in method 2DSL-1 since method 2DSL-1 was missing loops and was stretched on the target. From the qualitative evaluations, the knitted shapes by method 2DSL-2 possessed the target 3D and were most likely to have the accurate dimensions among all. Unfortunately, method 3DSL-2 failed to reconstruct the target 3D. To prove that method 2DSL-2 could preserve and reconstruct the target 3D, subsequent quantitative evaluations were carried out.

Table 5.7 and Table 5.8 listed out the loop density values of method 3DSL-2 and method 2DSL-2 when in a relaxed state and on the target for three interior areas. The tolerance remained  $\pm 5\%$ . By checking the relaxed loop density of all six samples, correct knitting was confirmed since the values were within tolerance. The results of loop density on target object of method 3DSL-2 were cohering to its qualitative evaluation results that most of the wpc and cpc values were beyond tolerance. The total average percentage differences of wpc and cpc of method 3DSL-2 were -10.31% and -6.55%. The readings which were more than -5% meant

that the loops in those areas were stretched. Very few readings were within the tolerance but those could be in the areas of extra fabric. Taking the second cpc measurement of sample 3DSL-2 II as an example, it was 0.03% and was very close to its value in the relaxed state, but this measurement was taken from the side bumps. After all, most of its poor loop density values proved that method 3DSL-2 failed to possess the target 3D. For method 2DSL-2, the readings were satisfied that all were within  $\pm 5\%$ . Even the measurements were taken near the linking seam, the results were within the tolerance though were slightly higher than the others, around -4.75% for wpc. And this told that samples by method 2DSL-2 on the target were not under stretch and had sufficient amount of loops in proper positions to form the target 3D.

Therefore, from the qualitative evaluations and quantitative evaluations, method 2DSL-2 could successfully reconstruct the target 3D and proved the revised flattened planes could minimise the area preservation errors. And the poor performances of method 3DSL-2 in both evaluations confirmed that it could not preserve the target geometry and led to shape distortion. Besides, there was a difference proven between the two loop alignment methods.

The possible reason for method 3DSL-2's failure was that the 2D knitting mechanism was incompatible with knitting the 3D straight lines. Checking back to the researches on calculating the distortion from 3D to 2D with flexible fabrics by Ng and Yu (2006b & 2006c), the length of the cutting edge of a 3D shape from its front view became different after flattening. As flatbed weft knitting was a mechanism in 2D, knitting the 3D straight lines directly was actually knitting the flattened 2D curved lines in straight. And thus the knitted shape by method 3DSL-2

became a distorted plane shown in Figure 5.27. The loops were aligned following the straight lines in 2D in fact, leading to a flat plane and losing its original 3D. Not only the area was distorted, the length of edges was also lengthened that formed the crimps and creases in the linking seams. The finished shape no longer possessed the required 3D. So loops alignment following the 3D parallel straight lines of a positive Gaussian curvature surface could not reconstruct the 3D from the area-preserving plane.

And the loop alignment method 2DSL-2 based on the horizontal lines to be marked onto the planes was successful because the direction of the dimensional information of the planes allowed loops to be aligned in the same direction of knitting, matching with the 2D knitting mechanism. Hence, knitting could preserve the planar area and resume the 3D. That was why loop alignment method 2DSL-2 could reconstruct the target 3D.

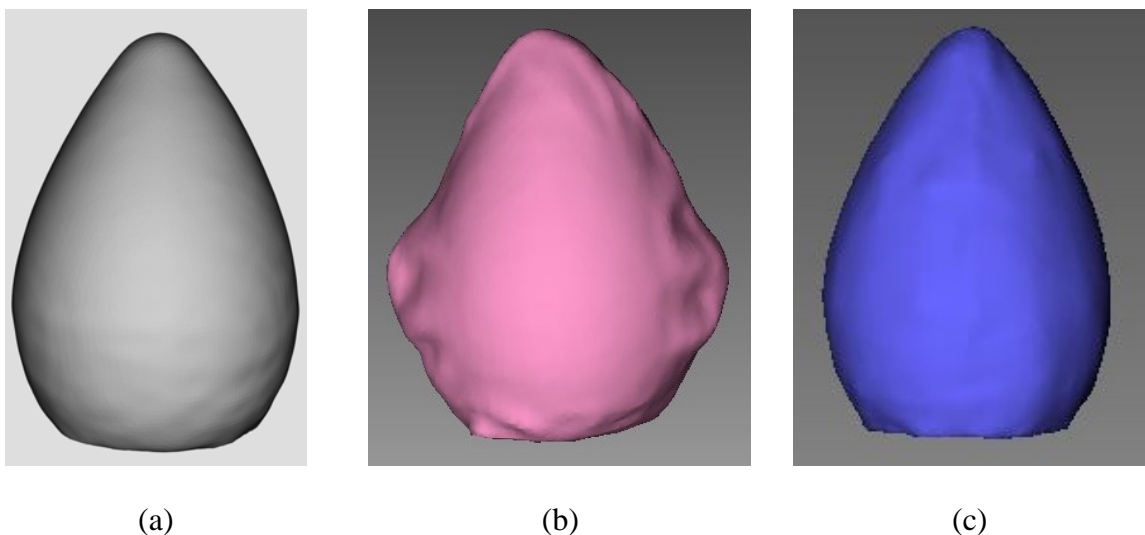


Figure 5.25 The front view of scanned images of (a) target image, (b) 3D knitted shape by method 3DSL-2 and (c) 3D knitted shape by method 2DSL-2

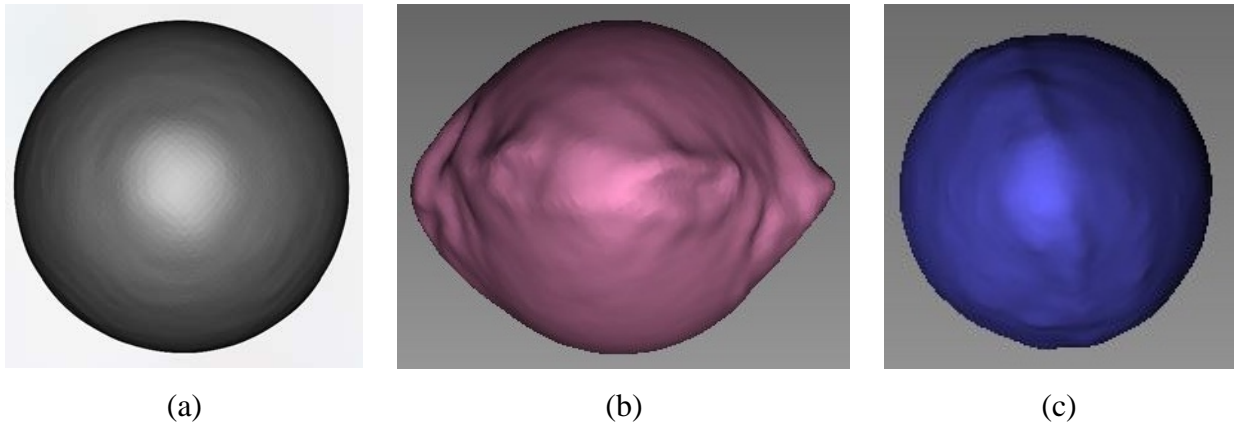


Figure 5.26 The top view of scanned images of (a) target image, (b) 3D knitted shape by method 3DSL-2 and (c) 3D knitted shape by method 2DSL-2

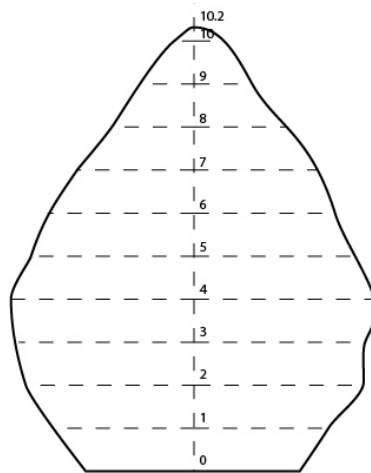


Figure 5.27 An illustration of the shape induced by method 3DSL-2

Item	Descriptions	Bumps / Folds	Crimps	Stretched Loops	Wavy Seam	Contour
Positive Gaussian Curvature 3DSL-2 I	Presence	Yes	Yes	Yes	Yes	Front view: distorted Top view: pointed sides
	Location	Two sides	Linking seams	Bulgiest Part	Two sides	
	Remarks	N/A				
Positive Gaussian Curvature 3DSL-2 II	Presence	Yes	Yes	Yes	Yes	Front view: distorted Top view: pointed sides
	Location	Two sides	Linking seams	Bulgiest Part	Two sides	
	Remarks	N/A				
Positive Gaussian Curvature 3DSL-2 III	Presence	Yes	Yes	Yes	Yes	Front view: distorted Top view: pointed sides
	Location	Two sides	Linking seams	Bulgiest Part	Two sides	
	Remarks	N/A				

Table 5.5 Table of appearance observation of three samples of positive

Gaussian curvature by method 3DSL-2

Item	Descriptions	Bumps / Folds	Crimps	Stretched Loops	Wavy Seam	Contour
Positive Gaussian Curvature 2DSL-2 I	Presence	No	No	No	No	Front view: accurate Top view: accurate
	Location					
	Remarks	Presence of partial knitting marks				
Positive Gaussian Curvature 2DSL-2 II	Presence	No	No	No	No	Front view: accurate Top view: accurate
	Location					
	Remarks	Presence of partial knitting marks				
Positive Gaussian Curvature 2DSL-2 III	Presence	No	No	No	No	Front view: accurate Top view: accurate
	Location					
	Remarks	Presence of partial knitting marks				

Table 5.6 Table of appearance observation of three samples of positive

## Gaussian curvature by method 2DSL-2

Item and Area		wpc	% diff	cpc	% diff
Working loop density		6.5617		8.9286	
Positive Gaussian Curvature 3DSL-2 I	Relax	6.451612903	-1.68%	8.695652174	-2.61%
	On object	6.106870229	-6.93%	8.196721311	-8.20%
	On object	5.357142857	-18.36%	8.108108108	-9.19%
	On object	6.153846154	-6.22%	8.450704225	-5.35%
	Average on object	5.872619747	-10.50%	8.251844548	-7.58%
Positive Gaussian Curvature 3DSL-2 II	Relax	6.451612903	-1.68%	8.849557522	-0.89%
	On object	5.797101449	-11.65%	8.196721311	-8.20%
	On object	5.357142857	-18.36%	8.333333333	-6.67%
	On object	6.18556701	-5.73%	8.955223881	0.30%
	Average on object	5.779937106	-11.91%	8.495092842	-4.86%
Positive Gaussian Curvature 3DSL-2 III	Relax	6.557377049	-0.07%	8.771929825	-1.75%
	On object	5.970149254	-9.02%	8.695652174	-2.61%
	On object	6.153846154	-6.22%	7.647058824	-14.35%
	On object	5.882352941	-10.35%	8.510638298	-4.68%
	Average on object	6.002116116	-8.53%	8.284449765	-7.21%
Total Average on object		5.884890989	-10.31%	8.343795718	-6.55%

Table 5.7 Table of loop density of the three samples by Method 3DSL-2

Item and Area		wpc	% diff	cpc	% diff
Working loop density		6.5617		8.9286	
Positive Gaussian Curvature 2DSL-2 I	Relax	6.666666667	1.60%	9.259259259	3.70%
	On object	6.315789474	-3.75%	9.090909091	1.82%
	On object	6.349206349	-3.24%	9.206349206	3.11%
	On object	6.4	-2.46%	9.090909091	1.82%
	Average on object	6.354998608	-3.15%	9.129389129	2.25%
Positive Gaussian Curvature 2DSL-2 II	Relax	6.611570248	0.76%	9.090909091	1.82%
	On object	6.25	-4.75%	8.928571429	0.00%
	On object	6.4	-2.46%	9.206349206	3.11%
	On object	6.451612903	-1.68%	8.988764045	0.67%
	Average on object	6.367204301	-2.96%	9.041228227	1.26%
Positive Gaussian Curvature 2DSL-2 III	Relax	6.666666667	1.60%	9.259259259	3.70%
	On object	6.557377049	-0.07%	8.860759494	-0.76%
	On object	6.52173913	-0.61%	8.823529412	-1.18%
	On object	6.25	-4.75%	8.928571429	0.00%
	Average on object	6.443038727	-1.81%	8.870953445	-0.65%
Total Average on object		6.388413878	-2.64%	9.013856934	0.95%

Table 5.8 Table of loop density of the three samples by Method 2DSL-2

## 5.7 Conclusion

After two rounds of experiments, the theory for the 3D pattern for knitted objects of surface with positive Gaussian curvature was established. Loop alignment method 3DSL-1 and 2DSL-1 failed because of the wrong assumption of symmetrical shape leading to errors in the area-preserving planes. So a well area-preserved plane was critical to the 3D pattern. Loop alignment method 3DSL-2 and 2DLS-2 were carried out with a revised 2D plane which used the entire surface of the target for flattening. The proper and area-preserved planes were derived and they allowed the two proposed methods to deduce their possibilities of 3D reconstruction. The differences of the two proposed loop alignment methods were proven. The loop alignment method based on the 2D straight lines worked while the one based on the 3D straight lines failed. The assumption was correct. The main idea of successful 3D shape knitting was that loop alignment must be compatible with the flatbed knitting constrains, the knitting mechanism in 2D. And with proper 3D data cloud



conversion, any surface with positive Gaussian curvature or zero Gaussian curvature could be repeated with this study. The experience achieved and theory developed were used in the next chapter of the last type surface, negative Gaussian curvature.

## CHAPTER 6

### NEGATIVE GAUSSIAN CURVATURE

In the two previous chapters, a surface with zero Gaussian curvature and a surface with a range of positive Gaussian curvature values were experimented. A theory on 3D pattern for knitted objects with concrete evidence from 3D data cloud conversion to 3D shape knitting was established. In this chapter, a surface with negative Gaussian curvature was used to experiment if the established theory and procedures were feasible. A chair in hyperbolic shape was used and it could be separated into two halves at its neck so that the final knitted shape could be put onto the target without over-stretched. Figure 6.1 showed a digital image of the target with its surface to be experimented indicated in red. Its edges in grey were not considered here as there was a change of curvature type from negative to positive or zero. Integration of curvature types on one surface was out of the scope of this study.

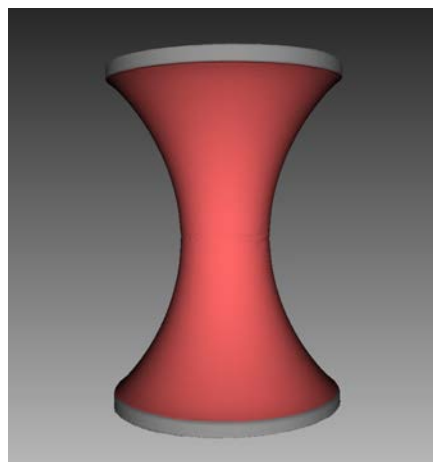


Figure 6.1 A digital image of the shape with a surface with negative Gaussian curvature indicated in red

## **6.1 3D Data Cloud Conversion**

The procedures for 3D data cloud conversion were well established. The target object would be first scanned for data cloud acquisition and processed preliminarily, then features of the processed data were recognised and extracted and finally the 3D surface mapped with mesh were flattened into a 2D plane for later 3D shape knitting.

### **6.1.1 3D Data Acquisition and Processing**

By using Artec Eva handheld 3D scanner, the 3D data cloud of the target object was obtained. With the aid of the Artec Studio CAD system, the data cloud underwent preliminary processing including eliminating useless frames, removing general noise, filling holes and rotation of xyz-axis. The finished data cloud was subject to features recognition.

### **6.1.2 Feature Recognition and Extraction**

As a hyperboloid, the target was in a convex shape. By using the suggested Sobel mask (Leong et al., 2006) (Figure 6.2), the points of the extreme convex and the turning points between the experimental surface and the grey edges shown in Figure 6.1 were achieved. And the mentioned curve fitting method generated smooth curves between the working surface and the useless edges and vertical lines

in the four directions, front, back, left and right, with the reference to the marking tape.

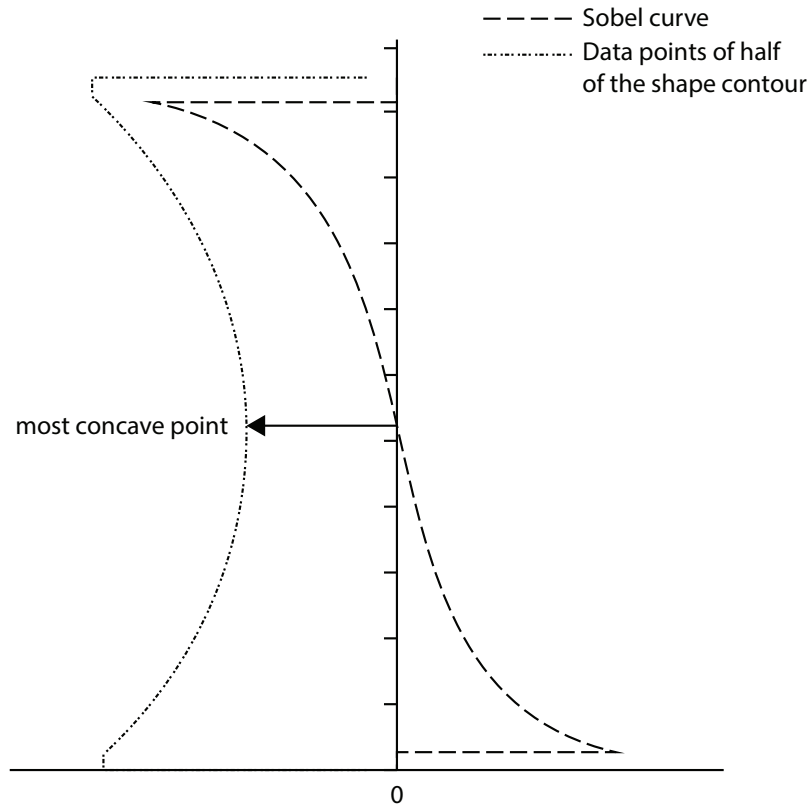


Figure 6.2 A diagram of Sobel mask of half of the target shape of negative Gaussian curvature

### 6.1.3 Polygonal Mesh Mapping and Flattening

The case of the target of negative Gaussian curvature was opposite to the one of positive Gaussian curvature though they were actually sharing the same idea. For the more convex areas, the triangulation mesh was denser with smaller triangles.

Figure 6.3 showed part of the triangulation on the target.

To avoid simultaneous distortions during flattening, cuts were inserted to preserve surface area. Due to the geometric properties of the target surface with negative Gaussian curvature, only vertical cuts were added. The cuts slashed the plane with empty spaces in olive-shape along the width indicated in grey in Figure 6.4. Referring to the established procedures for handling vertical cuts in previous chapter, these cuts should be extended to separate the plane into two. One cut was already extended to separate the 3D surface into a 2D plane and it formed two curved side edges. If the other three cuts in the middle of the plane were also extended, the whole plane would become four individual planes. However, if the plane were not separated, it was impossible to be knitted down with its surface area preserved using a flatbed knitting machine. By considering the knitting constrains, discussion on the plane continued in next section.

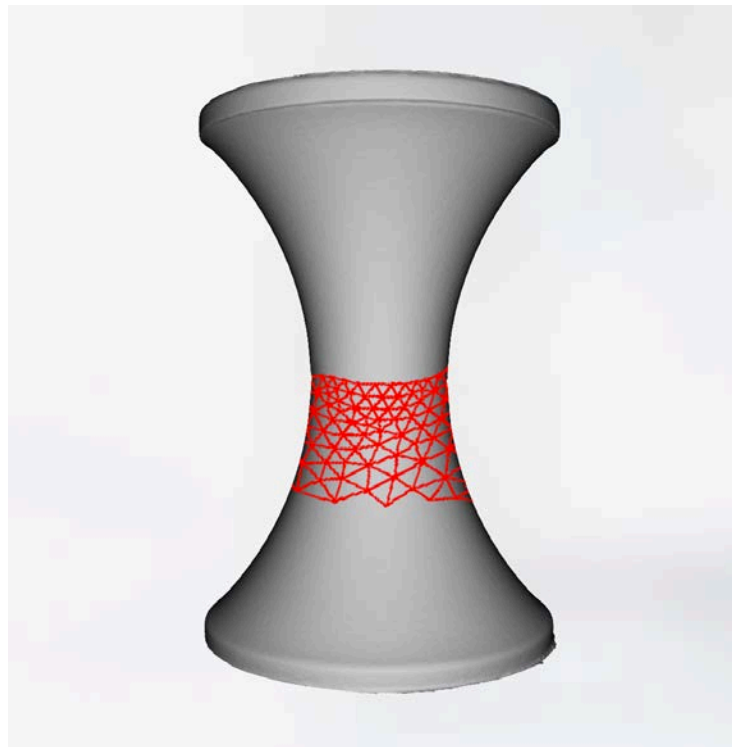


Figure 6.3 An illustration of mesh mapping with smaller triangles on the convex area of the surface with negative Gaussian curvature

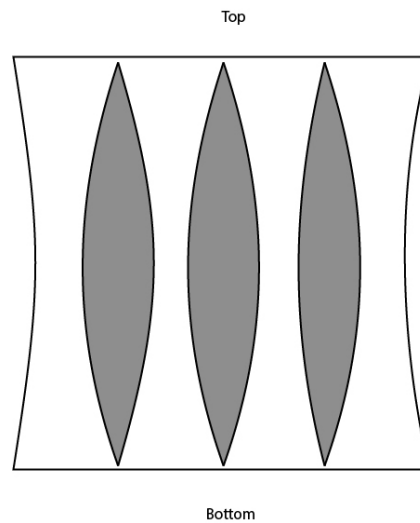


Figure 6.4 The flattened plane of the surface with negative Gaussian curvature with olive-shape empty space indicated in grey

## 6.2 3D Shape Knitting

In this section, the plane derived from the target surface with negative Gaussian curvature was brought to loop alignment, knitting sequence preparation and the knitting process. However, the plane could not be simply knitted otherwise its dimension could not be preserved. Discussing on the plane was raised and a method to handle this plane for 3D shape knitting was proposed.

### 6.2.1 Loop Alignment

The target surface was flattened into a 2D plane, but the plane in Figure 6.4 was not favourable for knitting with area preservation. If the plane were separated into four pieces, it would result in four linking seams in the end. From the quantitative evaluation of positive Gaussian curvature, it was known that the

bulkiness of linking seams would lead to a slightly distorted loop density value due to pulling of seam. So the more intense the seams presented, the more distortion existed in the final shape, altering the dimensional accuracy. Also, linking all the seams was time-consuming. It reduced the effectiveness and efficiency of the whole process. Therefore, separating the plane into four was not a good choice.

From the experience of positive Gaussian curvature chapter, partial knitting was capable of handling horizontal cuts with the surface area sustained. Therefore, if the plane was rotated  $90^\circ$  as in Figure 6.5 and the vertical empty space became horizontal, knitting could be possible. The curved starting and ending edges could be done by partial knitting. As there were no horizontal cuts in the original plane, the plane did not need to be separated but knitted as a whole. In this case, measurement taking and loop alignment were based on this rotated plane.

Loop alignment was based on the 2D straight lines as the conclusion from previous chapter. A vertical reference line was marked in the middle of the plane, the lowest point of the plane was set at 0 cm on the reference line and the numbers continued up to the top at an interval of 1 cm. Horizontal lines were also marked perpendicularly to the vertical reference line in 1 cm interval and extra horizontal lines were added to corner points, highest and lowest points of the empty spaces and the top point. Measuring all the heights and widths of the plane, a knitting sequence was calculated with the reference to the experimental cpc as 8.9286 cm and wpc as 6.5617 cm. Figure 6.6 showed the rotated plane marked with measurement lines.

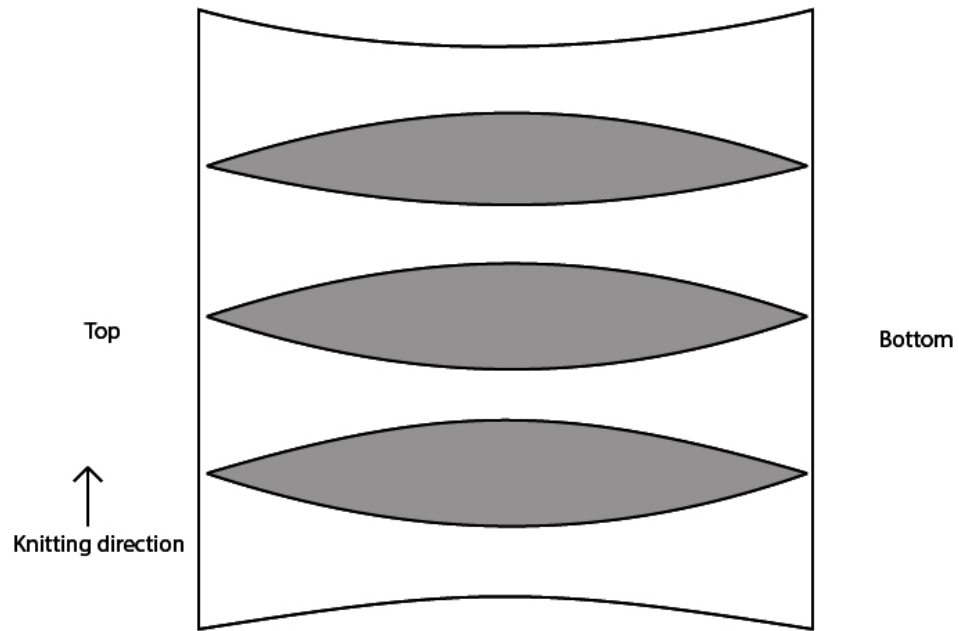


Figure 6.5 A 90° rotated plane of the target

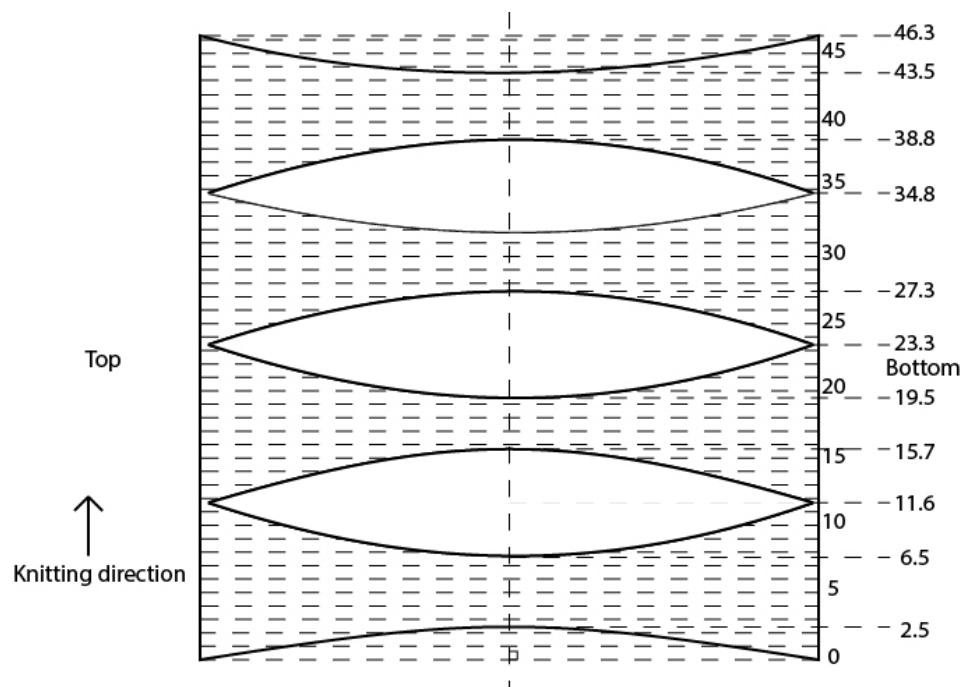


Figure 6.6 The rotated plane marked with measurement lines for loop alignment



### 6.2.2 Knitting Validation

With the prepared knitting sequence and the finished knitting programme by Shima Seiki Knit CAD system shown in Figure 6.7, knitting with 2/30 100% Merino wool using Shima Seiki SES-122S machine was executed. Normal routine of double checking and adjustment of machine setting and knitting process with trial fabrics were carried out. The knitted shape was reproduced three times.

By considering the knitted fabric would be linked at its starting and ending curved edges to form its 3D, the knitting start-up trim was modified to waste knit which was formed by knitting a certain length of knitted fabric with waste yarn before actual sample. Since the waste knit could be unravelled after linking, the presence of the start-up trims such as 2 courses of tubular at least in the knitted sample and the bulkiness of linking seams could be spared. Waste knit also helped in knitting consistency since with a certain length of waste knit, the fabric roll would be activated when then comb released the fabric. A finished 3D knitted shape after washing and steaming was shown in Figure 6.8.

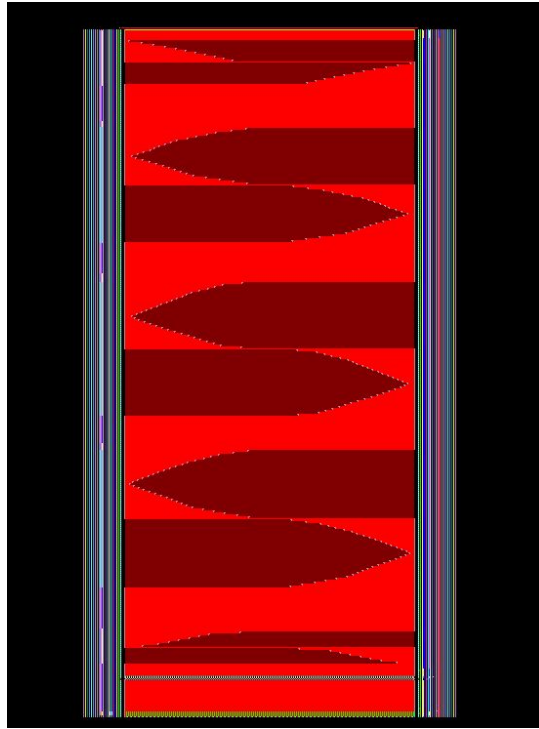


Figure 6.7 Knitting programme of the target object of negative Gaussian curvature



Figure 6.8 The knitted shape of surface with negative Gaussian curvature on the target

### 6.3 Evaluation

The three 3D knitted shape was put onto the target. As the target object could be parted in the middle, the knitted shapes' narrow neck did not need to pass through the wide base, preventing knitted shapes being over-stretched. The whole shape was put upright for evaluation each time, but the fabric edge could not stay on the upper edge of the target well due to gravity. And due to fabric curling of the edges, the fabric bottom edge did not lay well on the target object bottom edge. To cope with this problem, double tape was applied to the target edges to hold the fabric edges, seeing Figure 6.9. In order not to alter the knitted shape dimension laying on the target, double tape was not applied to the target body.

In the qualitative evaluation, the visual appearance of the knitted shapes and their 3D data cloud were compared with the target, shown in Figure 6.10. The shapes were fit on the target without any extra bumps, folds, crimps or fabric pulling from both the real products and scanned images. The linking seam of each was clean and straight, one was shown in Figure 6.10 (b). The partial knitting marks were more obvious on real products than in scanned images. The top and bottom edges were wavy even tapes were used. This was the caused by the natural knitted fabric edge curling and gravity. Table 6.1 listed the appearance observation of the samples. Generally speaking, from the qualitative evaluation, the knitted shapes possessed the target 3D.

The wpc and cpc of the three samples were measured and listed in Table 6.2. As the knitting direction of the samples was horizontal instead of vertical due to the

rotated plane, wpc and cpc were measured following the direction of loops. Knitting was correct since the loop density values of shapes in relaxed state were within tolerance. Most of the readings were acceptable that they were within the range of  $\pm 5\%$ , although one cpc value of shape I was just right at  $+5.00\%$ . However, one cpc value of shape II exceeded the tolerance at  $+6.67\%$ . The high value of that particular cpc measurement was caused by measuring a wale passing through several partial knitting marks that loops on the marks were slightly denser due to the pulling force of the previous loop. It should be known that the denser and tighter the loops were packed on the same wale, a higher cpc value would result. Nonetheless, the quantitative evaluation of the knitted shapes of negative Gaussian curvature was satisfied and it proved that the target 3D was successfully reconstructed.



Figure 6.9 Applying double tape to the target edge to hold the fabric edge

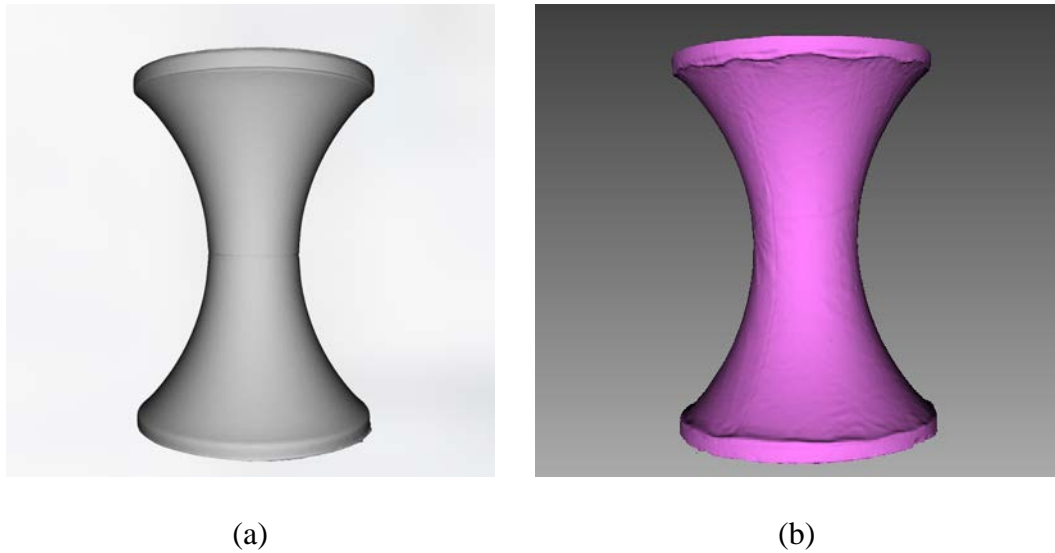


Figure 6.10 The scanned images of (a) target image, (b) 3D knitted shape of surface with negative Gaussian curvature

Item	Descriptions	Bumps / Folds	Crimps	Stretched Loops	Wavy Seam	Contour
Negative Gaussian Curvature I	Presence	No	No	No	No	Accurate
	Location					
	Remarks	Presence of partial knitting marks, wavy top and bottom edges				
Negative Gaussian Curvature II	Presence	No	No	No	No	Accurate
	Location					
	Remarks	Presence of partial knitting marks, wavy top and bottom edges				
Negative Gaussian Curvature III	Presence	No	No	No	No	Accurate
	Location					
	Remarks	Presence of partial knitting marks, wavy top and bottom edges				

Table 6.1 Table of appearance observation of three samples of negative Gaussian curvature

Item and Area		wpc	% diff	cpc	% diff
Working loop density		6.5617		8.9286	
Negative Gaussian Curvature I	Relax	6.535947712	-0.39%	9.090909091	1.82%
	On object	6.741573034	2.74%	9.375	5.00%
	On object	6.666666667	1.60%	9.230769231	3.38%
	On object	6.430868167	-1.99%	9.090909091	1.82%
	Average on object	6.613035956	0.78%	9.232226107	3.40%
Negative Gaussian Curvature II	Relax	6.557377049	-0.07%	9.174311927	2.75%
	On object	6.382978723	-2.72%	9.195402299	2.99%
	On object	6.315789474	-3.75%	9.302325581	4.19%
	On object	6.622516556	0.93%	9.523809524	6.67%
	Average on object	6.440428251	-1.85%	9.340512468	4.61%
Negative Gaussian Curvature III	Relax	6.711409396	2.28%	9.090909091	1.82%
	On object	6.818181818	3.91%	9.090909091	1.82%
	On object	6.52173913	-0.61%	8.823529412	-1.18%
	On object	6.41025641	-2.31%	9.090909091	1.82%
	Average on object	6.583392453	0.33%	9.001782531	0.82%
Total Average on object		6.545618887	-0.25%	9.191507035	2.94%

Table 6.2 Table of loop density of three samples of negative Gaussian curvature

## 6.4 Conclusion

The work on a surface with negative Gaussian curvature using the established procedures and theory was finished and it successfully preserved the surface area of the 3D shape and reconstructed its dimensions. Therefore, the 3D pattern for knitted objects of surface with negative Gaussian curvature was established.

The change of loop alignment direction, in other words, change of knitting direction, successfully tackled the fundamental problem of the 2D plane achieved from the surface with negative Gaussian curvature. As the normal weft knitting shaping techniques were not enough to knit a 2D plane with vertical cuts in the middle with the surface continued and with its surface area persevered at the same time, the more the vertical cuts there were, the more linking seams would be

required. So if knitting horizontally, the vertical cuts would become horizontal and could be achieved by partial knitting.

## CHAPTER 7

### CONCLUSION

The experiments were all finished and the study had come to an end. All three types of Gaussian curvatures, including zero Gaussian curvature, positive Gaussian curvature and negative Gaussian curvature, were investigated and all had positive results. A 3D knitting pattern for any freeform surface with a single type of Gaussian curvature was successfully established, from converting a 3D data cloud into a 3D knitted shape.

For an accurate 3D shape reconstruction, precise area preservation was the key to success, for both data cloud conversion and 3D shape knitting. In 3D data cloud conversion, the 3D surface was flattened into a 2D plane. It was all known that dimensional distortion in length, area and angle is unavoidable for all surfaces except surfaces with zero Gaussian curvature. As for mapping knitting loops onto the plane, surface area was determined to be preserved in the first priority in surface flattening. And in order to preserve surface area in flattening, cuts in different directions were inserted to the plane. The shape of horizontal cuts was achieved by partial knitting while vertical cuts were extended to separate the plane and then recombined by linking afterwards.

However, it should also be known that the more the vertical cuts inserted to a plane, the more the linking seams were resulted. And as linking seams had certain thickness in which there were two wales on each side in normal industrial production for fine gauge, the thickness of the seam against the target object surface induced a



pulling force to the neighbour loops and resulted a less dense loop density. So if there were more vertical cuts, the loop density of the knitted shape would be more affected. And linking all the seams were time-consuming, lowering the effectiveness and efficiency of the process. Therefore, by considering the property of the plane, change of knitting direction from vertical to horizontal by rotating the plane  $90^\circ$  was a feasible way to tackle a plane with more vertical cuts than horizontal cuts originally. It was concluded that the direction for loop alignment should not only be restricted to the uprightness of the target shape after all.

For 3D shape knitting, area preservation relied on the loop alignment method which was based on the measurement taking method of a plane. From Chapter 5, it was concluded that the method of taking dimensional measurements from the 2D plane determined the final shape. If the area of the plane was not preserved in loop alignment, the final shape would be distorted. And in order to preserve the planar area, the loop alignment method must be compatible with the 2D knitting mechanism. The dimensions of the plane must be directly taken from the 2D plane by marking a vertical reference line and horizontal straight lines perpendicular to the vertical reference line as the height and width of the plane respectively. That was why method 2DSL-2 which was the method based on the 2D straight lines could successfully reconstruct the target 3D while method 3DSL-2 based on the 3D straight lines failed. Again, as the parallels of latitude as in Cartography became 2D curved lines after flattening, direct knitting these curved lines was actually knitting them in straight due to the restriction of knitting mechanism in 2D. The final shape must be distorted. For method 3DSL-1 and 2DSL-1, they both failed was due to a distorted plane induced by a wrong assumption of the target being symmetric.

Going back to the linking seam issue, in the chapter of negative Gaussian curvature, linking seam was not affecting the loop density values, although there was only one linking seam in each sample. In fact, there was not a single linking wale under the seam at all. Since that linking seam was linking two courses together, the useless knits or waste knits were unravelled after linking. However, in the chapters of zero and positive Gaussian curvature, each seam was linking two wales together instead. It was known that it needed some fabrics for easier linking in production. And in order to minimise the bulkiness of linking seams, two wales as allowance on each side were spared for linking. If it was linking two courses together, more allowance could be spared as they could be unravelled later on. For some factories, to keep the knitted product seams consistent for a more appealing appearance, they also kept two courses of allowance on each side for linking two courses together. Nonetheless, these four courses of allowance were not considered in this study.

Moreover, from the experimental evaluations, it was concluded that both qualitative and quantitative evaluations were important to assess the 3D shape accuracy. A shape was considered inaccurate when it had excess fabrics such as appearance of bumps, folds or crimps and inadequate amount of fabrics such as fabric pulling, elongated loops or loose loop density exceeding the tolerance. Each evaluation method was required to assess either situation of excess fabrics or missing fabrics. The appearance and data cloud comparison as the qualitative evaluations could tackle distortion situations such as excess fabrics, but they were not a good method for evaluating missing fabrics as stretched loops were not easy to be noticed, especially for fine gauge knitted products. The loop density measurement as the

quantitative evaluation was a useful method to find out inadequate amount of fabrics and stretched loops, but it was not good for finding out excess fabrics when only looking at the numbers. Since the loops in an excess fabric area was in a relaxed state, by simply comparing the loop density values, it was impossible to know if the loops were in their proper positions or in an excess fabric area.

All in all, the study on 3D pattern for knitted objects was successful. As a fundamental study, it provided basic information and knowledge in 3D knitting. For its application, in the academic field, it can be a base for further 3D knitting research; and in the fashion industry field, it can be a unique idea for knitting a 3D form apparel with a 2 needle-bed flatbed knitting machine. Since this study was examining surfaces of a single type of Gaussian curvature each time, future work on investigating surfaces with integration of curvature types can be held. Or a new 3D pattern for knitted objects by using a four-needle-bed knitting machine could be done in the future.

## REFERENCE

- Andymsp, (2010). *Cylinder* [Graphic], Retrieved April 9, 2015 from: <https://boundlessadvantages.wordpress.com> CC NC
- Anthroscan.[http://www.human-solutions.com/apparel industry/anthroscan en.php](http://www.human-solutions.com/apparel%20industry/anthroscan%20en.php), 2015.
- Artec. <http://artec3d.com>, 2014
- Au, K. F. (2011). *Advances in knitting technology*. Cambridge : Woodhead : In association with the Textile Institute.
- Azariadis, P. N. (2002). An evolutionary algorithm for generating planar developments of arbitrarily curved surfaces. *Computers in Industry*, 47, 357-68.
- Atchison, S., & Pilant, M. (2011). *A mathematical history of cartography*. Texas: Texas A&M University.
- Belcastro, S. M. (2009). Every topological surface can be knit: a proof. *Journal of Mathematics and the Arts*, 3 (2), 67-83.
- Benítez, J., & Thome, N. (2004). Application of differential geometry to cartography. *International Journal of Mathematical Education in Science and Technology*, 35 (1), 29-38.
- Bezdek, J. C. (1981). *Pattern recognition with fuzzy objective function algorithms*. New York: Plenum Press.
- Bлага, M. Ciobanu, A.R., Dan, D. O., & Ionesi, S. D. (2011). Interactive application for computer aided design of 3d knitted fabrics. *Conference proceedings of "eLearning and Software for Education" (eLSE)*, 2, 433-440.
- Bodyshape. <http://www.bodyshapescanners.com/>, 2015.
- Brackenbury, T. (1992). *Knitted Clothing Technology*. Oxford: Blackwell Scientific Publications.
- Brunsmann, M. A., Daanen, H. M., & Robinette, K. M. (1997) Optimal postures and positioning for human body scanning, *Proceedings of International Conference on 3-D Digital Imaging and Modeling*, 226–273.
- Carmo, M. P. (1976). *Differential geometry of curves and surfaces*. London: Prentice-Hall.
- Choi, W., Kim, Y., & Powell, N. B. (2015). An investigation of seam strength and elongation of knitted-neck edges on complete garments by binding off processes. *The Journal of The Textile Institute*, 106 (3), 334-341.

Choi, W., & Powell, N. (2008). The development of specialized knitted structures in the creation of resist-dyed fabrics and garments. *The Journal of the Textile Institute*, 99, 253–264.

Creaform. <http://www.creaform3d.com/en>, 2015.

Cyberware. <http://www.cyberware.com>, 2015.

Dekker, L., Douros, I., Buxton, B., & Treleaven P (1999). Building symbolic information for 3D human body modelling tom range data. *3-D Digital Imaging and Modelling Proceedings*, 388-97.

Desbrun, M., Meyer, M., & Alliez, P. (2002) Intrinsic parameterizations of surface meshes. *Comput Graph Forum*, 21(3), 209–18.

Floater, M. S., & Hormann, K. (2005). *Advances in multiresolution for geometric modelling: Surface parameterization: a tutorial and survey*. Berlin: Springer Berlin Heidelberg.

Floater, M. S. (1997) Parametrization and smooth approximation of surface triangulations. *Computer Aided Geometric Design*, 14(3), 231–250.

Gallier, J. H. (2011). *Geometric methods and applications for computer science and engineering*. New York: Springer Science+Business Media.

Google, *Patents of Shima : Knit design method and device WO 2003032203 A1*. Retrieved May 4, 2016 from <http://www.google.com/patents/WO2003032203A1?cl=en>

Hills, R. L. (1989). William Lee and his knitting machine. *The Journal of The Textile Institute*, 80 (2), 169-184.

Hormann, K., & Greiner, G. (1999) *Mips: An efficient global parameterization method. Curve and surface design*. St Malo: Vanderbilt University Press.

Huang, C. Y., Zhang, X. & Cui, L. (2007). Study on collar pattern design of sweater based on body measurement. *Wool Textile Journal*, 3, 53-55.

Huang, H. Q. (2011). *Development of 2D block patterns from fit feature-aligned flattenable 3D garments*. Hong Kong: Institute of Textiles and Clothing, The Hong Kong Polytechnic University.

Igarashi, Y., Igarashi, T., & Suzuki, H. (2008). Knitting a 3D model. *Computer Graphics Forum*, 27 (7), 1737-1743.

Kieff (2012). *Point cloud torus* [Graphic], Retrieved April 2, 2015 from: [http://upload.wikimedia.org/wikipedia/commons/4/4c/Point\\_cloud\\_torus.gif](http://upload.wikimedia.org/wikipedia/commons/4/4c/Point_cloud_torus.gif) CC NC

- Knitting Industry (2016a). *Shima Seiki to hold Global 3D Knitting Seminar & Workshop in US*. Retrieved May 4, 2016 from <http://www.knittingindustry.com/shima-seiki-to-hold-global-3d-knitting-seminar-workshop-in-us/>
- Knitting Industry (2016b). *Shima Seiki to present latest machinery at Techtexil North America*. Retrieved May 4, 2016 from <http://www.knittingindustry.com/flat-knitting/shima-seiki-to-present-latest-machinery-at-techtexil-north-america/>
- Köller, K. (2011). *Hyperboloid* [Graphic], Retrieved April 9, 2015 from: <http://www.mathematische-basteleien.de/hyperboloid.htm> CC NC
- Kumar, R. G. V., Srinivasan, P., Holla, D. V., Sharstry, K. G., & Prakash, B. G. (2003). Geodesic curve computations on surfaces. *Computer Aided Design*, 20 (2), 119-33.
- Lanius, C. (2003). *Mathematics of cartography: What are maps?*. Retrieved March 19, 2015 from Rice University, Department of Mathematics Web site: <http://math.rice.edu/~lanus/pres/map/mapdef.html>
- Leong, I. F., Fang, J. J., & Tsai, M. J. (2007). Automatic body feature extraction from a market-less scanner human body. *Computer-Aided Design*, 39, 568-582.
- Levy, B., Petitjean, S., Ray, N., & Maillot, J. (2002). Least squares conformal maps for automatic texture atlas generation. *ACM Transactions on Graphics (TOG): Proceedings of ACM SIGGRAPH 2002*, 21(3), 362–371.
- Liu, Z., Mitani, J., Fukui, Y., & Nishihara, S. (2008). A new 3D shape retrieval method using Spherical Healpix. *Journal of Information Processing*, 16, 190-200.
- Lo, D. (2015). *Finite element mesh generation*. Boca Raton: CRC Press.
- Ma, Y., & Lamar, T. A. M. (2013). Three-dimensional shaping for knitted garments. *Research Journal of Textile and Apparel*, 17 (3), 128-139.
- Maghrabi, H. A., Vijayan, A, Wang, L., & Deb, P. (2015). Design of seamless knitted radiation shielding garments with 3D body scanning technology. *Proceedings of the 1st International Design Technology Conference (DesTech 2015): Procedia Technology*, 20 (C), 123-132.
- Mahbub, R., Wang, L. & Arnold, L. (2014). Design of knitted three-dimensional seamless female body armour vests. *International Journal of Fashion Design, Technology and Education*, 7 (3), 198-207.
- Matković, V. M. P. (2010). The power of fashion: the influence of knitting design on the development of knitting technology, *TEXTILE*, 8 (2), 122-146.
- Mccann, J., Albaugh, L., Narayanan, V., Grow, A., Matusik, W., Mankoff, J., & Hodgins, J. (2016). A compiler for 3D machine knitting. *ACM Transactions on Graphics (TOG)*, 35 (4), 1-11 [ Peer Reviewed Journal].

- Mccartney, J., Hinds, B. K., & Chong, K. W. (2005). Pattern flattening for orthotropic materials. *Computer-Aided Design*, 37, 631-644.
- Ng, R., & Yu, W. (2006a). Distortion theory of stereographic draping with rigid fabric. *Sen'i Gakkaishi*, 62 (3), 52-57.
- Ng, R., & Yu, W. (2006b). Distortion theory of stereographic draping with flexible fabric on surface of constant curvature. *Sen'i Gakkaishi*, 62 (4), 67-73.
- Ng, R., & Yu, W. (2006c). Distortion theory of stereographic draping with flexible fabric on general surface: part I - geometric analysis. *Sen'i Gakkaishi*, 62 (4), 74-80.
- Osada, R., Funkhouser, T., Chazelle, B., & Dobkin, D. (2002). Shape distributions. *ACM Transactions on Graphics*, 21 (4), 807-832.
- Pan, Z. X., Ge, Y. B., Wei, B., & Yang, J. (2009). The three-dimensional design in shaping knitting wear. *China Textile Leader*, 11, 97-98.
- Parida, L., & Mudur, S. P. (1993). Constraint-satisfying planar development of complex surfaces. *Computing Aided Design*, 25 (4), 225-232.
- Polking, J. C. (2000). *Mapping the Sphere*. Retrieved January 23, 2015 from Rice University: Department of Mathematics Web site: <http://math.rice.edu/~polking/cartography/cart.pdf>
- Quickfur (2012). *Some thoughts on the hypersphere*. [Graphic], Retrieved April 9, 2015 from: <http://hi.gher.space/forum/viewtopic.php?f=27&t=1688> CC NC
- Radvan, C. (2013). Inclusively designed womenswear through industrial seamless knitting technology. *Fashion Practice*, 5 (1), 33-58.
- Ray, S. C. (2012). *Fundamentals and advances in knitting technology*. New Delhi: Woodhead Publishing India Pvt. Ltd.
- Raz, S. (1991). *Flat knitting: The new generation*. Bamberg: Meisenbach.
- Shaffer, A., & Starler, E. D. & (2002). Smoothing an overlay grid to minimise linear distortion in texture mapping. *ACM Transactions on Graphics*, 21 (4), 874-890.
- Sheffer, A. (2002). Spanning tree seams for reducing parameterisation distortion of triangulated surface. *Shape Modeling International, 2002: International Conference on Shape Modelling and Applications*, 61-68.
- Shima Seiki (2006). *Creating shaping pattern guide*. Japan: Shima Seiki.
- Song, G., Wu, J. & Wei, Y. (2006). Computer-aided design of three-dimensional knitwear. *The Journal of the Textile Institute*, 97 (6), 549-552.

Spencer, D. J. (2001). *Knitting technology a comprehensive handbook and practical guide*. Cambridge: Woodhead Publishing Limited.

Stitch World (2015). *Stitch World*. Retrieved March 3, 2017 from <http://news.apparelresources.com/events-news/germany-shima-seiki-present-ispo-expo-seamless-knitting-machines-3d-design-system/>

Tae, J. K., Sung, M. K. (1999). Development of three-dimensional apparel CAD system: Part II: prediction of garment drape shape. *International Journal of Clothing Science and Technology*, 12 (1), 39-49.

Tae, J. K., Sung, M. K. (2002). Garment pattern generation from body scan data. *Computer-Aided Design*, 35 (7), 611-618.

Tatsushi, F., Tsuyoshi, M., Masashi, Y., Hirohisa, S., & Hidenori, I. (1998). A generating method for 3-dimensional knitting cloth shapes. *Conference: Computer Vision - ACCV'98, Third Asian Conference on Computer Vision, Hong Kong, China*, 474-481.

TC<sup>2</sup>. <http://www.tc2.com/>, 2015.

TriForm. <http://www.wvl.co.uk/>, 2015.

Underwood, J. (2009). *The design of 3D shape knitted preforms*. Melbourne: School of Fashion and Textiles, RMIT University.

Vranic, D. V., & Saupe, D. (2002). Description of 3D-shape using complex function on the sphere. *Proc. IEEE International Conference on Multimedia (ICME)*, 1, 177-180.

Wang, C. L., Chen, S. F., & Yuen, M. F. (2002). Surface flattening based on energy model. *Computing Aided Design*, 34 (11), 823-833.

Wang, C. L., Wang, Y., & Tang, K. (2004). Reduce the stretch in surface flattening by finding cutting paths to the surface boundary. *Computer Aided Design*, 36 (8), 665-677.

Wang, M. J., Wu, W. W., Lin, K. C., Yang S. N., & Lu J. M. (2007). Automated anthropometric data collection from three-dimensional digital human models. *The International Journal of Advanced Manufacturing Technology*, 32, 109-115.

Xu, Y. H., Yuan, X. L., & Qin, W. Y. (2009). Local Knitting Technology in Sweater Design. *Wool Textile Journal*, 39 (5), 45-49.

Yang, S. M., & Mao, L. L. (2009). Application of retiring knit in woollen sweater design. *Wool Textile Journal*, 1, 44-48.

Yoshizawa, S., Belyaev, A., & Seidel, H. P. (2004). A fast and simple stretch-minimizing mesh parameterization. *International conference on shape modeling and applications*, 200-208.